Studies on modulation of immune responses by poultry red mite, *Dermanyssus gallinae*, and development of the novel control strategies

（ワクモによる宿主免疫応答の調節と
新規制御法の開発に関する研究）

Sotaro FUJISAWA

CONTENTS

ABBREVIATIONS

PRM	poultry red mite
NFM	northern fowl mite
TFM	tropical fowl mite
IL	interleukin
TNF	tumor necrosis factor
SGE	salivary gland extract
NO	nitric oxide
RNA-Seq	RNA sequencing
Dg	*Dermanyssus gallinae*
Cys	cystatin
Ctr1	copper transporter 1
APMAP	adipocyte plasma membrane-associated protein
PBS	phosphate-buffered saline
QV	quality value
Contig	contiguous sequence
FPKM	fragments per kilobase of exon per million reads mapped
CPM	counts per millions
FDR	false discovery rate
IPR	InterProScan
GO	gene ontology
KEGG	Kyoto Encyclopedia of Genes and Genomes
CC	cellular component
MF	molecular function
BP	biological process
qRT-PCR	quantitative reverse transcription polymerase chain reaction
IFN	interferon
NIE	non-infested experimental
NIC	non-infested commercial
b.e.	before exposure
a.e.	after exposure
PBMCs	peripheral blood mononuclear cells
SME	soluble mite extract
ELISA	enzyme-linked immunosorbent assay
TGF	transforming growth factor

CCL	C-C chemokine ligand
CCR	C-C chemokine receptor
Treg	regulatory T
CTLA4	cytotoxic T-lymphocyte antigen 4
PD	programmed death
PD-L1	PD-ligand 1
IRF	interferon regulatory factor
Arg2	arginase 2
RACE	rapid amplification of cDNA ends
ORF	open reading frame
LCM	laser capture microdissection
Elf1a1	elongation factor 1-α-1
BSA	bovine serum albumin
SDS	sodium dodecyl sulfate
PBST	PBS containing 0.05% Tween-20
SR	survival rate
RC	reproductive capacity
CI	confidential interval
SDS-PAGE	SDS polyacrylamide gel electrophoresis

NOTES

The contents of Chapter I have been published in *Parasitology International*.

Fujisawa S, Murata S, Isezaki M, Oishi E, Taneno A, Maekawa N, Okagawa T, Konnai S, Ohashi K. 2020. Transcriptome dynamics of blood-fed and starved poultry red mites, *Dermanyssus gallinae*. *Parasitology International* **78**: 102156.

The contents of Chapter II are under consideration for publication in *Parasitology International* and *BMC Immunology*.

Fujisawa S, Murata S, Sato T, Oishi E, Taneno A, Konnai S, Ohashi K. Short communication: Investigation of peripheral blood responses in chickens infested with *Dermanyssus gallinae*. *Parasitology International* **In revision**.

Fujisawa S, Murata S, Isezaki M, Sato T, Oishi E, Taneno A, Maekawa N, Okagawa T, Konnai S, Ohashi K. Suppressive modulation of host immune responses by *Dermanyssus gallinae* infestation. *BMC Immunology* **In submission**.

The contents of Chapter III have been published in *Vaccine* and *Vaccines*, and will be published in *Parasitology*.

Fujisawa S, Murata S, Isezaki M, Ariizumi T, Sato T, Oishi E, Taneno A, Maekawa N, Okagawa T, Ichii O, Konnai S, Ohashi K. Characterization of a copper transporter 1 from *Dermanyssus gallinae* as a vaccine antigen. *Parasitology* **In press**.

Fujisawa S, Murata S, Takehara M, Aoyama J, Morita A, Isezaki M, Win SY, Ariizumi T, Sato T, Oishi E, Taneno A, Maekawa N, Okagawa T, Ichii O, Konnai S, Ohashi K. 2021. *In vitro* characterization of adipocyte plasma membrane-associated protein from poultry red mites, *Dermanyssus gallinae*, as a vaccine antigen for chickens. *Vaccine* **39**: 6057-6066.

Fujisawa S, Murata S, Isezaki M, Ariizumi T, Sato T, Oishi E, Taneno A, Maekawa N, Okagawa T, Ichii O, Konnai S, Ohashi K. 2021. Characterization of a novel cysteine protease inhibitor from poultry red mites and its potential application as a vaccine for chickens. *Vaccines* **9**: 1472.

PREFACE

The invasion of blood-feeding ectoparasites, the poultry red mites (*Dermanyssus gallinae*, PRMs), the northern fowl mites (*Ornithonyssus sylviarum*, NFMs), and the tropical fowl mites (*Ornithonyssus bursa*, TFMs) is a significant threat to egg-laying hens worldwide, causing considerable economic losses to the poultry industry. Among these mite species, PRMs have been found across a large number of countries and regions, particularly in European countries, Asian countries such as Iran, China, and Japan, and the countries in Latin America including Brazil [Sparagano *et al*., 2014; Mirzaei *et al*., 2016; Thomas *et al*., 2018]. The life cycle of PRMs consists of five stages: eggs, larvae, protonymphs, deutonymphs, and adults. While larvae do not feed on blood, nymphs and adults require blood meal for the development into subsequent stages and egg development [Chauve, 1998]. Protonymphs and deutonymphs molt after blood feeding and develop into the next life stages. In contrast, adult female PRMs feed blood several times, and then, they lay 4–8 eggs and produce about 30 eggs in their lifetime [Chauve, 1998]. PRMs typically infest chickens every 2-4 days, and complete their life cycle, from egg to adult, within 2 weeks [Sparagano *et al*., 2014]. PRMs infest chickens predominantly in the darkness, and they usually stay on hosts for 0.5 to 1.5 hours for blood feeding. After blood feeding, the majority of PRMs leave the hosts and stay in cracks and crevices of the poultry houses during the daytime [Sparagano *et al*., 2014]. Thus, PRMs efface themselves during the day, which make it hard to find them, whereas they can rapidly increase their numbers in favorable conditions.

Currently, more than 80% of laying hen's farm in several European countries and 85% of those in Japan are contaminated with PRMs [Sparagano *et al*., 2014]. Mass infestation with PRMs causes various health problems in chickens, such as anemia, depression, impaired immune responses, reduction in egg production, and sometimes causes death in young chickens. A previous study reported a ten-fold increase in mortality rate of chickens as a result of heavy infestation with PRMs [Cosoroaba, 2001]. The annual economic costs associated with the loss of production and the control of PRMs was estimated to be approximately €360 million for the EU egg industry in 2017 (*https://coremi.eu/home.html*) and €66.85 million in Japan [Mul *et al*., 2009; Sparagano *et al*., 2009]. In addition, PRMs occasionally infest mammalian species, including humans, and cause skin lesions, pruritis, and dermatitis, implicating that PRM-infestation could be an occupational hazard for poultry farm workers [Abdigoudarzi *et al*., 2014; Di Palma *et al*., 2018]. Furthermore, several literatures showed that PRMs potentially transmit several avian pathogens such as avian pox virus, avian influenza virus,

Salmonella Gallinarum, and spirochetes [Moro *et al*., 2009; Huong *et al*., 2014; Sommer *et al*., 2016; Pugliese *et al*., 2019] as well as zoonotic pathogens such as *Erysipelothrix rhusiopathiae* [Eriksson *et al*., 2009]. Collectively, the infestation with PRMs could be serious issues in both aspects of veterinary hygiene and public health, and therefore, the control of PRMs is a crucial matter for the poultry industry.

Hematophagous ectoparasites secrete various effector molecules into their saliva that modulate host physiological responses to maintain undisturbed blood feeding. Hemostatic responses including blood clotting, platelet aggregation, and vasoconstriction are the primal host defensive reaction against intrusion by mouthparts of parasites into the host skin [Kotál *et al*., 2015]. These acute responses are accompanied by the activation of host immune systems; keratinocytes, endothelial cells, and leukocytes, including dendritic cells and macrophages, which are present in the sites of infestation, produce pro-inflammatory chemokines and cytokines, such as interleukin (IL)-8, IL-1β, and tumor necrosis factor (TNF)-α, for the recruitment of inflammatory cells including neutrophils, resulting in inflammatory responses [Wikel, 2013; Šimo *et al*., 2017]. Moreover, during secondary infestation, T and B cells produce cytokines and antibodies against salivary or mouthpart-derived molecules to augment inflammation and activate complement, mast cells, and basophils [Brossard and Wikel, 2004; Bowman and Nuttall, 2008; Wikel, 2013]. Meanwhile, several studies have demonstrated that salivary proteins of hematophagous ectoparasites, such as serine protease inhibitors, interrupt host hemostasis and pain signaling [Ribeiro and Mather, 1998; Champagne, 2005; Hughes, 2013; Ibelli *et al*., 2014]. Additionally, these ectoparasites produce a variety of immunosuppressants to mitigate both innate and adaptive immune responses; for instance, tick saliva or salivary gland extract (SGE) attenuates the production of nitric oxide (NO) and inflammatory cytokines including TNF-α and IL-1β from macrophages [Kuthejlová *et al*., 2001; Chen *et al*., 2012], and impairs the proliferation and functions of dendritic cells [Oliveira *et al*., 2008; Skallova *et al*., 2008] and lymphocytes [Gillespie *et al*., 2001; Hannier *et al*., 2003]. These immunosuppressive functions of salivary factors were also reported in mosquitoes [Cross *et al*., 1994; Schneider *et al*., 2004]. Importantly, the suppressive modulation of host immunity caused by the infestation is considered to be closely associated with pathogen transmission [Schneider *et al*., 2004; Schneider and Higgs, 2008; Kazimirova and Stibraniova, 2013; Liu and Bonnet, 2014; Nuttall, 2019; Guerrero *et al*., 2020].

These findings evoke the idea that the infestation with PRMs may modulate host physiological states. Notably, since PRMs can rapidly expand their population in favorable conditions, chickens raised at poultry houses severely contaminated would be exposed to PRMs more heavily and chronically, compared to the hosts affected by ticks

or mosquitoes. Therefore, PRM-infestation might cause immunosuppression and pose increased risks of infection with avian pathogens. Indeed, a previous report demonstrated that the protein composition in the plasmas of chickens was altered by the infestation with PRMs, representing that PRM-infestation contributes to the attenuated humoral immunity [Kowalski and Sokół, 2009]. The immunomodulatory effects of PRM-infestation were further supported by decreased levels of antibody titers in PRM-infested chickens vaccinated against avian infectious agents [Kaoud and El-Dahshan, 2010], and by the reduced percentages of lymphocytes in chickens raised at PRM-eroded farms [Koziatek-Sadłowska and Sokół, 2020]. Collectively, consistent with the observations in ticks and mosquitoes, PRMs could modulate host immunological states during infestation. However, the details of immune reactions in chickens infested with PRMs, including cytokine expression profiles, have yet to be elucidated.

Currently, the control of PRMs mainly depends on the exhaustive sanitary management of the premises and the use of synthetic acaricides such as organic phosphorus, carbamates, and pyrethroids. However, as PRMs have a trait to conceal themselves in hideaways, they could escape from these treatments [Flochlay *et al*., 2017]. In addition, even All-In-All-Out production system is not enough to eradicate PRMs because they can survive for a long period, up to 8 months, without a blood meal in severe conditions [Chauve, 1998; Axtell, 1999; Sparagano *et al*., 2014], and infest new flocks. Moreover, improper and continuous use of acaricides could cause various social problems; for instance, in 2017, an “egg scandal”, the contamination of eggs with fipronil, a broad-spectrum insecticide, broke out in at least 40 European countries, resulting in the recall of millions of eggs and the loss of millions of dollars [Smulders *et al*., 2018; Tu *et al*., 2019]. To avoid such social issues, the use of synthetic acaricides is strictly regulated in many countries, especially in Europe [Sparagano *et al*., 2014]. Furthermore, recently, the emergence of acaricide-resistant PRMs has been reported worldwide [Thind and Ford, 2007; Murano *et al*., 2008, 2015; Marangi *et al*., 2009]. Although novel synthetic acaricides are developed, the acquisition of the resistance in PRMs may be inevitable. Indeed, a new synthetic acaricide, which is a phoxim-based product and was approved in European countries in 2010, demonstrated tremendous acaricidal effect at the beginning of its introduction. However, PRMs resistant to phoxim emerged within just 1 year after the introduction [Meyer-Kühling *et al*., 2007; Zdybel *et al*., 2011]. Collectively, current countermeasures are insufficient to control PRMs in the poultry sector, and therefore, the development of alternative control strategies are strongly aspired. To date, several non-chemical approaches have been under consideration. These alternatives subsume biological control including predatory species that feed on PRMs [Ali *et al*., 2012; Lesna

et al., 2012], or microbials, such as fungi, that are pathogenic for PRMs [Steenberg and Kilpinen, 2003; Kaoud and El-Dahshan, 2010; Tavassoli *et al*., 2011]. In addition, some non-chemical biopesticides, such as spinosad, which are more friendly to the environment, showed toxicities on PRMs [George *et al*., 2010; Liebisch *et al*., 2011]. Nonetheless, various problems need to be overcome to put these strategies into practice. Both predators and fungi require specific environmental conditions to act [Ali *et al*., 2012; Lesna *et al*., 2012], which could cause the variation in their efficacies dependent on the climates. Furthermore, it has been reported that the residual efficacies of biopesticides are shorter than chemicals, and their safety on vertebrates and environment are still controversial [Chauve, 1998; Abdel-Ghaffar *et al*., 2009]. Owing to these issues, most of the alternative strategies hit setbacks and are yet to be ready for field application.

The development of acaricide-resistance in ticks, such as *Rhipicephalus* (*Boophilus*) *microplus*, is also a social issue threatening livestock industry as well as human health [Abbas *et al*., 2014; Rodriguez-Vivas *et al*., 2018]. As a novel and non-chemical measure, the anti-tick vaccine has been in the limelight because of its lower risk of the contamination in the environment and of the development of acaricide-resistance [de la Fuente and Kocan, 2006; de la Fuente and Contreras, 2015]. Anti-tick vaccines interfere with the functions of tick molecules by antibodies produced in vaccinated hosts, resulting in the disruption of homeostasis or interruption of physiological activities such as blood feeding, digestion, or reproduction (Figure 1) [Willadsen, 2004]. Two types of molecules can be considered as vaccine antigens based on their targets [Nuttall *et al*., 2006]. The first type of the targets includes proteins secreted into their saliva ("exposed" antigens) that facilitate attachment to the host skin [Tsuda *et al*., 2001], suppression of host immune reactions [Wikel, 1996; Mori *et al*., 2010], and inhibition of coagulation [Narasimhan *et al*., 2004], contributing to the maintenance of undisturbed blood feeding. The second includes proteins expressed in the midgut ("concealed" antigens). Since the ingested blood is accumulated in the midgut, antigens in midguts could be efficiently exposed to antibodies contained in the blood sucked from vaccinated hosts [Willadsen *et al*., 1989; Willadsen, 2004]. Heretofore, a number of antigen candidates have been examined, and the vaccine targeting Bm86, a plasma membrane protein expressed in the midgut of *R. microplus*, exhibited tremendous efficacies and commercially used in the field [Willadsen *et al*., 1995].

Of late years, researches on the development of vaccines against PRMs are getting vigorous on the basis of the success in ticks [Arkle *et al*., 2008]. Several studies have identified antigen candidates and examined their efficacies [Bartley *et al*., 2012; Wright *et al*., 2016; Lima-Barbero *et al*., 2019]. However, efficacies of anti-PRM vaccine have

yet to be sufficiently observed in practical application in the field [Bartley *et al*., 2017], and no vaccine against PRMs is commercially available. Therefore, investigation of antigens for more effective vaccines is necessary to establish the control strategies by vaccination. Whilst ticks infest hosts and continue blood feeding for a longer period (3–10 days or more [Ribeiro and Francischetti, 2003]), the period of blood feeding by PRMs is much shorter than that by ticks. Hence, concealed antigens are expected to be more suitable as vaccine antigens against PRMs. In addition, considering the mechanism of vaccine described above, molecules that play essential roles in PRMs' physiological activities, such as blood digestion or egg development, are desirable as vaccine antigens. Moreover, since antibodies produced in vaccinated hosts exert their effects after the ingestion by PRMs, antigens should be highly expressed in PRMs, especially in blood fed states. To investigate antigen candidates, therefore, biological characteristics including gene expression profiles of PRMs should be analyzed in each feeding state. Notably, previous reports have demonstrated that gene expression patterns of ticks were greatly changed in response to blood feeding. For instance, gene expression profiles in the midguts and ovaries of *Ixodes ricinus* were drastically altered after blood feeding [Kotsyfakis *et al*., 2015]. Besides, the expressions of genes involved in metabolic processes in the midguts of *Ornithodoros erraticus* and *Haemaphysalis flava* were significantly upregulated after blood feeding [Xu *et al*., 2016; Oleaga *et al*., 2018]. In PRMs, meanwhile, a previous study performed transcriptome analysis by RNA sequencing (RNA-Seq) using RNA sample from mixed life stages, sexes, and feeding states [Schicht *et al*., 2014]. However, transcriptome dynamics between blood-fed and starved PRMs have yet to be investigated.

In this study, to scrutinize the host physiological responses against PRM-infestation in detail and to develop a novel strategy for the control of PRMs by vaccination approaches, in Chapter I, comprehensive transcriptome analysis was performed using blood-fed and starved PRMs by RNA-Seq. The gene expression patterns were then compared between each feeding state to investigate the biological characteristics of PRMs in detail. In Chapter II, the immunological states of chickens infested with PRMs were analyzed to assess the immunomodulatory effects of PRM-infestation on the hosts. Then, in Chapter III, to develop the vaccination strategy as a novel method to control PRMs, antigen candidates for the vaccine were explored from the data obtained by RNA-Seq analysis conducted in Chapter I. Three newly-identified antigen candidates, cystatin-like molecule (*D. gallinae*-cystatin: Dg-Cys), copper transporter 1-like molecule (*D. gallinae*-copper transporter 1: Dg-Ctr1), and adipocyte plasma membrane-associated protein-like molecule (*D. gallinae*-adipocyte plasma membrane-associated protein: Dg-APMAP)

were characterized and evaluated for their potential as vaccine antigens *in vitro*.

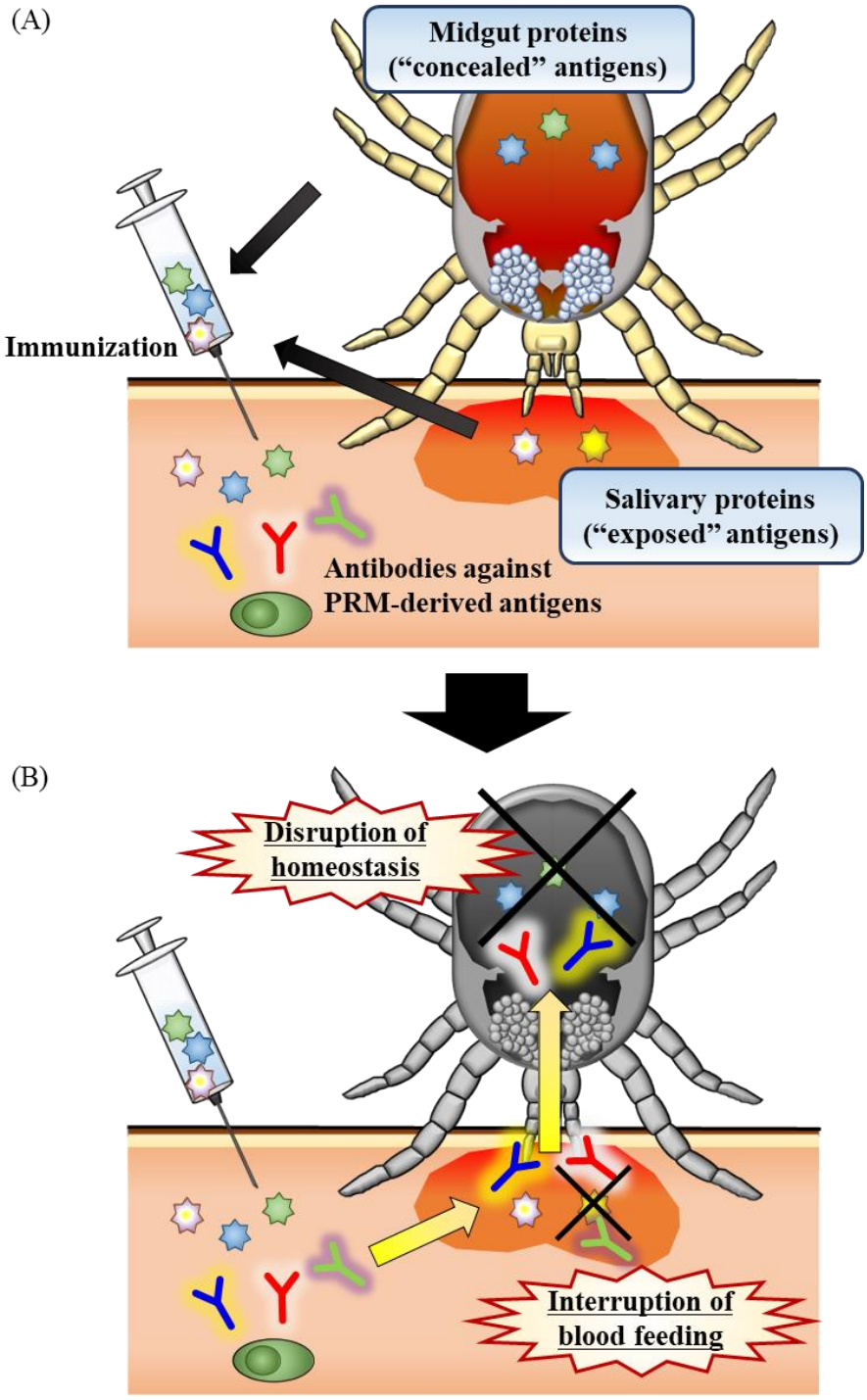

Figure 1. The mechanism of the vaccine against hematophagous ectoparasites.
(A) Hosts are immunized with parasite-derived antigens, including salivary proteins ("exposed" antigens) that contribute to the maintenance of undisturbed blood feeding, and midgut proteins ("concealed" antigens) that play essential roles in parasites' lives. (B) Antibodies produced in immunized hosts exert anti-parasite effects by interrupting blood feeding or by disrupting homeostasis.

CHAPTER I

Comparative analyses of transcriptomes in blood-fed and starved poultry red mite, *Dermanyssus gallinae*

INTRODUCTION

PRMs are one of the most noxious blood-feeding ectoparasites of chickens and are prevalent in many countries, especially European countries and Asian countries including Japan [Sparagano *et al*., 2014; Mirzaei *et al*., 2016; Thomas *et al*., 2018]. Massive PRM-infestation initiates a variety of negative impacts on chickens, including anemia, depression, and decrease in egg production and quality, resulting in significant economic losses to the poultry industry [Cosoroaba, 2001]. Currently, the use of synthetic acaricides is the most common strategy to protect poultry sector from PRM-invasion. However, since PRMs are nocturnal and conceal themselves in hideaways during daytime [Chauve, 1998], they could survive acaricide treatment. Furthermore, the emergence of PRMs that are resistant against acaricides has been widely reported [Thind and Ford, 2007; Murano *et al*., 2008, 2015; Marangi *et al*., 2009]. Therefore, the development of novel control methods is urgently required, and recently, anti-PRM vaccine has been spotlighted as a promising strategy for the prevention of PRMs [Arkle *et al*., 2008]. However, efficacies of vaccines previously developed have been found to be insufficient for the practical application in the field [Bartley *et al*., 2017], and thus, antigens for more effective vaccines should be investigated.

Anti-PRM vaccines induce the disruption of homeostasis and/or reduction of fecundity in PRMs by interrupting the functions of PRM-derived antigens by antibodies produced in vaccinated chickens. Considering this mechanism, vaccine antigens should be essential molecules for PRMs' lives. Additionally, since antibodies produced by the host would be ingested by PRMs along with blood feeding, molecules expressed in PRMs constitutively or at least in a blood-fed state are desirable as vaccine antigens. Importantly, several studies have demonstrated that the gene expression profiles of ticks, hematophagous ectoparasites which are biologically related to PRMs, were dramatically altered after blood feeding; for instance, the gene expression patterns in the salivary gland and the midgut of *I. ricinus* were exceedingly different between blood-fed and starved states [Kotsyfakis *et al*., 2015]. Collectively, to search for antigen candidates, it is important to understand the biological characteristics of PRMs in each feeding state. Previously, researchers have conducted a transcriptome profiling of PRMs by RNA-Seq analysis using mixed sexes and life stages of blood-fed PRMs, demonstrating that some metabolic processes were active [Schicht *et al*., 2014]. However, the dynamics of gene expression patterns in response to blood feeding in PRMs have yet to be examined. Therefore, in this chapter, to explore effective antigens for the development of anti-PRM vaccines, the RNA-Seq analysis using each feeding state of PRMs was conducted, and

the biological characteristics of PRMs was investigated by comparing the gene expression patterns between blood-fed and starved PRMs.

MATERIALS AND METHODS

PRM samples

Mixed life stages and sexes of PRMs were obtained from an egg-laying farm in Japan. A part of the dark red, round PRMs were designated as "blood-fed PRMs" on morphological observation and were isolated within 2 days of mite collection. The remaining PRMs were maintained at 25°C in 70% humidity for a 2-week period, and designated as "starved PRMs". PRM samples were stored at −80°C until use.

RNA isolation and cDNA synthesis

Isolated PRM samples were washed twice with phosphate-buffered saline (PBS, pH7.2) and thoroughly homogenized with a 1.5-mL homogenization pestle for a 1.5 mL microcentrifuge tube (Scientific Specialties, Inc., Lodi, CA, USA) in 600 μL of buffer RLT Plus (RNeasy Plus Mini Kit, Qiagen, Hilden, Germany). Total RNA was isolated using the RNeasy Plus Mini Kit according to the manufacturer's instructions.

RNA-Seq

RNA-Seq was conducted using the total RNA isolated from mixed life stages and sexes of blood-fed and starved PRMs as described above. All the following procedures were performed at Hokkaido System Science Co., Ltd., Hokkaido, Japan.

1. Construction of cDNA library and sequencing

The qualities of RNA samples were examined using an Agilent 2100 Bioanalyzer (Agilent Technologies, Böblingen, Germany). A cDNA library was prepared using the TruSeq Stranded mRNA Sample Prep Kit (Illumina, Inc., San Diego, CA, USA), according to the standard protocol. Paired-end sequencing was performed using HiSeq (Illumina, Inc.), according to the manufacturer's instructions.

2. Sequence assembly

The adaptor sequences added to construct the cDNA library (5′-AGA TCG GAA GAG CAC ACG TCT GAA CTC CAG TCA C-3′, 5′-AGA TCG GAA GAG CGT CGT GTA GGG AAA GAG TGT-3′) were removed from raw reads with cutadapt software v1.1 (*https://cutadapt.readthedocs.org/en/stable/*). The read sequences which indicated low quality values (QV) were trimmed using Trimmomatic software v0.32 (*http://www.usadellab.org/cms/index.php?page=trimmomatic*). The regions in which QVs were lower than 20 were excluded, and the read sequences that had more than 50 bp

were used for further analyses. The trimmed reads were assembled to create contiguous sequences (contigs) with Trinity software v2.4.0 (*https://github.com/trinityrnaseq/trinityrnaseq/wiki*). *De novo* sequence assembly was conducted using the read sequences obtained from both mite-samples. Raw sequence data were deposited in DDBJ/ENA/GeneBank (BioSample accessions: SAMD00228960, SAMD00229086).

3. Expression analyses

The expression intensities of each contig were analyzed and compared between blood-fed and starved PRMs in accordance with the Trinity assembly and analysis pipeline [Haas *et al*., 2013]. The trimmed reads were mapped to the contigs described above using Bowtie2 software v2.3.2 (*http://bowtie-bio.sourceforge.net/bowtie2/index.shtml*). The trimmed reads were also mapped to the genome sequence of the chicken (*Gallus gallus*, NCBI: txid9031) using TopHat software v2.0.14 (*http://tophat.cbcb.umd.edu/*), and chicken-derived contigs were removed. The expected expression intensity (fragments per kilobase of exon per million reads mapped; FPKM) of each contig was calculated both in blood-fed and starved PRMs using RSEM package v1.3.0 for R (*http://deweylab.biostat.wisc.edu/rsem/*). FPKM values were compared between blood-fed and starved PRMs using edgeR package v3.8.6 for R (*http://bioinf.wehi.edu.au/edgeR/*). To minimize the rate of false positives, the genes with a logarithmic value of their counts per millions ($\log_2$CPM, outputted by edgeR package) less than 0 were excluded from analyses. The *p*-value and false discovery rate (FDR) were adjusted using the edgeR package to estimate statistical significances.

4. Functional annotation

The contigs were converted into amino acid sequences using the 'getorf' program from the EMBOSS package v6.6.0 (*http://emboss.sourceforge.net/*) and applied to the InterProScan (IPR) program v5.32-71.0 (*https://www.ebi.ac.uk/interpro/*) to add functional annotations based on their amino acid motifs and domains. The contigs considered as virus-derived products based on the IPR annotation were removed.

Bioinformatic analysis

A gene ontology (GO) and metabolic pathway enrichment analyses were conducted using the contigs, except for virus-derived genes and ribosomal RNA genes, using Shiny GO v0.61 (*http://bioinformatics.sdstate.edu/go/*) and according to Kyoto Encyclopedia of Genes and Genomes (KEGG) [Kanehisa and Goto, 2000], in accordance with each

transcript’s IPR annotation.

RESULTS

Sequencing and *de novo* assembly

The numbers of reads obtained by RNA-Seq were summarized in Table I-1. In total, 168,996,962 reads from blood-fed PRMs and 165,252,914 reads from starved PRMs were obtained. After read trimming, 167,594,546 reads (99.2%) and 163,337,310 reads (98.8%) were acquired from blood-fed and starved PRMs, respectively. To restrain the contamination with host-derived transcripts, the trimmed reads of blood-fed PRMs were mapped to the genome sequence of chicken, and 86,194 reads (0.05%) were considered as chicken-derived genes and excluded from the analysis (Table I-1). *De novo* sequence assembly using the trimmed reads obtained from both feeding states of PRMs resulted in the yield of 162,263 contigs. The average size of contigs was 1,013 bp (Table I-2), and 92.12% and 87.75% of reads from blood-fed and starved PRMs were mapped to the assembled contigs, respectively (Table I-1).

Expression analysis and functional annotation

Among the contigs acquired above, 40,642 contigs (24.9%) indicated detectable expression intensities, of which $\log_2$CPM were no less than 0 (Table I-3). In blood-fed PRMs, 37,900 genes were highly expressed (FPKM > 0), whereas the expression of 39,374 genes was observed in starved PRMs. Among them, 1,268 genes (3.1%) were expressed only in blood-fed PRMs, while 2,742 genes (6.7%) were detected only in starved PRMs. The contigs obtained were translated into their deduced amino acid sequences and functionally annotated in accordance with their amino acid motifs and domains. A total of 36,785 contigs (22.7%) were characterized for their functions, and 19,666 contigs (53.3%) were expressed with detectable intensities ($\log_2\text{CPM} \geq 0$). After excluding the contigs derived from viruses and ribosomal RNA genes, 19,114 genes were obtained and subjected to further analyses. The comparative analysis of gene expression between blood-fed and staved PRMs revealed that 2,154 genes were significantly upregulated in blood-fed PRMs, while the expression levels of 4,175 genes were higher in starved PRMs (Figure I-1).

GO and metabolic enrichment analysis

PRM-derived genes that showed significant differences in their expression intensities between the two feeding states were subjected to GO and metabolic enrichment analyses. Each gene was codified into three GO categories, consisting of cellular components (CC), molecular functions (MF), and biological processes (BP). Regarding the CC and MF

terms, the GO terms annotated frequently were found to be similar between each feeding state of PRMs, although there were some differences in the order of enrichment FDR (Table I-4). The top 5 CC terms were ‘Intracellular organelle’, ‘Organelle’, ‘Membrane-bounded organelle’, ‘Intracellular membrane-bounded organelle’, and ‘Cytoplasm’ in blood-fed PRMs. These were almost identical to those in starved PRMs, except for the difference in the order of the top 2 (Table I-4). In blood-fed PRMs, the top 5 categories with respect to MF were ‘Ion binding’, ‘Heterocyclic compound binding’, ‘Organic cyclic compound binding’, ‘Protein binding’ and ‘Transferase activity’, whilst the top MF term in starved PRMs was ‘Protein binding’, followed by ‘Ion binding’, ‘Organic cyclic compound binding’, ‘Heterocyclic compound binding’, and ‘Anion binding’ (Table I-5). Conspicuous differences were observed in the BP terms. In blood-fed PRMs, the top 3 terms were associated with metabolic processes, ‘Cellular nitrogen compound metabolic process’, ‘Heterocycle metabolic process’, ‘Organic cyclic compound metabolic process’ (Table I-6). In contrast, in starved PRMs, the majority of annotated BP terms corresponded to ‘Biological regulation’, ‘Regulation of biological processes’, and ‘Regulation of cellular processes’ (Table I-7). Additionally, within top 30 categories in starved PRMs, the next 5 categories related to the regulation of biological activities including metabolism were included, whereas these were not allocated to the categories in blood-fed PRMs (Tables I-6 and 7).

A metabolic pathway enrichment was also analyzed by mapping the contigs to the KEGG pathways [Kanehisa and Goto, 2000]. Regardless of feeding states, the most major pathway was that of ‘Metabolic pathway’, followed by ‘Oxidative phosphorylation’ and ‘Carbon metabolism’ in blood-fed PRMs, and ‘Endocytosis’ and ‘Purine metabolism’ in starved PRMs (Tables I-8 and 9). Notably, autophagy seemed to be more active in starved PRMs (Table I-9). To investigate the metabolic pathway active in each state, the contigs classified into ‘Metabolic pathways’ in Tables I-8 and 9 were ranked in accordance with their expression intensities, and the motifs/domains within the top 15 contigs were predicted based on the IPR descriptions. In blood-fed PRMs, the contigs associated with the phosphorylation of nucleotide diphosphates and adenosine triphosphate were expressed with high expression intensities, indicating that energy synthetic processes are highly active in blood-fed PRMs (Table I-10). In contrast, starved PRMs strongly expressed genes involved in gluconeogenesis and the β-oxidation of fatty acids (Table I-10). Finally, to examine the differences in expressions of genes related to energy synthesis, gluconeogenesis, and β-oxidation of fatty acids, the expression profiles of selected contigs were summarized in Table I-11 and in the scatter plot visualizing the relationship between statistical significance and relative changes in the expression levels (Figure I-2).

The significant upregulation of the expression of contigs related to energy synthesis in blood-fed PRMs was observed, while the downregulation of the expression of contigs associated with gluconeogenesis and β-oxidation of fatty acids was confirmed. Collectively, these data showed that gene expression patterns of PRMs, especially those involved in metabolic pathways, are dramatically altered in response to blood feeding.

Table I-1. The numbers of reads obtained in each process.

	Blood-fed	Starved
Raw data	168,996,962	165,252,914
Trimmed data	167,594,546	163,337,310
No. of reads mapped to chicken genome sequence (%)	86,194 (0.05)	-
Trimmed data (host-removed)	167,508,352	-
No. of mapped reads (%)	154,386,218 (92.12)	143,329,002 (87.75)
No. of unmapped reads (%)	13,208,328 (7.88)	20,008,308 (12.25)

Table I-2. Summary of the *de novo* assembly.

No. of contigs	Total length (bp)	Average contig length (bp)	Largest contig length (bp)	N50 contig length (bp)[a]
162,263	164,301,068	1,013	17,417	1,888

[a]The minimum contig required to cover 50% of the genomes.

Table I-3. Summary of the expression analysis and functional annotation.

Gene expression metrics	No. of contigs ($log_2CPM \geq 0$)	40,642
	Genes expressed in blood-fed PRMs ($log_2CPM \geq 0$, FPKM > 0)	37,900
	Genes expressed in starved PRMs ($log_2CPM \geq 0$, FPKM > 0)	39,374
	Genes expressed both in blood-fed and starved PRMs ($log_2CPM \geq 0$, both FPKM > 0)	36,632
Functional annotation metrics	Total no. of annotated contigs	36,785
	No. of annotated contigs ($log_2CPM \geq 0$)	19,666
	No. of annotated contigs ($log_2CPM \geq 0$, excluded virus-derived and ribosomal RNA genes)	19,114

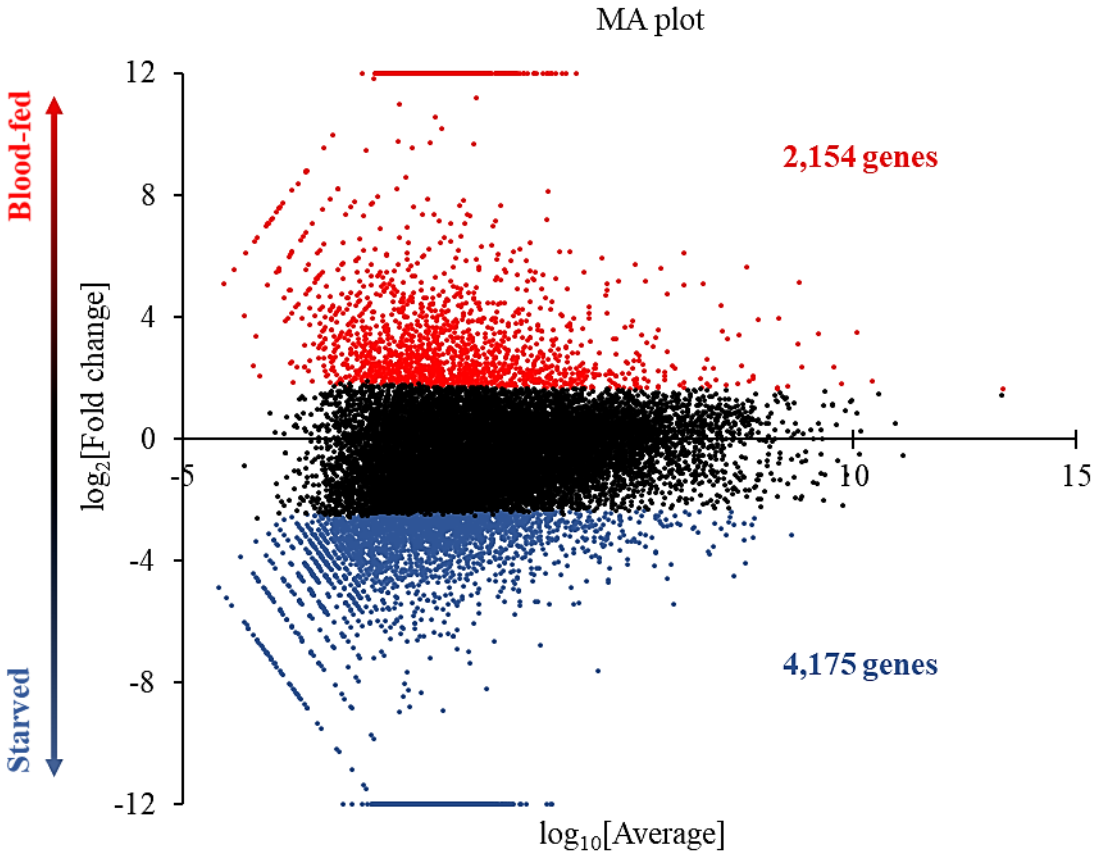

Figure I-1. Differences in gene expression patterns between blood-fed and starved PRMs.

The differences in gene expression pattern between blood-fed and starved PRMs were visualized, by displaying the fold change versus the averages of expression intensities (MA plot). The red dots indicate the genes expressed higher in blood-fed PRMs while the blue dots show those expressed higher in starved PRMs, representing a total of 2,154 and 4,175, respectively. The false discovery rate cut-off value was set to 0.01.

Table I-4. Top 10 GO categories with respect to "Cellular component".

	Enrichment FDR	No. of GO terms associated with each category	Total no. of GO terms classified into each category	Functional category
Blood-fed mites				
1	7.16E-95	572	4,051	Intracellular organelle
2	7.66E-95	574	4,082	Organelle
3	8.17E-93	533	3,645	Membrane-bounded organelle
4	1.34E-91	521	3,534	Intracellular membrane-bounded organelle
5	6.61E-87	499	3,380	Cytoplasm
6	7.35E-70	375	2,361	Cytoplasmic part
7	7.70E-59	336	2,166	Intracellular organelle part
8	1.62E-57	338	2,215	Organelle part
9	6.79E-54	321	2,110	Protein-containing complex
10	1.17E-37	276	1,989	Nucleus
Starved mites				
1	1.67E-101	762	4,082	Organelle
2	1.67E-101	758	4,051	Intracellular organelle
3	1.04E-97	701	3,645	Membrane-bounded organelle
4	3.34E-91	674	3,534	Intracellular membrane-bounded organelle
5	7.22E-88	648	3,380	Cytoplasm
6	7.15E-63	466	2,361	Cytoplasmic part
7	9.11E-58	422	2,110	Protein-containing complex
8	1.91E-56	403	1,989	Nucleus
9	1.98E-43	396	2,166	Intracellular organelle part
10	1.31E-42	400	2,215	Organelle part

GO terms were listed in descending order of statistical significance (FDR value).

Table I-5. Top 10 GO categories with respect to "Molecular function".

	Enrichment FDR	No. of GO terms associated with each category	Total no. of GO terms classified into each category	Functional category
Blood-fed mites				
1	1.32E-28	302	2,506	Ion binding
2	2.20E-23	346	3,251	Heterocyclic compound binding
3	2.74E-23	346	3,262	Organic cyclic compound binding
4	8.41E-21	270	2,405	Protein binding
5	1.11E-19	247	2,168	Transferase activity
6	6.08E-16	166	1,342	Small molecule binding
7	6.08E-16	161	1,284	Metal ion binding
8	7.30E-16	163	1,312	Cation binding
9	2.56E-15	96	609	RNA binding
10	4.81E-15	153	1,228	Nucleotide binding
Starved mites				
1	5.07E-72	493	2,405	Protein binding
2	8.12E-45	444	2,506	Ion binding
3	6.43E-33	499	3,262	Organic cyclic compound binding
4	8.37E-33	497	3,251	Heterocyclic compound binding
5	1.25E-30	257	1,323	Anion binding
6	4.46E-30	258	1,342	Small molecule binding
7	1.87E-28	357	2,168	Transferase activity
8	3.10E-24	228	1,228	Nucleotide binding
9	3.10E-24	228	1,228	Nucleoside phosphate binding
10	1.41E-23	237	1,312	Cation binding

GO terms were listed in descending order of statistical significance (FDR value).

Table I-6. Top 30 GO categories with respect to "Biological process" (Blood-fed mites).

	Enrichment FDR	No. of GO terms associated with each category	Total no. of GO terms classified into each category	Functional category
1	1.20E-73	407	2,601	Cellular nitrogen compound metabolic process
2	1.07E-66	355	2,191	Heterocycle metabolic process
3	6.05E-66	357	2,229	Organic cyclic compound metabolic process
4	3.20E-65	352	2,193	Cellular aromatic compound metabolic process
5	6.31E-65	345	2,128	Nucleobase-containing compound metabolic process
6	3.91E-51	518	4,498	Macromolecule metabolic process
7	5.42E-42	403	3,330	Cellular macromolecule metabolic process
8	3.88E-41	270	1,826	Nucleic acid metabolic process
9	3.96E-39	261	1,776	Gene expression
10	6.27E-39	298	2,186	Biosynthetic process
11	3.23E-38	293	2,149	Organic substance biosynthetic process
12	2.95E-37	286	2,096	Cellular biosynthetic process
13	1.22E-35	404	3,554	Organonitrogen compound metabolic process
14	1.65E-32	220	1,495	RNA metabolic process
15	1.20E-28	156	929	Small molecule metabolic process
16	4.59E-27	220	1,629	Cellular component organization or biogenesis
17	4.72E-27	214	1,564	Cellular nitrogen compound biosynthetic process
18	2.65E-25	78	307	Nucleobase-containing small molecule metabolic process
19	1.97E-24	211	1,602	Macromolecule biosynthetic process
20	4.14E-24	208	1,578	Cellular macromolecule biosynthetic process
21	3.51E-22	97	498	RNA processing
22	3.63E-22	257	2,210	Cellular protein metabolic process
23	1.14E-21	76	332	NcRNA metabolic process
24	2.61E-21	67	268	Nucleoside phosphate metabolic process
25	2.70E-21	165	1,185	Heterocycle biosynthetic process
26	2.70E-21	205	1,629	Macromolecule modification
27	2.70E-21	167	1,206	Organic cyclic compound biosynthetic process
28	1.77E-20	86	430	Organophosphate metabolic process
29	1.92E-20	65	263	Nucleotide metabolic process
30	2.48E-20	37	87	Nucleoside triphosphate metabolic process

GO terms were listed in descending order of statistical significance (FDR value).

Table I-7. Top 30 GO categories with respect to "Biological process" (Starved mites).

	Enrichment FDR	No. of GO terms associated with each category	Total no. of GO terms classified into each category	Functional category
1	3.45E-88	608	3,035	**Biological regulation**
2	6.87E-74	533	2,681	**Regulation of biological process**
3	1.68E-65	496	2,534	**Regulation of cellular process**
4	3.10E-65	594	3,330	Cellular macromolecule metabolic process
5	1.07E-63	500	2,601	Cellular nitrogen compound metabolic process
6	1.07E-63	725	4,498	Macromolecule metabolic process
7	1.66E-61	442	2,191	Heterocycle metabolic process
8	4.31E-61	446	2,229	Organic cyclic compound metabolic process
9	5.09E-61	441	2,193	Cellular aromatic compound metabolic process
10	6.25E-60	430	2,128	Nucleobase-containing compound metabolic process
11	2.72E-53	423	2,186	Biosynthetic process
12	2.38E-52	416	2,149	Organic substance biosynthetic process
13	5.29E-51	406	2,096	Cellular biosynthetic process
14	7.53E-49	312	1,434	**Regulation of metabolic process**
15	3.58E-48	317	1,480	Cellular component organization
16	4.07E-47	355	1,776	Gene expression
17	7.64E-45	297	1,387	**Regulation of macromolecule metabolic process**
18	1.06E-44	321	1,564	Cellular nitrogen compound biosynthetic process
19	1.06E-44	356	1,826	Nucleic acid metabolic process
20	2.85E-44	270	1,206	Organic cyclic compound biosynthetic process
21	5.15E-44	310	1,495	RNA metabolic process
22	5.94E-44	328	1,629	Cellular component organization or biogenesis
23	1.22E-43	264	1,174	Aromatic compound biosynthetic process
24	2.18E-43	562	3,554	Organonitrogen compound metabolic process
25	2.22E-43	265	1,185	Heterocycle biosynthetic process
26	6.23E-43	258	1,143	Nucleobase-containing compound biosynthetic process
27	1.38E-42	245	1,059	Organelle organization
28	7.00E-41	279	1,321	**Regulation of cellular metabolic process**
29	1.17E-40	231	990	**Regulation of gene expression**
30	3.15E-39	274	1,311	**Regulation of primary metabolic process**

GO terms were listed in descending order of statistical significance (FDR value).
GO terms associated with the regulation of biological activities were shown in bold.

Table I-8. Top 30 functional categories of the predicted KEGG pathways (Blood-fed mites).

	Enrichment FDR	No. of GO terms associated with each category	Total no. of GO terms classified into each category	Functional category
1	5.82E-37	181	1,022	Metabolic pathways
2	9.25E-10	25	83	Oxidative phosphorylation
3	2.63E-05	22	109	Carbon metabolism
4	0.000106	23	129	Protein processing in endoplasmic reticulum
5	0.000178	6	10	Thiamine metabolism
6	0.000231	15	68	Ribosome biogenesis in eukaryotes
7	0.000294	12	47	RNA degradation
8	0.000726	10	37	Nucleotide excision repair
9	0.000954	11	46	Aminoacyl-tRNA biosynthesis
10	0.001248	9	33	Basal transcription factors
11	0.001405	16	92	Purine metabolism
12	0.0017	9	35	Fanconi anemia pathway
13	0.001835	11	52	Pyrimidine metabolism
14	0.001835	8	29	RNA polymerase
15	0.001835	8	29	Homologous recombination
16	0.002168	8	30	DNA replication
17	0.003236	7	25	Galactose metabolism
18	0.003236	7	25	Base excision repair
19	0.005515	17	119	RNA transport
20	0.006342	6	21	Terpenoid backbone biosynthesis
21	0.007869	6	22	Starch and sucrose metabolism
22	0.007951	10	55	Biosynthesis of amino acids
23	0.008149	5	16	Fructose and mannose metabolism
24	0.008149	7	30	Fatty acid degradation
25	0.008149	10	56	mRNA surveillance pathway
26	0.008149	6	23	Notch signaling pathway
27	0.009113	13	87	Glutathione metabolism
28	0.009113	11	67	Amino sugar and nucleotide sugar metabolism
29	0.009584	15	109	Spliceosome
30	0.009584	13	88	Ubiquitin mediated proteolysis

GO terms were listed in descending order of statistical significance (FDR value).

Table I-9. Top 30 functional categories of the predicted KEGG pathways (Starved mites).

	Enrichment FDR	No. of GO terms associated with each category	Total no. of GO terms classified into each category	Functional category
1	1.51E-29	213	1,022	Metabolic pathways
2	1.89E-09	39	134	Endocytosis
3	2.35E-07	28	92	Purine metabolism
4	2.31E-06	21	63	FoxO signaling pathway
5	1.58E-05	29	119	RNA transport
6	1.71E-05	11	22	Starch and sucrose metabolism
7	1.74E-05	27	109	Carbon metabolism
8	1.74E-05	18	56	mRNA surveillance pathway
9	2.00E-05	11	23	Notch signaling pathway
10	0.000116	20	76	Wnt signaling pathway
11	0.000168	12	33	Basal transcription factors
12	0.000168	21	85	Autophagy
13	0.000286	10	25	Galactose metabolism
14	0.000642	6	10	Thiamine metabolism
15	0.000912	24	117	Peroxisome
16	0.001482	9	25	Base excision repair
17	0.001778	10	31	Propanoate metabolism
18	0.001973	12	43	Lysine degradation
19	0.002006	18	82	MTOR signaling pathway
20	0.002881	6	13	One carbon pool by folate
21	0.003313	12	46	Aminoacyl-tRNA biosynthesis
22	0.003562	10	35	Citrate cycle (TCA cycle)
23	0.003562	12	47	Valine, leucine and isoleucine degradation
24	0.003562	12	47	RNA degradation
25	0.003562	21	109	Spliceosome
26	0.004292	13	55	Biosynthesis of amino acids
27	0.004292	10	36	AGE-RAGE signaling pathway in diabetic complications
28	0.004952	7	20	Autophagy
29	0.004952	10	37	TGF-beta signaling pathway
30	0.005481	11	44	Alanine, aspartate and glutamate metabolism

GO terms were listed in descending order of statistical significance (FDR value).

Table I-10. Motifs/domains predicted by IPR IDs in the top 15 contigs that indicated high expression intensities and were associated with "Metabolic pathways" in tables I-8 and 9.

	IPR ID	FPKM	Predicted motifs/domains
Blood-fed mites			
1	IPR001564	1,591.02	Nucleoside diphosphate kinase
2	IPR019344	1,121.97	Mitochondrial F1-F0 ATP synthase subunit F, predicted
3	IPR006808	1,051.95	ATP synthase, F0 complex, subunit G, mitochondrial
4	IPR024571	719.13	ERAP1-like C-terminal domain
5	IPR000194	574.94	ATPase, F1/V1/A1 complex, alpha/beta subunit, nucleotide-binding domain
6	IPR008386	560.47	ATP synthase, F0 complex, subunit E, mitochondrial
7	IPR008387	559.59	ATP synthase-coupling factor 6, mitochondrial
8	IPR008181	559.27	Deoxyuridine triphosphate nucleotidohydrolase
9	IPR006721	492.98	ATP synthase, F1 complex, epsilon subunit, mitochondrial
10	IPR004205	427.30	Cytochrome b-c1 complex subunit 8
11	IPR000793	324.92	ATP synthase, alpha subunit, C-terminal
12	IPR002347	305.25	Short-chain dehydrogenase/reductase SDR
13	IPR006424	295.71	Glyceraldehyde-3-phosphate dehydrogenase, type I
14	IPR029055	258.72	Nucleophile aminohydrolases, N-terminal
15	IPR000711	255.54	ATPase, OSCP/delta subunit
Starved mites			
1	IPR008209	558.95	Phosphoenolpyruvate carboxykinase, GTP-utilizing
2	IPR004046	522.48	Glutathione S-transferase, C-terminal
3	IPR006089	280.24	Acyl-CoA dehydrogenase, conserved site
4	IPR000644	251.53	CBS domain
5	IPR024571	223.29	ERAP1-like C-terminal domain
6	IPR002347	182.58	Short-chain dehydrogenase/reductase SDR
7	IPR000183	145.65	Ornithine/DAP/Arg decarboxylase
8	IPR004839	137.06	Aminotransferase, class I/classII
9	IPR000836	113.69	Phosphoribosyltransferase domain
10	IPR033469	107.19	CYTH-like domain superfamily
11	IPR001805	101.38	Adenosine kinase
12	IPR003033	98.18	SCP2 sterol-binding domain
13	IPR000573	95.52	Aconitase A/isopropylmalate dehydratase small subunit, swivel domain
14	IPR001085	90.85	Serine hydroxymethyltransferase
15	IPR015590	90.71	Aldehyde dehydrogenase domain

Table I-11. The expression profiles of the representative genes associated with energy synthesis, gluconeogenesis, and the β-oxidation of fatty acid.

FPKM value		Contig No.	logFC*	$-\log_{10}$[FDR]	BLAST top hit (Accession No.)
Blood-fed	Starved				
1,591.02	458.05	DN45047_c0_g1_i1	2.15	2.24	nucleoside diphosphate kinase B-like (NDKB-like) [*Varroa destructor*] (XP_022653377.1)
1,051.95	202.66	DN42035_c4_g2_i2	2.77	3.38	ATP synthase subunit g, mitochondrial-like (ATPSG-like) [*Varroa destructor*] (XP_022653165.1)
559.59	175.48	DN43086_c0_g2_i1	2.05	2.08	ATP synthase-coupling factor 6, mitochondrial-like (ATPSCF6-like) [*Varroa destructor*] (XP_022643748.1)
427.30	107.62	DN40018_c2_g1_i1	2.34	2.57	ubiquinol-cytochrome C reductase complex (UCCR) [*Ixodes scapularis*] (AAY66915.1)
295.71	11.05	DN42158_c2_g1_i1	5.08	8.79	glyceraldehyde-3-phosphate dehydrogenase-like (GAPDH-like) [*Varroa destructor*] (XP_022655133.1)
80.18	558.95	DN41863_c2_g3_i3	-2.47	2.81	phosphoenolpyruvate carboxykinase, cytosolic [GTP]-like (PPCK-like) [*Varroa destructor*] (XP_022663562.1)
119.74	280.24	DN39874_c1_g1_i1	-0.89	0.62	isobutyryl-CoA dehydrogenase (IBCD) [*Tropilaelaps mercedesae*] (OQR74842.1)
14.38	251.53	DN44967_c0_g1_i3	-3.79	5.61	inosine-5'-monophosphate dehydrogenase 1-like isoform X1 (I5MD1-like) [*Varroa destructor*] (XP_022660176.1)

*log2[fold changes] of FPKM values (blood-fed/starved).

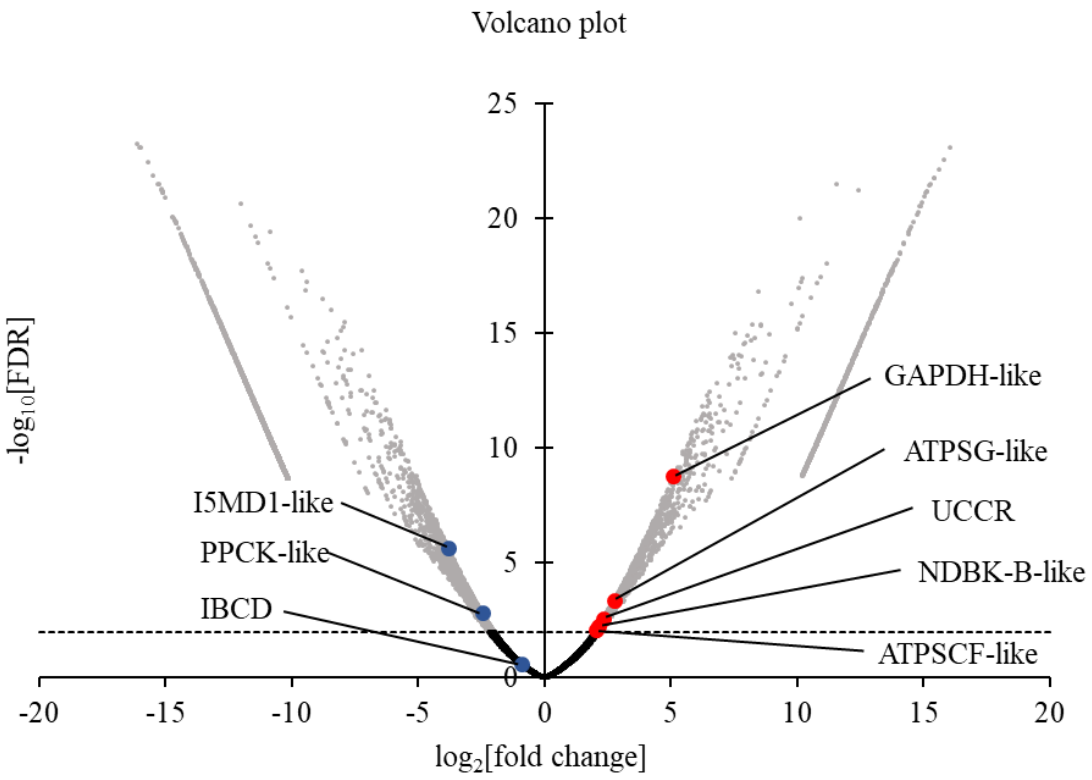

Figure I-2. Dynamics of gene expression patterns in response to blood feeding.
The relationship between the statistical significances (false discovery rate, FDR) and the fold change was visualized. The gray dots indicate the genes with significant differences in gene expression. The red dots indicate the representative genes involved in energy synthesis, whereas the blue dots reflect the representative genes associated with gluconeogenesis and β-oxidation. The FDR cut-off value was set to 0.01. NDKB: nucleoside diphosphate kinase B, ATPSG: ATP synthase subunit g, ATPSCF: ATP synthase-coupling factor, UCCR: ubiquinol-cytochrome C reductase, GAPDH: glyceraldehyde-3-phosphate dehydrogenase, PPCK: phosphoenolpyruvate carboxykinase, IBCD: isobutyryl-CoA dehydrogenase, I5MD1: inosine-5'-monophosphate dehydrogenase 1.

DISCUSSION

PRMs are obligatory blood-feeding ectoparasites [Chauve, 1998], evoking the idea that blood feeding would alter their physiology. Here, the comparative analysis of PRMs' transcriptome was performed between different feeding states to shed light on the dynamics in their gene expression after blood feeding.

The GO enrichment analyses revealed that the genes related to metal ion binding were more frequently expressed in blood-fed PRMs that are consistent with the results of a previous study on the transcriptome of the midguts of a tick *H. flava* [Xu *et al*., 2016], suggesting either that the transport, uptake, or storage of host blood-derived metal ions including ferrous or copper ion were promoted, or that PRMs responded to pro-oxidant agents, such as iron, which are released during blood digestion to protect themselves from oxidative tissue damage [Mohr and Killilea, 2018]. Thus, interruption of metal ion biding molecules could induce the breakdown of PRM homeostasis, leading to these molecules as targets for novel control strategies against PRMs, as exemplified by the potential of ferritin 2, the iron-storage protein, as a vaccine antigen in ticks [Hajdusek *et al*., 2010].

With respect to BP categories, a prominent difference in their frequencies was observed between blood-fed and starved PRMs. In starved PRMs, the terms associated with the regulation of various biological activities were comprised in the majority of the annotated terms, whilst these were not assigned in blood-fed PRMs. Although PRMs are dependent on nutrients exclusively from host-derived blood meal for the development and reproduction [Pritchard *et al*., 2015], they can survive for a long period of time without blood feeding [Nordenfors *et al*., 1999]. The present study showed that biological processes including metabolism are abrogated in starved PRMs in order to reduce the energy consumption to maintain their lives in the absence of sufficient nutrients. These differences in the metabolisms were further supported by the metabolic pathway enrichment analysis in this study. Energy synthetic processes including ATP synthesis were highly active in blood-fed PRMs. In contrast, starved PRMs predominantly expressed genes associated with β-oxidation of fatty acids, autophagy, and gluconeogenesis, and these responses were considered to be adaptive changes in metabolism during starvation [Cahill Jr, 2006; Müller *et al*., 2015].

Taken together, physiological conditions of PRMs, especially energy synthetic and metabolic processes, were drastically divergent among different feeding states. In this study, however, the probability that environmental contaminants on the PRMs' surface may have biased the results could not be excluded, albeit the expression intensities of genes derived from such contaminants were not significant. Besides, the data in the

present study may contain the transcripts from microbial symbionts. These symbionts play crucial roles in the physiology of arthropods, and their population would also be altered in response to blood feeding [Hunter *et al*., 2003; Zchori-Fein and Perlman, 2004]. Of note, in the present study, RNA-Seq was performed using Poly (A)-RNA; the transcripts derived from prokaryotes such as bacteria were mostly removed from the obtained data. Therefore, symbionts-derived transcripts would not significantly affect the data, although they cannot be excluded completely. Additionally, single samples from blood-fed and starved PRMs were examined. To verify the data, analyses using multiple samples would be desirable, or further experiments including the quantification of the expression levels of the PRM transcripts by quantitative reverse transcription polymerase chain reaction (qRT-PCR) [Ariizumi *et al*., 2021] are required.

SUMMARY

PRMs are one of the most harmful blood-feeding ectoparasites of avian species. Since blood meal is the only source of nutrients required for the development and reproduction of PRMs, the dynamics of their physiological status elicited by blood feeding are crucial information for better understanding of their biological characteristics. In this chapter, the transcriptomes of PRMs in blood-fed and starved states were comprehensively analyzed and compared. The expression of genes associated with energy synthesis and metabolic processes was drastically higher in a blood-fed state. In contrast, transcripts involved in the regulation of biological processes, fatty acid oxidation, autophagy, and gluconeogenesis were markedly expressed in a starved state. These data provide valuable information for investigating the targets of alternative PRM control methods, as well as for exploring their novel biological pathways related to blood digestion, molting, and reproduction.

CHAPTER II

Suppressive modulation of host immunological states caused by *Dermanyssus gallinae* infestation

INTRODUCTION

Infestation by hematophagous ectoparasites including tick species induces various host physiological responses. At the sites of infestation, hemostasis including blood coagulation is initially activated in response to mechanical injury caused by stings [Kotál *et al*., 2015]. Following this acute reaction, pro-inflammatory chemokines and cytokines, such as IL-8, IL-1β, and TNF-α, are produced by keratinocytes, endothelial cells, and immune cells which have a contact to parasites' saliva, and facilitate the recruitment of inflammatory cells [Wikel, 2013; Šimo *et al*., 2017]. Meanwhile, bugs secrete various effector molecules into their saliva, including immunosuppressants, to maintain an environment suitable for blood feeding; for instance, in tick species, SGE of *I. ricinus* impairs superoxide and NO production, phagocytic activities, and the production of Th1 cytokines including interferon (IFN)-γ and TNF-α by monocytes [Kuthejlová *et al*., 2001; Kýcková and Kopecký, 2006]. In addition, functions of lymphocytes as well as innate immune cells are also modulated by tick-derived molecules, as manifested by their reduced proliferation by SGE of *R. appendiculatus* and *Dermacentor andersoni,* and saliva of *I. ricinus* [Wikel, 1982; Ramachandra and Wikel, 1992; Rolníková *et al*., 2003]. Moreover, SGE from a mosquito *Aedes aegypti* attenuates the production of Th1 cytokines and IFNs [Cross *et al*., 1994; Schneider *et al*., 2004]. Notably, several studies have indicated that these immunosuppression by salivary factors are closely related to arbovirus transmission [Schneider *et al*., 2004; Schneider and Higgs, 2008; Guerrero *et al*., 2020].

In PRMs, previous studies demonstrated that chronic exposure to PRMs alters protein composition in the plasmas of infested chickens [Kowalski and Sokół, 2009], and that PRM-infestation reduces the levels of antibody productions in chickens immunized with vaccines against avian pathogens [Kaoud and El-Dahshan, 2010], suggesting that PRM-infestation contributes to the impairment of host humoral immunity. Besides, there was a non-significant negative correlation between the percentage of helper T cells and B cells in chickens raised at PRM-eroded cages and the number of PRMs, whilst the percentage of cytotoxic T cells was positively correlated with the number of PRMs [Koziatek-Sadłowska and Sokół, 2020]. These findings suggest that PRMs could modulate host immunity during blood feeding. However, details of immune responses, such as cytokine profiles, in chickens infested with PRM remain unclear.

In Chapter II, to investigate the immunological states of PRM-infested chickens, the expression of chicken-derived transcripts in blood-fed PRMs was initially analyzed using the dataset of RNA-Seq obtained in Chapter I. The RNA-seq data, obtained from blood-

fed PRMs in Chapter I, contained chicken-derived transcripts that were originated from chicken blood ingested by PRMs, and its profiles may reflect some of the responses in peripheral blood of PRM-infested chickens. In addition, the expression of representative cytokines and other molecules related to immune responses were compared between PRM-infested and non-infested chickens. Finally, to assess the direct effect of PRM-derived molecules on functional phenotypes of chicken immune cells, chicken peripheral blood cells or a macrophage-like cell line were stimulated with PRM-derived soluble extracts and gene expressions of cytokines and other immunomodulatory molecules were analyzed.

MATERIALS AND METHODS

RNA-Seq and data analysis

The data obtained from RNA-Seq analysis performed in Chapter I were used to analyze the expression intensities of chicken-derived genes in blood-fed PRMs. The adaptor sequences and the reads with low QVs were trimmed from raw reads as described in Chapter I. Trimmed reads were mapped to the genome sequence of the chicken (*Gallus gallus*, NCBI: txid9031) using TopHat software v2.0.14 (*http://tophat.cbcb.umd.edu/*), and the expected counts and FPKM of the transcripts were calculated using Cufflinks package v2.2.1 (*http://cufflinks.cbcb.umd.edu/*). All of the procedures were conducted at Hokkaido System Science Co., Ltd.

Plasma and peripheral blood mononuclear cells (PBMCs) of chickens

Heparinized fresh blood samples were collected from non-infested healthy chickens raised at the Field Science Center for Northern Biosphere, Hokkaido University (non-infested experimental (NIE) chickens) and a commercial egg-laying farm that is free from PRMs in Japan (non-infested commercial (NIC) chickens), or from an egg-laying farm eroded by PRMs in Japan ("Infested"). Additionally, blood samples were collected from non-infested chicks raised at a PRM-free coop (before exposure, b.e.) and from infested chickens that were transferred from a PRM-free coop to a PRM-eroded coop (after exposure, a.e.). Blood samples of b.e. and a.e. samples were collected from the same flock. Plasma was isolated from the blood by the centrifugation at 2,000 × *g* for 10 min, and PBMCs were isolated by density gradient centrifugation on Percoll solution (GE Healthcare, Chicago, IL, USA). Plasma and PBMCs were isolated within 48 h of blood sample collection.

RNA isolation and cDNA synthesis

Total RNA of PBMCs was isolated using TRI reagent (Molecular Research Center, Inc., Cincinnati, OH, USA) according to the manufacturer's instructions. Remaining DNA was removed from the isolated RNA with DNase I treatment (amplification grade; Thermo Fisher Scientific, Waltham, MA, USA) for 10 min at 65°C. cDNA synthesis from isolated RNA was performed with PrimeScript reverse transcriptase (TaKaRa Bio Inc., Shiga, Japan) using 200 pmol of oligo (dT) 18 primer (Hokkaido System Science Co., Ltd.).

Preparation of soluble mite extract (SME)

Approximately 500 mg of starved PRMs prepared as described in Chapter I were suspended in 5 mL of PBS supplemented with 200 U/mL of penicillin and 200 μg/mL of streptomycin (Thermo Fisher Scientific) and incubated at 37°C for 1 h. After washing twice with 10 mL of cold PBS, PRMs were suspended in 1 mL of cold PBS and homogenized by sonicating four times for 15 s on ice using an ultrasonic homogenizer UX-050 (Mitsui Electric, Chiba, Japan). The homogenate was then centrifuged at 20,000 × *g* for 20 min at 4 °C. The supernatant was collected as SME and filtrated with a 0.22 μm filter (Nihon Pall Ltd., Tokyo, Japan). SME was stored at −80°C until use.

Cell culture and stimulation

Chicken PBMCs isolated from NIE chickens as described above and the chicken HD-11 macrophage-like cell line transformed by a myc-containing MC29 retrovirus [Beug *et al*., 1979] were suspended in RPMI1640 medium (Sigma-Aldrich, St. Louis, MO, USA) supplemented with 10% heat-inactivated fetal bovine serum (Cell Culture Technologies LLC, Gravesano, Switzerland). PBMCs or HD-11 cells (2.0×10^6 cells) were cultured at 39°C and 5% CO_2 for 24 h in the presence of 1% of SME or sterilized PBS. The cells were collected and suspended with TRI reagent (Molecular Research Center, Inc.). RNA isolation and cDNA synthesis from the cells were conducted as described above.

qRT-PCR

Specific primer sets for the chicken cytokines, chemokines, and *β-actin* genes were designed and used (Table II-1). qRT-PCR was conducted using cDNA samples from chicken PBMCs or HD-11 cells using LightCycler480 System II (Roche Diagnostics, Mannheim, Germany) with TB Green Premix DimerEraser (TaKaRa Bio Inc.) according to the manufacturer's protocols. The cycling conditions consisted of initial denaturation at 95°C for 30 s, followed by 45 cycles of 95°C for 5 s, each annealing temperature listed in Table II-1 for 30 s, and 72°C for 30 s. To analyze primer pairs for their specificities, a melting curve analysis was subsequently conducted from 65°C to 95°C at a rate of 0.1°C/s. To construct the standard curves for quantification, serial dilutions of T-vector pMD20 (TaKaRa Bio Inc.) or pGEM-T Easy Vector (Promega Corporation, Madison, WO, USA) inserted with each amplicon were used. The mRNA expression of each target was presented as the ratio obtained by dividing the concentration of the target mRNA by that of *β-actin* mRNA.

Enzyme-linked immunosorbent assay (ELISA)

The concentrations of IL-1β, IL-10, and transforming growth factor (TGF)-β1 in the

plasma samples were analyzed by ELISA using the Chicken Interleukin 1β ELISA kit (CUSABIO TECHNOLOGY LLC, Wuhan, China), chicken IL-10 Do-It-Yourself ELISA (Kingfisher Biotech Inc., Saint Paul, MN, USA), and Chicken Transforming Growth factor β1 ELISA kit (CUSABIO TECHNOLOGY LLC), respectively, according to the manufacturer's instructions.

Statistics

Differences were analyzed using the Mann-Whitney *U* test for gene expression and ELISA analyses using samples from infested and non-infested chickens. For multiple comparisons, the Steel-Dwass test was performed. Wilcoxon signed rank test or Student's *t*-test was performed to analyze the difference in qRT-PCR analyses using PBMCs and HD-11 cells, respectively. For all tests, $p < 0.05$ was considered statistically significant.

Ethics statement

1. Genetic recombination experiments

All genetic recombination experiments were performed in accordance with the Manual for Safety Management on Genetic Recombination Experiments in Hokkaido University (Approval number: 2019-024).

2. Blood sample collection

The chicken blood samples used in this study were obtained with informed consent from the farm owners. Sample collection was performed in accordance with the procedures and guidelines of the Ethics Committee of the Faculty of Veterinary Medicine, Hokkaido University.

Table II-1. Primers used in real time quantitative RT-PCR.

Target gene	Primer sequences (5' - 3') F: forward; R: reverse	Annealing temperature (°C)	Accession no.
CCL4	F: TCTCGCTCTTCTCATCGCATC R: GAAGATGATGGCAGGCTTTGAG	60	NM_204720
CCR5	F: GTGGTCAACTGCAAAAAGCA R: GCCCGTTCAACTGTGTCG	58	NM_001271141
IL-1β	F: CGCTCACAGTCCTTCGACATC R: CCGCTCATCACACACGACATGT	60	NM_204628
IL-2	F: TTGGAAAATATCAAGAACAAGATTCATC R: TCCCAGGTAACACTGCAGAGTTT	60	AJ224516
IL-6	F: CTGTTCGCCTTTCAGACCTACC R: CATGGTGATTTTCTCTATCCAGTCC	60	AJ309540
IL-8	F: CTGCGGTGCCAGTGCATTAG R: AGCACACCTCTCTTCCATCC	58	NM_205498
IL-12	F: TGTCTCACCTGCTATTTGCCTTAC R: CTGGTGTCTCATCGTTCCACTC	60	AY262752
IFN-α	F: CCAGCACCTCGAGCAAT R: GGCGCTGTAATCGTTGTCT	58	AB021153
IFN-γ	F: CTCCCGATGAACGACTTGAG R: CTGAGACTGGCTCCTTTTCC	58	NM_205149
TNF-α	F: CGCTCAGAACGACGTCAA R: GTCGTCCCACACCAACGAG	60	MF801626
IL-10	F: CATGCTGCTGGGCCTGAA R: CGTCTCCTTGATCTGCTTGATG	60	NM_001004414
TGF-β1	F: TGAGTATTGGGCCAAAGAGCTG R: ACACGAAGAAGATGCTGTGG	58	JQ423909
TGF-β4	F: AGGATCTGCAGTGGAAGTGGAT R: CCCCGGGTTGTGTTGGT	60	M31160
CD25	F: CGAAGCAAGCAAACAATTCA R: ATGGTGCCAGTGGTAGGAAG	58	NM_204596
CTLA-4	F: CCACTGCCGAAGTAATGGAA R: TTGTCGCCTGTCTGTTTGAG	59	NM_001040091
PD-1	F: GGACTACGGTGTGCTGGAGTT R: TCTTTCCTCGCTCTGGTGTG	60	XM422723
PD-L1	F: TTCAGGGACGGATAAAGCTG R: CGTCTCTGAGCTTCACGTTG	58	XM424811
IRF4	F: AGCAGCCTGGAACAAGTCAT R: AGAGGCCCATCCCAGTAGAT	58	NM_204299
IRF5	F: GAGGGAGAGGAGGATCCAAG R: GACAGCTCCCCTGAGAACAG	59	NM_001031587
Arg2	F: GTTGAGGGATGTGGATCCTG R: GCATCGATGTCAAAGCTCAA	59	NM_001199704
β-actin	F: CCAACTGGGATGATATGGAGAAG R: AGGCATACAGGGACAGCACA	60	NM_205518

RESULTS

A pro-inflammatory chemokine C-C chemokine ligand (CCL) 4 was highly expressed in the blood of chickens infested with PRMs

To investigate the immunological states of PRM-infested chickens, the expression intensities of chicken-derived transcripts originated from chicken blood ingested by PRMs were analyzed based on their FPKM values. With respect to the molecules related to the immune reactions, high expression of *CCL4*, encoding C-C chemokine ligand 4, was observed (Table II-2). Although the transcripts of other cytokines and chemokines were also detected, their FPKM values were lower than the limit of quantification (FPKM = 0, Table II-3). To examine whether CCL4 expression was higher in PRM-infested chickens than non-infested chickens, expression levels of CCL4 mRNA and protein were assessed and compared in blood samples from PRM-infested chickens raised at a PRM-contaminated commercial egg-laying farm and NIE chickens maintained at a PRM-free experimental farm. In addition, considering that other extrinsic factors such as vaccination may affect immunological states, plasma from NIC chickens raised at a PRM-uncontaminated commercial laying hen's farm were also tested. The expressions of CCL4 mRNA and protein were higher in PBMCs of PRM-infested chickens compared to those of NIE and NIC chickens, while CCL4 was undetectable in the plasmas of NIE chickens (Figures II-1A and B). To further confirm that CCL4 expression was upregulated in response to PRM-infestation, the concentration of CCL4 in the plasmas collected from the same flock before and after exposure to PRMs (b.e. and a.e., respectively) was also examined. Although statistical analysis was not conducted because the concentration of CCL4 in 1 out of 8 b.e. samples was lower than the quantification limit, the concentration of CCL4 in a.e. samples was higher than that in b.e. samples (Figure II-1C). Collectively, PRM-infestation upregulates CCL4 expression in chickens.

Expression levels of inflammatory cytokines and interferons were not dramatically changed in response to PRM-infestation

Given that CCL4, a pro-inflammatory chemokine, was highly expressed in chickens from a PRM-contaminated farm, it was hypothesized that PRM-infestation induces inflammatory responses in chickens. Thus, the gene expression of pro-inflammatory cytokines, Th1 cytokines, and a type I IFN was examined in PBMCs of the infested and NIE chickens. While the expressions of *IL-1β* and *IL-8* mRNA were higher in the infested chickens than in NIE chickens, no difference in the mRNA expression of other pro-inflammatory cytokines, *IL-6*, *IL-12*, and *TNF-α*, was observed (Figure II-2A). In

addition, there was no significant difference in the expression levels of Th1 cytokines, *IL-2* and *IFN-γ*, and a type I IFN, *IFN-α* between the two groups (Figures II-2B and C). Notably, the infested chickens tended to exhibit lower expression of *C-C chemokine receptor 5* (*CCR5*), a receptor of CCL4, compared to NIE chickens (Figure II-2D), although no statistical significance was observed. These results suggest that PRM-infestation downregulates the expression of CCR5 to inhibit the recruitment of inflammatory cells driven by CCL4 in chickens.

Expression levels of immunosuppressive factors were higher in PRM-infested chickens

Next, the expression of anti-inflammatory cytokines, IL-10, TGF-β1, and TGF-β4, and other immunosuppressive molecules was examined in PBMCs of PRM-infested and NIE chickens. The mRNA expressions of *IL-10* and *TGF-β1* were significantly higher in the infested chickens than in NIE chickens, while there was no difference in the expression of *TGF-β4* between the infested and NIE chickens (Figure II-3A). In addition, the mRNA expression of CD25, a marker for regulatory T (Treg)-like cells in chickens [Shanmugasundaram and Selvaraj, 2011], and immune checkpoint molecules, cytotoxic T-lymphocyte antigen 4 (CTLA-4), programmed death (PD)-1 and PD-ligand 1 (PD-L1), was examined. The expression levels of *CD25*, *CTLA-4*, and *PD-1* were significantly higher in the infested chickens than in NIE chickens, whereas no difference in the expression of *PD-L1* was observed (Figure II-3B).

PRM-infestation potentially upregulated the expressions of anti-inflammatory cytokines

To evaluate protein levels of cytokines whose gene expression was upregulated in infested chickens, the concentrations of IL-1β, IL-10, and TGF-β1 in plasma samples collected from PRM-infested, NIE, and NIC chickens were compared. No difference in IL-1β concentration between the NIE and infested groups was observed, whereas IL-1β concentration in NIC chickens was significantly higher than that in NIE and PRM-infested chickens (Figure II-4). Although IL-10 was not detected in both NIE and NIC chickens, it was detectable in 8 out of 11 infested chickens (Figure II-4), indicating that the plasma concentration of IL-10 in infested chickens was high, consistent with the kinetics of mRNA expression observed in PBMCs from the infested chickens. The concentration of TGF-β1 in the plasma from the infested chickens tended to be higher than that in NIE chickens, although NIC chickens tended to have higher concentrations of TGF-β1 than NIE chickens (Figure II-4). However, statistical differences were not

determined among the three groups, as NIE and NIC chickens included samples that were below the quantitation limit. These data suggest that chickens chronically infested with PRMs are in an immunosuppressive state.

To further examine whether PRM-infestation modulates cytokine expressions, the concentrations of IL-1β, IL-10, and TGF-β1 in the plasmas collected from b.e. and a.e. chickens were examined. Statistical analyses were not applicable because samples that were below the quantitation limit were included in each analysis. IL-1β concentrations in a.e. chickens were lower than those in b.e. chickens, and 3 out of 8 a.e. samples showed values less than the quantitation limit (Figure II-5). In contrast, the concentrations of IL-10 and TGF-β1 were higher in a.e. chickens than in b.e. chickens, as expected. The numbers of samples exhibited values less than quantitation limit were 6 out of 8 b.e. samples and 1 out of 8 a.e. samples in the assay for IL-10, and 6 out of 7 b.e. samples and 1 out of 7 a.e. samples in the assay for TGF-β1 (Figure II-5). Taken together, following exposure to PRMs, the production of anti-inflammatory cytokines, IL-10 and TGF-β1, is increased, whereas the plasma concentration of IL-1β is reduced in blood of the infested chickens.

PRM-derived soluble extracts modulated the expression of cytokines in chicken PBMCs

To investigate the direct effects of PRM-derived molecules on chicken immune cells, PBMCs from NIE chickens were cultured in the presence of soluble extract derived from PRM (SME). Remarkably, the mRNA expression of *IFN-α*, a representative cytokine that contributes to the innate immune response, was significantly decreased in response to SME exposure (Figure II-6A). In contrast to the results observed in Figures II-2A and B, the mRNA expression of several Th1 cytokines was significantly upregulated in the presence of SME (*IL-2* and *IFN-γ*, Figure II-6A). Consistent with the results of infested and NIE samples, *IL-1β* expression was upregulated whereas *CCR5* expression was significantly downregulated in SME-stimulated cells, while there was no difference in *CCL4* expression (Figures II-6A and B). Regrading anti-inflammatory cytokines, the treatment with SME drastically upregulated the expression of *IL-10*, whereas the expression level of *TGF-β1* was not affected (Figure II-6C). As higher expressions of other immunosuppressive molecules, *CD25*, *CTLA-4*, and *PD-1*, in PBMCs from PRM-infested chickens were observed (Figure II-3B), the effect of SME on the expressions of these molecules was assessed. The mRNA expressions of *CD25* and *CTLA-4* were significantly downregulated by SME stimulation (Figure II-6D). On the other hand, the treatment with SME significantly upregulated the mRNA expressions of *PD-1* and *PD-*

L1 (Figure II-6E). Thus, PRM-derived SME activated certain subsets of chicken immune cells, perhaps mainly T cells, and upregulated the expression of pro-inflammatory and Th1 cytokines, whilst decreased the expression of *IFN-α* and upregulated the expression of *IL-10* and immune checkpoint molecules, *PD-1* and *PD-L1*. These data suggest that PRM-derived molecules have the potential to suppress host immune responses, although the inflammatory response could be activated by PRM-infestation.

PRM-derived SME polarized macrophages to the M2-like phenotype

In chickens raised at a commercial farm chronically infested with PRMs, the mRNA expressions of *CD25*, a marker for Treg-like cells in chickens, and immune checkpoint molecules, *CTLA-4* and *PD-1*, were upregulated (Figure II-3B), while treatment with SME did not stimulate the expression of *CD25* and *CTLA-4* in chicken PBMCs (Figure II-6C). These data show that the suppressor cells which are different from Treg-like cells, may be responsible for the expression of immunosuppressive cytokines during the initial phase of infestation. To examine this hypothesis, the gene expression of cytokines and related molecules were analyzed in HD-11, a chicken macrophage-like cell line, in the presence of SME. The mRNA expressions of *TNF-α*, *IFN-α*, *IFN-γ*, and *CCR5* were significantly downregulated by the treatment with SME, while *IL-1β* expression was upregulated (Figures II-7A and B). In contrast, SME exposure significantly increased the expressions of *IL-10* and *PD-L1* (Figure II-7C), whilst *TGF-β1* expression was downregulated. Finally, to characterize the functional phenotype of HD-11 cells stimulated with SME, the expression levels of interferon regulatory factor (IRF)-5, which regulates inflammatory M1 macrophage polarization [Krausgruber *et al*., 2011], and IRF4 and arginase 2 (Arg2), which are considered markers for M2 macrophages [Satoh *et al*., 2010; Hardbower *et al*., 2016] were examined. The mRNA expression of *IRF5* was significantly downregulated in SME-exposed HD-11 cells, whereas *IRF4* and *Arg2* were highly expressed in response to SME-stimulation (Figure II-7D). Taken together, PRM-derived molecules seemed to suppress inflammation in chickens by mediating the polarization of macrophages into the M2-like phenotype. The hypothetical mechanism of host immune modulation caused by PRM-infestation was summarized in Figure II-8.

Table II-2. Top 20 chicken-derived transcripts in PRMs.

Rank	Gene ID	Genes	FPKM value
1	*HBA1*	Haemoglobin subunit alpha 1	6,679.91
2	*HBBA*	Haemoglobin beta, subunit A	2,055.28
3	*ATP6*	ATP synthase F0 subunit 6	1,308.59
4	*COII*	Cytochrome c oxidase subunit 2	1,017.79
5	*GABARAP*	GABA type A receptor-associated protein	788.36
6	*FTH1*	Ferritin heavy chain 1	770.68
7	*CCL4*	C-C motif chemokine ligand 4	514.07
8	*ND1*	NADH dehydrogenase subunit 1	482.68
9	*COX3*	Cytochrome c oxidase subunit 3	441.17
10	*B2M*	Beta-2-microgloblin	372.99
11	*COX7B*	Cytochrome c oxidase subunit 7B	341.00
12	*HBM*	Haemoglobin subunit alpha-D	332.53
13	*LAMTOR5*	Late endosomal/lysosomal adaptor and MAPK and MTOR activator 5	331.58
14	*BF1*	MHC class I alpha chain 1	308.63
15	*ITM2B*	Integral membrane protein 2B	302.77
16	*COX1*	Cytochrome c oxidase subunit 1	294.16
17	*C26H6orf106*	Uncharacterized	284.68
18	*RHOA*	RhoA	270.93
19	*PEX16*	Peroxisomal membrane protein PEX16	250.57
20	*UBB*	Polyubiquitin-B	236.88

Spliceosomal and ribosomal RNA genes are not included.

Table II-3. Chicken-derived transcripts related to immune responses detected in blood-fed PRMs that are present within top 1,000.

Rank	Gene ID	Genes	FPKM value
103	*IRF5*	Interferon regulatory factor-5	0
145	*IL2RA*	Interleukin-2 receptor subunit alpha	0
254	*IL17REL*	Interleukin-17 receptor E-like	0
373	*IFNG*	Interferon gamma	0
374	*IL26*	Interleukin 26	0
375	*IL22*	Interleukin 22	0
555	*TNFRSF13C*	Tumor necrosis factor receptor superfamily member 13C	0
636	*IL2RB*	Interleukin-2 receptor subunit beta	0
758	*IL17RA*	Interleukin-17 receptor A	0
883	*CD9*	CD9	0
903	*CD86*	CD86	0
929	*CD4*	CD4	0
982	*TNFRSF1A*	Tumor necrosis factor receptor superfamily member 1A	0

Spliceosomal and ribosomal RNA genes are not included.

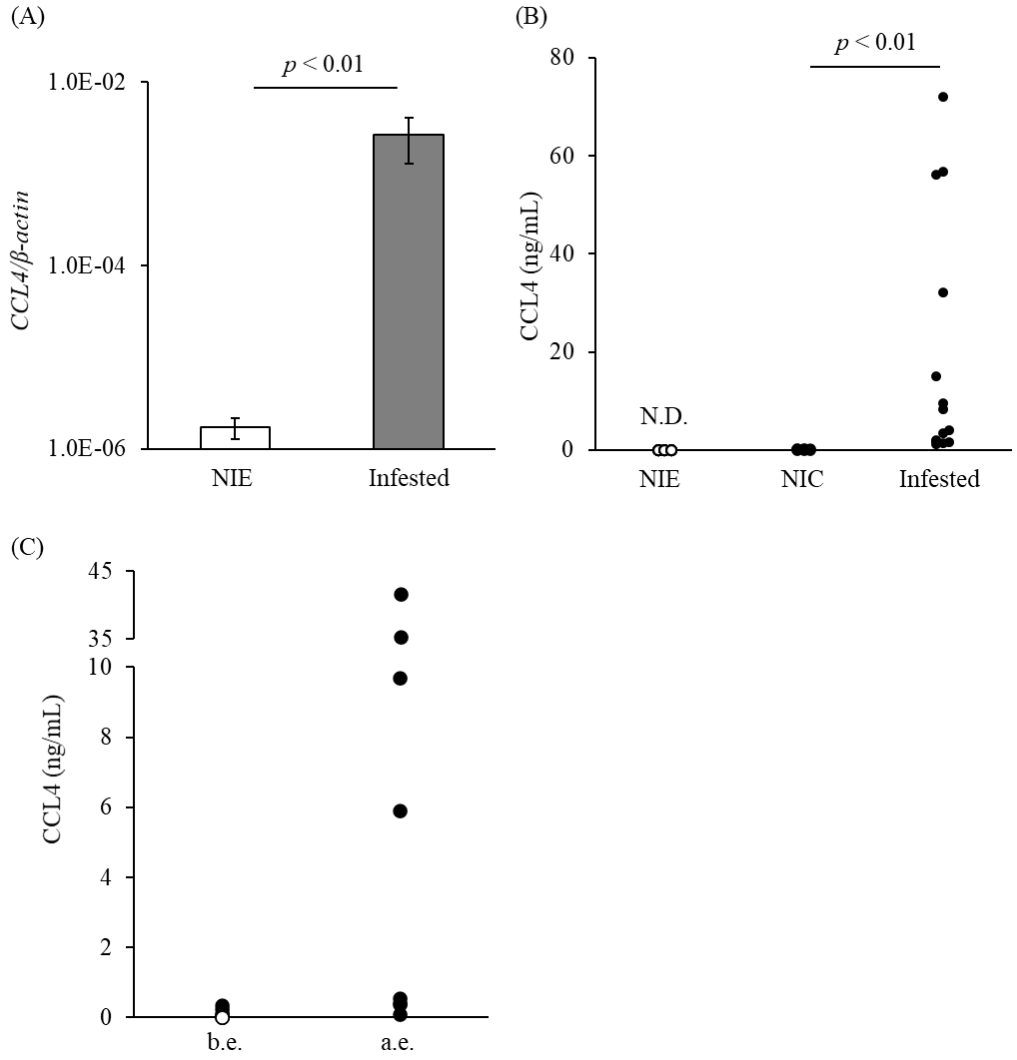

Figure II-1. Expression of CCL4 in PRM-non-infested and infested chickens.

(A) The mRNA of *CCL4* in PBMCs collected from non-infested experimental (NIE) chickens raised at an experimental farm without contamination with PRMs (n = 11) and infested chickens from a PRM-eroded commercial laying hen farm (n = 16) were examined by qRT-PCR. The extent of the expression of *CCL4* was calculated by dividing the copy number of *CCL4* by that of *β-actin*. Data are presented as mean ±standard error of the mean. (B and C) Plasma concentration of CCL4 in (B) NIE chickens (n = 13), non-infested commercial (NIC) chickens raised at a PRM-free laying hen farm (n = 8), and infested chickens (n = 14), or in (C) chickens before transfer to productive farm (before exposure to PRMs; b.e., n = 8) and infested chickens after transfer to productive farm (after exposure to PRMs; a.e., n = 8) were determined by ELISA. Statistical significance was determined using the Mann-Whitney U test.

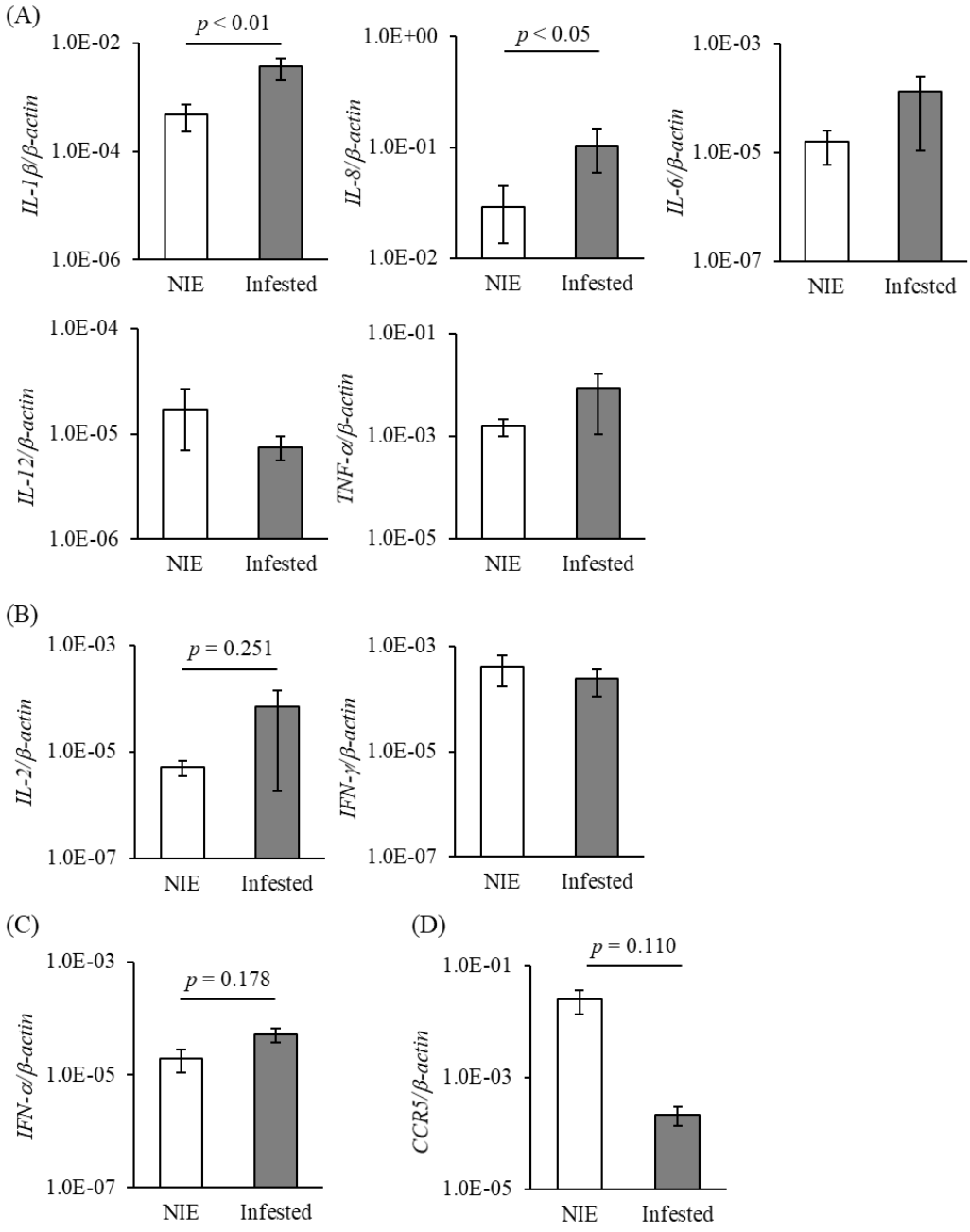

Figure II-2. Gene expressions of inflammatory cytokines, Th1 cytokines, a type I interferon, and a chemokine receptor in PRM-non-infested and infested chickens.
The mRNA of (A) inflammatory and (B) Th1 cytokines, (C) a type I interferon, and (D) *CCR5*, a receptor of CCL4 in PBMCs collected from non-infested experimental (NIE) chickens raised at a PRM-free experimental farm (n = 11) and infested chickens from a PRM-eroded commercial laying hen farm (n = 16) were examined by qRT-PCR. The extent of the expression of target genes was calculated by dividing the copy number of each target by that of *β-actin*. Data are presented as mean ±standard error of the mean. Statistical analysis was performed using the Mann-Whitney *U* test.

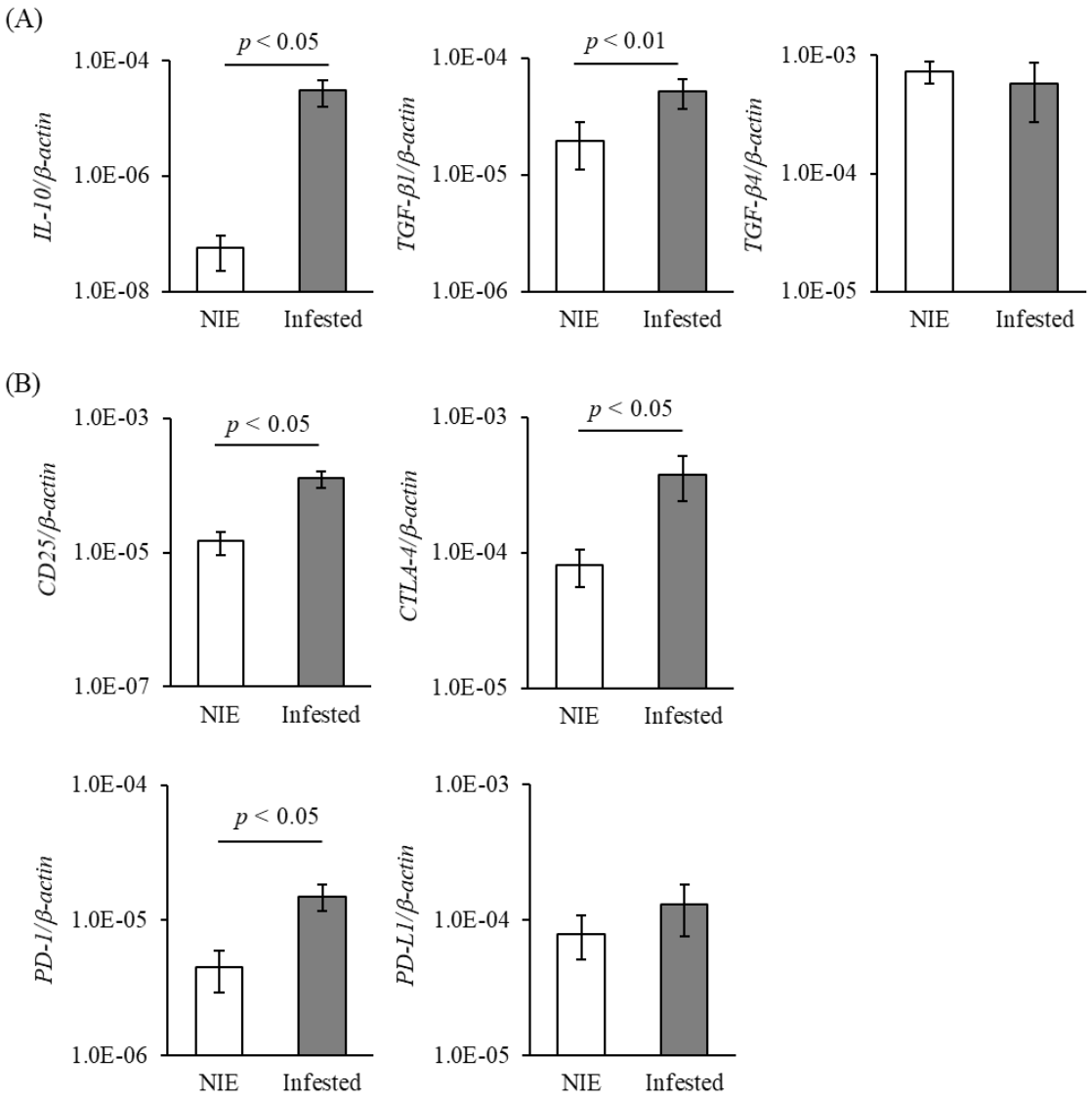

Figure II-3. Gene expressions of anti-inflammatory cytokines and the molecules related to the immunosuppression in PRM-non-infested and infested chickens.

The mRNA levels of (A) anti-inflammatory cytokines and (B) *CD25*, a marker for regulatory T-like cells in chickens, and immune checkpoint molecules in PBMCs collected from non-infested experimental (NIE) chickens raised at an experimental farm without contamination with PRMs (n = 11) and infested chickens from a PRM-eroded commercial laying hen's farm (n = 16) were examined by qRT-PCR. The extent of the expression of target genes was calculated by dividing the copy number of each target by that of *β-actin*. Data are presented as mean ± standard error of the mean. Statistical significance was determined using the Mann-Whitney U test.

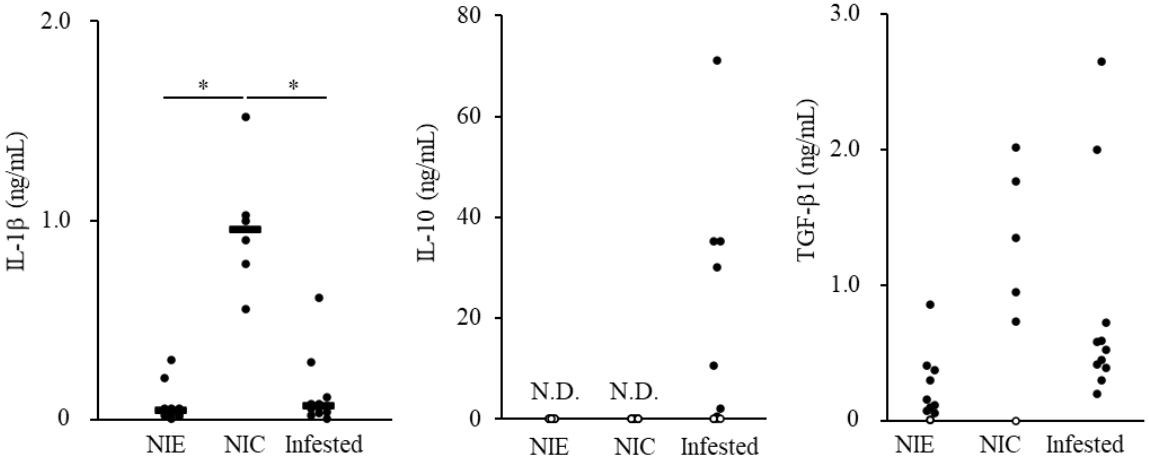

Figure II-4. Plasma concentrations of IL-1β, IL-10, and TGF-β1 in non-infested and infested chickens.

The concentrations of IL-1β, IL-10, and TGF-β1 in the plasma samples collected from non-infested chickens raised at a PRM-free experimental farm (NIE), non-infested commercial (NIC) chickens raised at a PRM-free laying hen's farm, and infested chickens from a PRM-eroded commercial laying hen farm were determined by ELISA. IL-1β, NIE: $n = 13$, NIC: $n = 6$, Infested: $n = 12$; TGF-β1, NIE: $n = 12$, NIC: $n = 6$, Infested: $n = 12$; IL-10, NIE: $n = 10$, NIC: $n = 6$, Infested: $n = 11$. Statistical differences were analyzed using the Steel-Dwass test. White circles indicate samples that were less than the quantitation limit. *$p < 0.05$. N.D.: not detected.

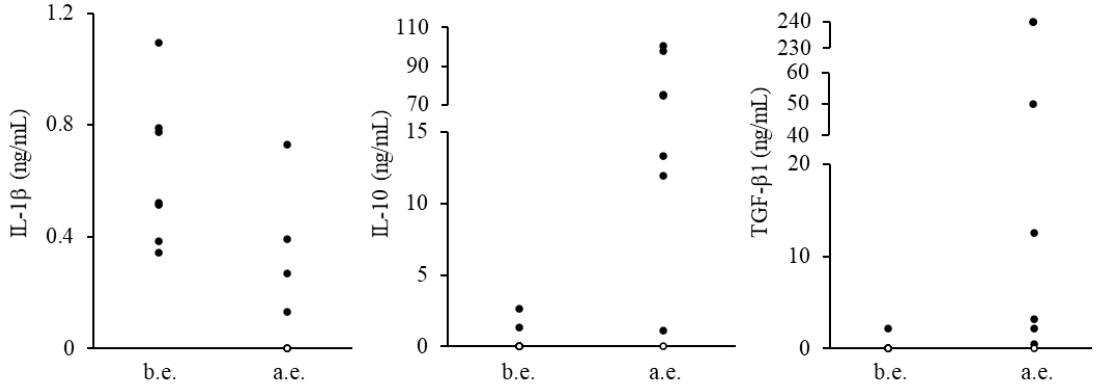

Figure II-5. Changes in plasma concentrations of cytokines after-exposure to PRMs. The concentrations of IL-1β, IL-10, and TGF-β1 in the plasma samples collected from non-infested chickens raised at a PRM-free coop (before exposure to PRMs; b.e.) and infested chickens that were transferred from a PRM-free coop to PRM-contaminated coop (after exposure to PRMs; a.e.) were determined by ELISA. IL-1β and TGF-β1, b.e.: n = 7, a.e.: n = 7; IL-10, b.e.: n = 8, a.e.: n = 8. White circles indicate samples that were less than the quantitation limit.

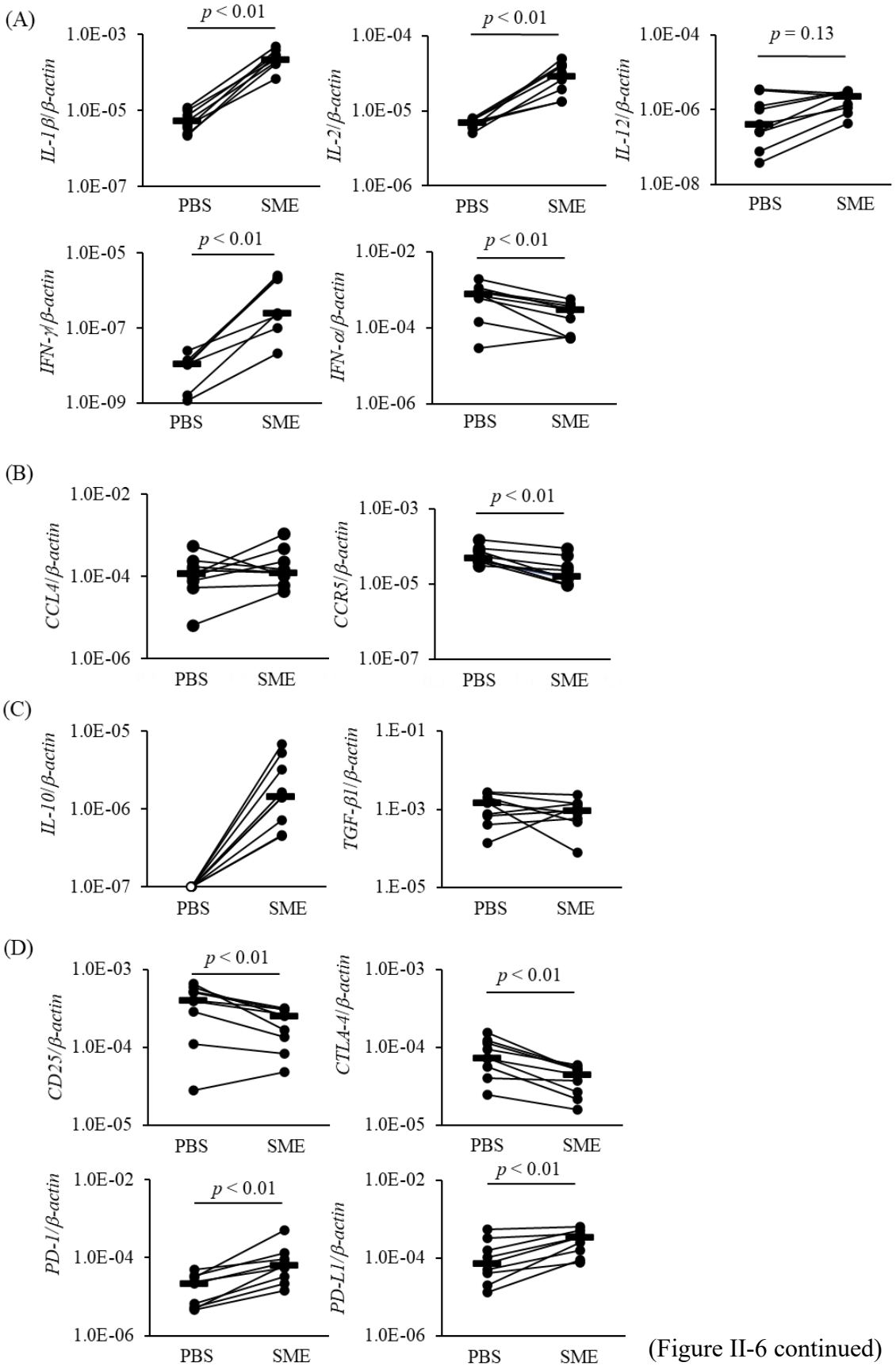

(Figure II-6 continued)

Figure II-6. Gene expressions of cytokines and the molecules related to immunosuppression in SME-stimulated chicken PBMCs.

PBMCs collected from non-infested experimental (NIE) chickens raised on a PRM-free experimental farm were cultured with soluble mite extract (SME) or PBS for 24 h (n = 9). Gene expression of (A) pro-inflammatory cytokines, Th1 cytokines, and a type I interferon, (B) *CCL4* and *CCR5*, (C) anti-inflammatory cytokines, and (D) *CD25*, a marker for Treg-like cells in chickens, and the immune checkpoint molecules were examined by qRT-PCR. The extent of the expression of target genes was calculated by dividing the copy number of each target by that of *β-actin*. Statistical significance was determined using the Wilcoxon signed-rank test. White circles indicate samples that were less than the quantitation limit.

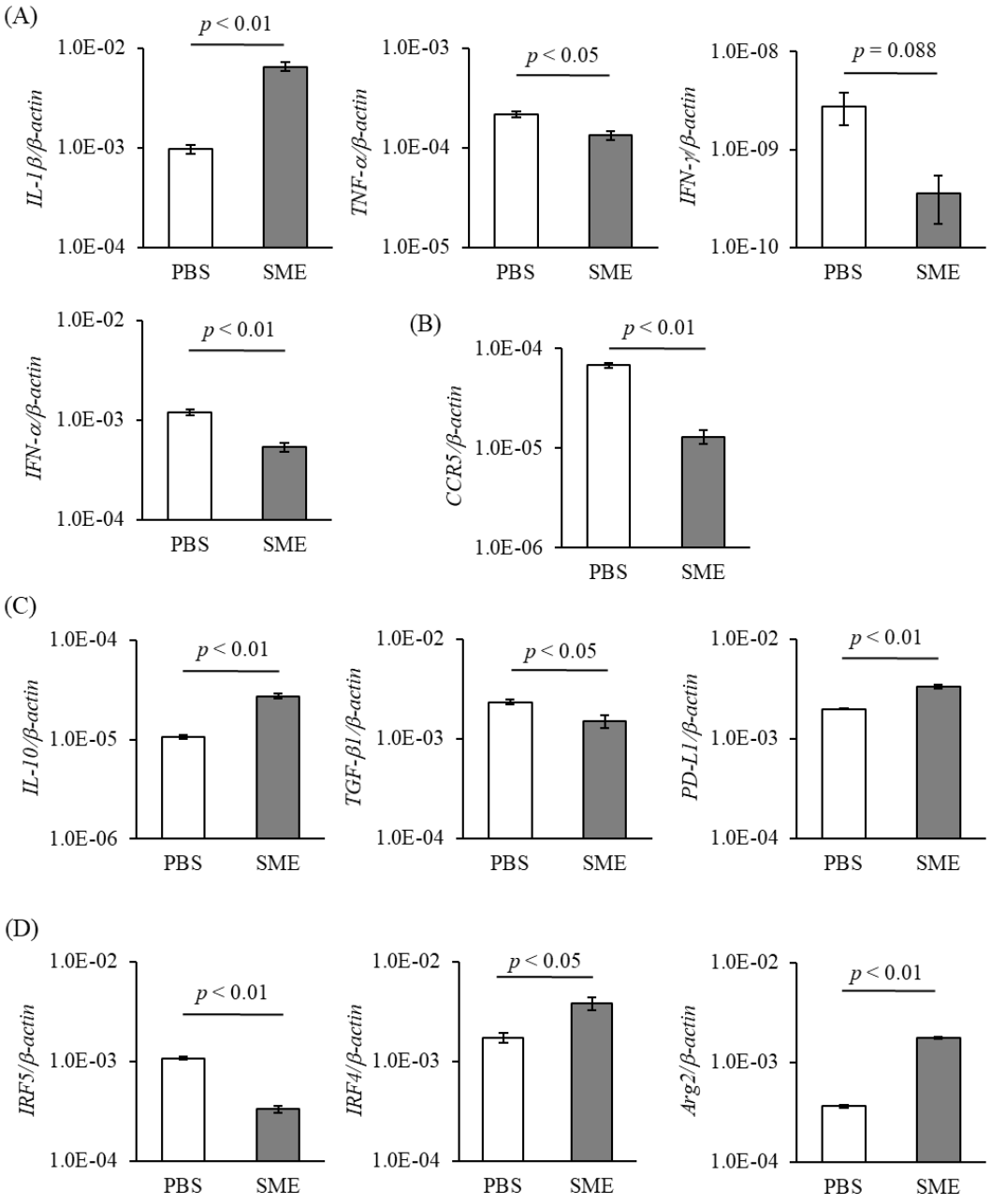

Figure II-7. Changes in gene expressions of chicken macrophages in response to SME exposure.

HD-11 chicken macrophages were cultured with SME or PBS for 24 h (n = 5). Gene expressions of (A) *IL-1β*, *IFN-γ*, *TNF-α*, and *IFN-α*, (B) *CCR5*, (C) anti-inflammatory cytokines and an immune checkpoint molecule, *PD-L1*, (D) the molecules related to the polarization of macrophages to M1 or M2 phenotypes, were examined by qRT-PCR. The extent of the expression of target genes was calculated by dividing the copy number of each target by that of *β-actin*. Statistical significance was determined using Student's *t*-test.

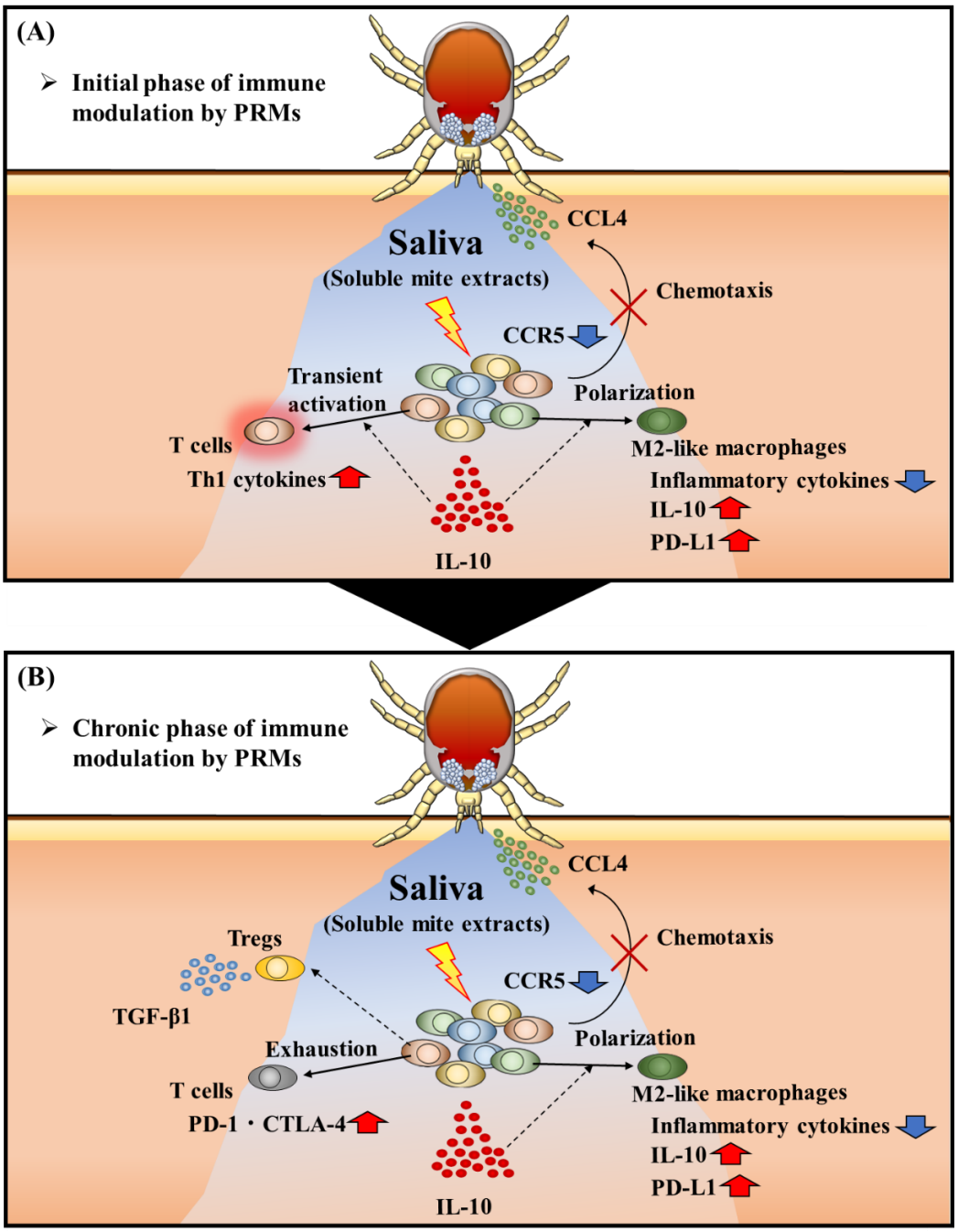

Figure II-8. The theory of host immune modulation by PRM-infestation.

(A) In acute phase of infestation, PRM-derived molecules reduce the expression of CCR5 in immune cells and interrupt the recruitment of inflammatory cells to the site of infestation. In addition, PRM-infestation elicits the polarization of macrophages into the M2-like phenotype, while T cells are transiently activated. IL-10 is a potential regulator of these cell type-selective modulation. (B) Chronic infestation further attenuate host immune responses as represented by T-cell exhaustion and differentiation of Treg-like cells.

DISCUSSION

To date, mounting literatures have reported that hematophagous arthropods such as ticks and mosquitoes secrete various effector molecules into their saliva and modulate host immunological states during infestation [Cross *et al*., 1994; Mejri *et al*., 2002; Schneider *et al*., 2004; Brake and Pérez de León, 2012; Kotál *et al*., 2015]. This not only contributes to the maintenance of a suitable environment for undisturbed blood feeding but also facilitates pathogen transmission [Schneider *et al*., 2004; Schneider and Higgs, 2008; Šimo *et al*., 2017; Nuttall, 2019; Guerrero *et al*., 2020]. Therefore, to understand host responses, especially immune responses, against infestation with ectoparasites is important for the establishment of control strategies of infectious diseases as well as parasitical burdens. The present study revealed that the immunological states of chickens chronically exposed to PRMs were suppressively modulated and that PRM-derived molecules potentially elicit the polarization of macrophages into the M2-like phenotype, resulting in immunosuppression of hosts.

RNA-Seq analysis using blood-fed PRMs revealed that a chemokine CCL4 was particularly expressed in chicken's blood ingested by PRMs. CCL4 is produced by various cell types including epithelial cells, platelets, and lymphocytes, and recruits immune cells, such as natural killer cells, T cells, and monocytes, to mount the inflammatory response [Uguccioni *et al*., 1995; Dairaghi *et al*., 1998]. Since *CCL4* expression in PBMCs was not increased by SME treatment, the upregulation of CCL4 might be stimulated by mechanical skin injury caused by the penetration of the mouthparts of PRMs, as reported in tick infestation [Kotál *et al*., 2015]. Hence, the upregulation of CCL4 might also be mediated by other ectoparasites, including NFMs and TFMs. In spite of the upregulation of CCL4, the increase in mRNA expressions of pro-inflammatory cytokines and Th1 cytokines were not observed except for *IL-1β*, while the gene expression of another pro-inflammatory chemokine *IL-8* was upregulated. A pervious study has reported that saliva from a tick *R. sanguineus* downregulated the cell-surface expression of CCR5, a receptor of CCL4 [Oliveira *et al*., 2008]. Consistent with this previous finding, gene expression of *CCR5* tended to be decreased in PRM-infested chickens compared to that in non-infested chickens. Moreover, SME stimulation significantly downregulated the expression of *CCR5* in PBMCs and HD-11 cells *in vitro*. Several studies have demonstrated the inhibitory properties of tick saliva against a variety of chemokines, including CCL2, CCL3, CCL11, and IL-8 [Hajnická *et al*., 2001; Vancová *et al*., 2007]. Therefore, the interruption of chemokine activities might be one of the key immunomodulatory functions of tick saliva to inhibit the migration and activation of

immune cells and subsequently to suppress the host inflammatory responses. Further studies are required to elucidate the interaction of PRM saliva to chemokine activities.

Throughout this study, in contrast to other pro-inflammatory cytokines, gene expression of *IL-1β* in PRM-infested chickens tended to be higher than that in non-infested chickens; an opposite tendency was observed in the plasma concentration of IL-1β. IL-1β is primarily synthesized as a pro-IL-1β, an inactive precursor, in the cytoplasm and processed by the cysteine protease caspase-1 to be a mature IL-1β, which is secreted from the cells [Li *et al*., 1995; Qu *et al*., 2007]. Several studies have revealed that cysteine protease inhibitors are contained in tick saliva [Kotsyfakis *et al*., 2006; Sajiki *et al*., 2020], and therefore, cysteine protease inhibitors present in PRM saliva may inhibit the processing of cytoplasmic pro-IL-1β and reduce the plasma concentration of mature IL-1β.

Several studies have reported the potential of tick saliva to suppress the production of pro-inflammatory and Th1 cytokines, including TNF-α and IFN-γ, and to induce the expression of immune checkpoint molecules [Chen *et al*., 2012; Poole *et al*., 2013; Sajiki *et al*., 2021]. Consistent with these findings, PRM-derived SME attenuated the expression of IFNs and inflammatory cytokines in HD-11 chicken macrophages, and remarkably, treatment with SME induced the polarization of macrophages into the anti-inflammatory M2-like phenotype. Meanwhile, certain subsets of immune cells, probably T cells, were activated by stimulation with SME, as represented by the increased expression in Th1 cytokines, *IL-2* and *IFN-γ*, in SME-exposed PBMCs. This contradictory may be explained by cell-type selective modulation driven by IL-10, a cytokine that possesses pleiotropic functions. IL-10 is known to function as an anti-inflammatory cytokine on macrophages, whereas it activates inflammatory potentials of $CD8^+$ T cells, depending on the expression level of its low-affinity receptor IL-10Rβ [Saxton *et al*., 2021]. In this study, the expression of IL-10 was significantly upregulated in PRM-infested chickens and SME-stimulated PBMCs and HD-11 cells, showing that IL-10 may mediate immunomodulation caused by PRM-infestation as a critical regulator. Further experiments, including the blockade of IL-10, are warranted to elucidate the detailed molecular mechanisms in modulation of host immunological states mediated by PRM-derived molecules.

Chickens raised at farms continuously contaminated with PRMs are expected to be chronically exposed to PRMs. In PBMCs from chickens chronically infested with PRMs, the expression of immune checkpoint molecules, *CTLA-4* and *PD-1*, were significantly upregulated, indicating that severe or chronic infestation with PRMs could cause exhaustion of T cell. Notably, the expression of *PD-L1* in PBMCs and HD-11 cells was upregulated by the stimulation with SME; its continuous expression potentially

contributes to the development of T-cell exhaustion. As another possibility indicative of immunosuppressive state, Treg-like cells would be increased in chickens chronically suffered from PRM-infestation, as shown by the increased expression of *CD25* in PBMCs from PRM-infested chickens. In addition, the higher expression of TGF-β1 in PRM-infested chickens seems to represent an increase in Treg-like subpopulations [Vignali *et al*., 2008], as M2-like HD-11 macrophages polarized by SME-stimulation did not exhibit increased expression in *TGF-β1*. In contrast, the expressions of *TGF-β1*, *CD25*, and *CTLA-4* were not upregulated in SME-exposed PBMCs, suggesting that transient exposure to PRM-derived molecules could not facilitate the differentiation of T cells into Treg-like subpopulations. Although additional experiments including flow cytometric analyses are required to elucidate the involvement of Treg-like cells in an immunosuppressive state in chickens chronically infested with PRMs, T-cell responses seem to be mitigated in affected chickens.

In the present study, the samples collected from farms continuously eroded by PRMs were used to analyze the immunological states in the affected chickens. However, the experiments in this study did not directly prove the effect of PRM-infestation on host immune reactions. In addition, SME used for cell culture experiments contains not only molecules secreted in PRMs' saliva but also soluble proteins from other tissues, such as the midgut and hemosome. Techniques to only harvest saliva or salivary glands from PRMs have yet to be developed due to their small size. Considering these limitations, samples from chickens experimentally infested with PRMs should be analyzed to corroborate the modulation of host immunity caused by PRM-infestation.

SUMMARY

During infestation, hematophagous arthropods, such as ticks and mosquitoes, secrete various factors that interfere with host physiological responses, including immune responses, to sustain an environment for blood feeding. Since the immunosuppression caused by infestation with hematophagous arthropods contributes to pathogen transmission and decreased efficacy of vaccines, it is necessary to understand the modulation of host immune reactions against the infestation. However, immune responses in chickens, including cytokine expression profiles, against PRM-infestation has yet to be fully elucidated.

In Chapter II, according to chicken-derived transcripts obtained by RNA-Seq analysis using blood-fed PRMs, a pro-inflammatory chemokine *CCL4* showed high expression intensity and was highly expressed in PRM-infested chickens compared to non-infested chickens. However, there is no difference in the expression of Th1 and inflammatory cytokines between PRM-infested and non-infested chickens, and the gene expression of *CCR5*, a receptor of CCL4, in PBMCs from the infested chickens were lower than that in the non-infested chickens. In contrast, the expression of anti-inflammatory cytokines, IL-10 and TGF-β1, and other molecules related to immunosuppression, such as immune checkpoint molecules, was significantly higher in the infested chickens. These results suggest that chronic infestation with PRMs suppressively modulates host immunological states in chicken. In addition, cell culture experiments using SME revealed that PRM-derived molecules directly mitigate host inflammatory responses, as represented by the polarization of chicken macrophage-like cells when stimulated with SME into the anti-inflammatory M2-like phenotype. Additional experiments, including experimental infestation with PRMs, are required to corroborate immunosuppression caused by PRM-infestation.

CHAPTER III

Identification and characterization of novel antigen candidates for the development of vaccines against *Dermanyssus gallinae*

INTRODUCTION

Currently, the control of PRMs is mainly dependent upon spraying the cages with synthetic chemical acaricides. However, continuous use of acaricides could result in various problems, including the contamination of products and environment with acaricides [Smulders *et al*., 2018; Tu *et al*., 2019], as well as the development of acaricide-resistance in PRMs [Thind and Ford, 2007; Murano *et al*., 2008, 2015; Marangi *et al*., 2009]. Recently, vaccination has been highlighted as an alternative strategy for the control of PRMs, and researchers have examined several antigen candidates for their anti-PRM potentials [Bartley *et al*., 2012; Wright *et al*., 2016; Lima-Barbero *et al*., 2019]. Efficacies of these vaccine antigens, however, have not been observed to be sufficient to control PRMs in the field [Bartley *et al*., 2017]. Therefore, explorations of antigens for more effective vaccines are necessary to improve vaccination strategies.

In ticks, two types of molecules can be considered as vaccine antigens. The first type of the molecules includes proteins produced in salivary glands and secreted into saliva ("exposed" antigens) that support blood feeding and adhesion to the host [Wikel, 1996; Tsuda *et al*., 2001]. The second includes molecules expressed in the midguts ("concealed" antigens); midgut antigens could be exposed to antibodies produced in vaccinated host, as ingested blood is accumulated in the midguts [Willadsen *et al*., 1989; Willadsen, 2004]. Since PRMs infest chickens for shorter periods (0.5 to 1.5 h [Chauve, 1998; Pritchard *et al*., 2015]) than ticks, concealed rather than exposed antigens may be more appropriate as antigen targets for anti-PRM vaccine. In addition, since the concept of anti-PRM vaccine is to damage PRMs by interfering the functions of PRM molecules with antibodies ingested during blood feeding, antigens for vaccines are required to be the molecules which play important roles in biological activities of PRMs, including blood digestion. Furthermore, the molecules expressed on the plasma membrane are more desirable as manifested by prominent efficacies of vaccines targeting plasma membrane protein, Bm86, in ticks [Rand *et al*.,1989; Azhahianambi *et al*., 2009].

In Chapter III, antigen candidates for anti-PRM vaccines were investigated from the dataset obtained by RNA-Seq analysis in Chapter I, and three candidate molecules were identified: a cystatin-like molecule (Dg-Cys), a copper transporter-1-like molecule (Dg-Ctr1), and an adipocyte plasma membrane-associated protein-like molecule (Dg-APMAP). Several studies have reported that cystatins are associated with various physiological processes in ticks, including blood digestion and egg development [Grunclová *et al*., 2006; Schwarz *et al*., 2012]. Ctr1 is a plasma membrane protein which mediates the uptake of copper ion, and the copper ion plays a critical role in respiration

[Muttkowski, 1921], immunity [Christensen *et al*., 2005; Lu *et al*., 2014], and metal homeostasis and detoxification [Amiard *et al*., 2006; Perez and Noriega, 2014; Rivera-Perez *et al*., 2017] in arthropods. Meanwhile, the physiological importance of APMAP in arthropods has yet to be documented; however, APMAP is considered as a protein expressed on the plasma membrane and exhibited a marked expression intensity among plasma membrane proteins identified in the dataset of RNA-Seq analysis, indicating its potential as a candidate antigen. In this study, these molecules were characterized and analyzed for their potentials as vaccine antigens *in vitro*. Additionally, to assess the potential application of the identified antigens for "cocktail vaccines", the effects of mixed plasmas containing antibodies against multiple antigens were examined.

MATERIALS AND METHODS

PRM samples

Blood-fed PRMs were obtained as described in Chapter I. Starved PRMs were collected after incubating for a 1-week period at 25°C in 70% humidity. Some blood-fed and starved PRMs were fixed with 70% ethanol, and eggs, larvae, protonymphs, deutonymphs, and adults were morphologically identified and collected separately under microscopic observation. The remaining PRMs were kept at 4°C in 70% humidity until use for the *in vitro* feeding assay, or stored at −80°C. RNA was isolated as described in Chapter I, and cDNA synthesis from isolated RNA was performed as described in Chapter II.

Identification of the full-length nucleotide sequences of Dg-Cys, Dg-Ctr1, and Dg-APMAP in PRMs

The transcripts of *Dg-Cys*, *Dg-Ctr1*, and *Dg-APMAP* were obtained by RNA-Seq analysis described in Chapter I. To identify the full-length nucleotide sequence of the cDNA encoding *Dg-Cys* transcript, rapid amplification of cDNA ends (RACE) was conducted using total RNA from blood-fed PRMs and the primers 5′ GSP1–3 and 3′GSP1–2, with 5′ and 3′ RACE Systems (Thermo Fisher Scientific). To determine the nucleotide sequences of the open reading frame (ORF) of *Dg-Ctr1* and *Dg-APMAP*, PCR was performed with Ex Taq polymerase (TaKaRa Bio Inc.) using cDNA from blood-fed PRMs and the primers as follows: for *Dg-Ctr1*: DgCtr1-F and R; for *Dg-APMAP*: DgAPMAP-ORF-F and R, DgAPMAP-seq-F1–3, and DgAPMAP-seq-R1–3. Sequence analyses were performed using a GenomeLab GeXP Genetic Analysis System (SCIEX, Framingham, MA, USA) according to the manufacturer's instructions. Primers were listed in Table III-1. The signal peptide domain, the transmembrane site, and the active site were predicted using the software systems SignalP v4.1 (*http://www.cbs.dtu.dk/services/SignalP/*), TMHMM v2.0 (*http://www.cbs.dtu.dk/services/TMHMM/*), and InterProScan program v5.32-71.0, respectively. The phylogenetic trees were generated by MEGA software version X [Kumar *et al*., 2018], using a maximum likelihood method with 1,000 bootstrap replicates and a JTT matrix-based model [Jones *et al*., 1992], by using a discrete Gamma distribution (+G) and assuming that a certain fraction of sites is evolutionarily invariable (+I), to improve the tree topology.

Laser-capture microdissection

The cDNA of the salivary glands, midguts, and ovaries from PRMs were prepared using tissue samples extracted by laser-capture microdissection (LCM) as previously described [Ichii *et al*., 2017]. Briefly, mixed life stages of starved PRMs were fixed with Carnoy solution, embedded in paraffin, cut into 5-μm sections, and mounted on glass slides coated with LCM films (Meiwafosis, Tokyo, Japan). Sections were then stained with 1% toluidine blue, and tissues were dissected with MicroBeam Rel.4.2 (Carl Zeiss, Oberkochen, Germany) following manufacturer's instructions. Total RNA from each tissue was isolated using the RNAqueous-Micro Kit (Thermo Fisher Scientific) according to the manufacturer's protocols, and cDNA was synthesized with SuperScript First-Strand Synthesis System for RT-PCR (Thermo Fisher Scientific) using 300 pmol random hexamer primer (Hokkaido System Science Co., Ltd.).

Gene expression analyses

The expression of *Dg-Cys*, *Dg-Ctr1*, and *Dg-APMAP* mRNA in each feeding state, life stage, and tissue was analyzed by RT-PCR using Ex Taq polymerase (TaKaRa Bio Inc.) and specific primers Dg-Cys F/R, Dg-Ctr1-RT-F/R, and Dg-APMAP-RT-F/R. As an internal control, *elongation factor 1-α-1*-like (*Elf1a1*), was amplified using the primers Elf1a1-F/R [Ariizumi *et al*., 2021]. Primers used are listed in Table III-2. Since the RNA samples isolated from salivary glands were of small amount and low quality, the detection of targets in cDNA samples synthesized from salivary glands was performed by nested RT-PCR using the same primer set.

qRT-PCR

To quantify the expression of *Dg-Cys*, *Dg-Ctr1*, and *Dg-APMAP* mRNA at each life stage and feeding state of PRMs, qRT-PCR was conducted using each cDNA samples , except for that obtained from eggs, using LightCycler480 System II (Roche Diagnostics) and TB Green Premix DimerEraser (TaKaRa Bio Inc.) according to the manufacturer's instructions. To amplify the target genes and *Elf1a1*, primers used in gene expression analyses were used. The PCR conditions consisted of an initial denaturation at 95°C for 30 s, followed by 45 cycles of 95°C for 5 s, 60°C for 30 s, and 72°C for 30 s. To assess primer pairs for their specificities, a melting curve analysis was subsequently performed from 65°C to 95°C at a rate of 0.1°C/s. To generate standard curves for quantification, serial dilutions of T-vector pMD20 (Takara Bio Inc.) inserted with *Dg-Cys*, *Dg-Ctr1*, *Dg-APMAP*, or *Elf1a1* were used. Each sample was tested three times, and mRNA expression of target genes was calculated as a ratio by dividing the concentration of target mRNA by

that of *Elf1a1* mRNA.

Flow cytometric analysis

To confirm the expression of Dg-Ctr1 on the plasma membrane, the FLAG epitope-tagged recombinant Dg-Ctr1 protein was generated. The ORF of the *Dg-Ctr1* was amplified using the primers FLAG-Dg-Ctr1-F/R (Table III-2) and the PCR product was digested with EcoRV-HF (New England Biolabs, Ipswich, MA, USA) and KpnI-HF (New England Biolabs). The digested fragment was cloned into the vector pCXN2.1-FLAG (kindly provided by Dr. Takehiko Yokomizo, Juntendo University, Tokyo, Japan [Niwa *et al*., 1991]). Then, the plasmid was digested with NcoI-HF (New England Biolabs) and KpnI-HF (New England Biolabs), and the digested fragment was sub-cloned into the pIEx-4 vector (Merck, Kenilworth, NJ, USA) (pIEx4-FLAG-Dg-Ctr1). pIEx4-FLAG-Dg-Ctr1 and pIEx4-FLAG (mock) were transfected into Sf9 insect cells using *Trans*IT-Insect Transfection Reagent (Mirus Bio LLC, Madison, WI, USA), according to the manufacturer's protocols. Cells were collected at 72 h after the transfection, and stained with Anti DYKDDDDK Monoclonal Antibody (2H8; TransGenic Inc., Fukuoka, Japan) or a mouse IgG2a isotype control (HOPC-1; SourthernBiotech, Birmingham, AL, USA). Cells were then washed three times with PBS containing 1% bovine serum albumin (BSA; Sigma-Aldrich) (1% BSA-PBS) and stained with phycoerythrin-conjugated anti-mouse IgG (H+L) polyclonal antibody (Beckman Coulter, Fullerton, CA, USA). Cells were washed twice with 1% BSA-PBS and analyzed by FACS Verse (BD Biosciences, San Jose, CA, USA).

Preparation of recombinant proteins

Recombinant proteins of Dg-Cys, Dg-Ctr1, and Dg-APMAP were expressed as fusion proteins with the His-tag by using the BIC system (TaKaRa Bio Inc.). The whole protein lacking its signal peptide of Dg-Cys and the N-terminal sides of the extracellular regions of Dg-Ctr1 were expressed (Dg-Cys-his and Dg-Ctr1-N-his). Regarding Dg-APMAP, to investigate the optimal size and position of fragments to promote expression and secretion of recombinant proteins, five expression plasmids containing different regions of the extracellular region of Dg-APMAP (Dg-APMAP-N-his: N-terminal side of the extracellular region, Dg-APMAP-C-his: C-terminal side of the extracellular region, Dg-APMAP-N2-his: N-terminal side of the extracellular region without the strictosidine synthase domain, Dg-APMAP-D-his: strictosidine synthase domain, Dg-APMAP-C2-his: C-terminal side of the extracellular region without the strictosidine synthase domain) were prepared (Figure III-8B) as well as the entire extracellular region (Dg-APMAP-his).

PCR was performed using cDNA synthesized from blood-fed PRMs described above, with KOD-Plus-Neo (TOYOBO Co., Ltd., Osaka, Japan) and primers containing the homologous recombination sites (Table III-3). Each amplicon was integrated into the cloning site of the pBIC4 vector (TaKaRa Bio Inc.) by homologous recombination and introduced into *Brevibacillus* competent cells (*Brevibacillus* Expression System, TaKaRa Bio Inc.). The transformed bacteria were cultured in 2SY (Dg-Cys-his) or TM medium (Dg-Ctr1-N-his and Dg-APMAP-N-his) at 32°C, following the manufacturer's protocols. The recombinant proteins were purified from the supernatants using Ni Sepharose 6 Fast Flow (Thermo Fisher Scientific, Waltham, MA, USA) (Dg-Cys-his) or TALON metal affinity resin (Clontech Laboratories, Inc., Mountain View, CA, USA) (Dg-Ctr1-N-his and Dg-APMAP-N-his). The buffer was replaced to PBS using SnakeSkin Dialysis Tubing (Thermo Fisher Scientific) overnight at 4°C. The purified proteins were mixed with 2 × sodium dodecyl sulfate (SDS) buffer (125 mM Tris-HCl, pH 6.8, 4% SDS, 10% 2-mercaptoethanol, and 20% glycerol), boiled for 5 min, separated using an SDS-polyacrylamide gel, and stained with Coomassie brilliant blue (FUJIFILM Wako Pure Chemical Corporation, Osaka, Japan) to confirm the purity of each protein. The concentration of proteins was determined using Pierce BCA Protein Assay Kit (Thermo Fisher Scientific) according to the manufacturer's instructions.

Enzymatic activity of Dg-Cys-his

The inhibitory properties of Dg-Cys-his against cysteine proteases, cathepsin L, S, and B were examined using the SensoLyte Rh110 Cathepsin L Assay Kit (ANASPEC, Fremont, CA, USA), SensoLyte 520 Cathepsin S Assay Kit (ANASPEC), and SensoLyte 520 Cathepsin B Assay Kit (ANASPEC), respectively, following the manufacturer's protocols. As a negative control, BSA diluted in PBS was used.

Immunization of chickens with recombinant proteins

Plasmas were prepared from chickens immunized with Dg-Cys-his, Dg-Ctr1-N-his, or Dg-APMAP-N-his. Each protein was mixed with light liquid paraffin as an adjuvant (20 μg/mL). Chickens (Dg-Cys-his and Dg-Ctr1-N-his, Hy-Line Brown; Dg-APMAP-N-his, specific pathogen-free chickens, VALO BioMedia) at 3 weeks of age were subcutaneously immunized with the recombinant proteins or PBS as the control as follows: Dg-Cys-his, 20 μg of the protein or PBS (n = 4 and 2: Cys1–4 and PBS-Cys1 and 2, respectively); Dg-Ctr1-N-his, 10 or 20 μg of the protein or PBS (n = 3, each: Ctr1–3, Ctr4–6, and PBS-Ctr1–3, respectively); Dg-APMAP-N-his, 20 μg of the protein or unimmunized (n = 4, each: APM1–4 and UN1–4, respectively). Four weeks later, the

heparinized blood was collected from APM1–4 and UN1–4, and Cys1–4, PBS-Cys1 and 2, Ctr1-6, and PBS-Ctr1–3 were immunized with the same doses of same antigens, respectively. The heparinized blood was collected 3 weeks after the second immunization, and the immune plasmas were isolated by centrifugation at 2,000 × *g* for 10 min. Experiments on Dg-Cys-his and Dg-Ctr1-N-his were conducted at Experimental Animal Facility, Faculty of Veterinary Medicine, Hokkaido University, and Immunization of Dg-APMAP-N-his was performed at Choka Research Institute, Vaxxinova Japan K.K., Tochigi, Japan.

ELISA

Antibody titers in the immune plasmas were determined by ELISA. The purified Dg-Cys-his, Dg-Ctr1-N-his, or Dg-APMAP-N-his was coated on the wells of 96-well plates (Sumitomo Bakelite Co., Ltd, Tokyo, Japan) (100 ng/well) with carbon-bicarbonate buffer (pH9.0). After 16 h, the solution was aspirated, and PBS containing 0.05% Tween-20 (PBST) with 1% BSA was added to each well and incubated at 37°C for 2 h. The wells were washed five times with PBST, and two-fold serial dilutions of plasma samples from 2,000× to 64,000× with PBS were added. After incubation for 1 h at 25°C, the wells were washed five times with PBST and incubated with anti-chicken IgY peroxidase rabbit antibody (Sigma-Aldrich) for 1 h at 25°C. The wells were then washed five times with PBST and finally, reacted with the TMB one-component substrate (Bethyl Laboratories, Montgomery, TX, USA) for approximately 20 min at 25°C in the dark. The reaction was quenched with 0.18 M H_2SO_4, and the absorbance was measured at 450 nm. The assays were performed in duplicate.

Western blotting

The production of specific antibodies against Dg-Cys-his, Dg-Ctr1-N-his, and Dg-APMAP-N-his was examined by western blotting. Purified recombinant proteins were separated in an SDS-polyacrylamide gel and transferred to polyvinylidene difluoride membranes (Merck Millipore, Burlington, MA, USA). The membranes were blocked overnight at 4°C with PBST containing 1% skim milk. The membranes were incubated with each immune plasma at 25°C, washed with PBST, and incubated with anti-chicken IgY peroxidase rabbit antibody at 25°C (Sigma-Aldrich). Finally, the peroxidase signal was visualized by incubating the membranes with Immobilon Western Chemiluminescent HRP substrate (Merck Millipore).

***In vitro* feeding assay**

1. Evaluation of the potential of Dg-Cys, Dg-Ctr1, and Dg-APMAP as vaccine antigens

The potentials of Dg-Cys, Dg-Ctr1, and Dg-APMAP as vaccine antigens were examined by *in vitro* feeding assay [Ariizumi *et al*., 2021]. Heparinized fresh chicken blood was collected from healthy chickens maintained at the Field Science Center for Northern Biosphere, Hokkaido University, and incubated at 40°C until use. Immune plasmas from each group were pooled separately. After centrifugation at 2,000× *g* for 10 min, the plasma was replaced with an equal volume of pooled immune plasmas described above. Approximately 100 starved PRMs of mixed life stages were collected in each artificial feeding device as previously described (Figure III-1 [Ariizumi *et al*., 2021]). The devices were capped with rubber caps type 2 (GE Healthcare) and the rubber cap was penetrated using a 27-G needle (TERUMO CORPORATION, Tokyo, Japan) for ventilation. The top of devices was filled with 400 μl of blood containing immune plasmas, and blood feeding was performed for 4 h at 40°C in a dark, humid condition with modest shaking. Only blood-fed PRMs were then collected in Pasteur pipettes (day 0) and maintained at 25°C in 70% humidity during the observation period. The number of dead PRMs were monitored for 1 week or 10 days, and the numbers of newborn larvae and protonymphs were counted at the last day of the observation period. The anti-PRM properties of immune plasmas were evaluated based on the following criteria:

1) The survival rate (SR):

$$\mathrm{SR}\ (\%) = \left(1 - \frac{\text{No. of dead PRMs on day 7 or 10}}{\text{No. of blood-fed PRMs}}\right) \times 100$$

2) The reproductive capacity (RC)

$$\mathrm{RC} = \frac{\text{No. of newborn larvae and protonymphs on day 7 or 10}}{\text{No. of blood-fed adults}}$$

Adults and nymphs were collected separately and the survival rate was analyzed independently.

2. Evaluation of the efficacy of the "cocktail vaccine"

To examine the effects of the "cocktail vaccine", pooled immune plasmas of Dg-Cys

were mixed with an equal volume of those of Dg-Ctr1 or Dg-APMAP. As a control, equal volumes of pooled plasmas PBS-Cys 1 and 2 were mixed with those of pooled plasmas PBS-Ctr1–3 or UN1–4, respectively. *In vitro* blood feeding was performed as described above using adult PRMs, and the SR was monitored for a 10-day period.

Statistics

For gene expression analyses, differences were assessed using the Mann-Whitney *U* test. For *in vitro* feeding assay, the SR and RC between the groups were compared by Fisher's exact test. The odds ratio and 95% confidential interval (CI) was estimated. In addition, to analyze the difference in the SR, Kaplan-Meier curves were constructed and a log-rank test was performed. For multiple comparisons, Fisher's multicomparison test was conducted and a p value was adjusted by Holm method. For all tests, $p < 0.05$ was considered statistically significant.

Ethics statement

1. Genetic recombination experiments

All genetic recombination experiments were performed in accordance with the Manual for Safety Management on Genetic Recombination Experiments in Hokkaido University (Approval number: 2019-024).

2. Animal experiments

Immunizations of chickens with Dg-Cys-his and Dg-Ctr1-N-his were approved by the Institutional Animal Care and Use Committee, Hokkaido University (Approval numbers: 16-0004 and 20-0051), and all experiments were conducted according to the relevant guidelines and regulations of the Faculty of Veterinary Medicine, Hokkaido University, which has been fully accredited by the Association for Assessment and Accreditation of Laboratory Animal Care International. Immunization of chickens with Dg-APMAP-N-his was performed in accordance with relevant guidelines and regulations of Choka Research Institute, Vaxxinova Japan K.K., and the procedure was approved by the Animal Care and Use Committee, Vaxxinova Japan K.K. (Approval number: AR007-C-EX-036).

Table III-1. Primers used in gene cloning and sequencing.

Primer	Primer sequences (5' - 3')
5' GSP-1	ACCGATCACTACAAACTGCA
5' GSP-2	CAACAGCAGCAGCAGTACGA
5' GSP-3	AGTACGAATAAACACGCGCG
3' GSP-1	CCAAACGGTCTCCGTACTGT
3' GSP-2	CCGTACTGTCGGACGAAATC
Dg-Ctr1-F	AGGACGGTGCAATTCTCAAC
Dg-Ctr1-R	GTGTTGGCTGGTTGGTGTTT
DgAPMAP-ORF-F	GCAGAGCAGAGCAGAGCACGG
DgAPMAP-ORF-R	GTGGTGAGGCGGGCTCGAATG
DgAPMAP-seq-F1	ATTCCGCTCGACTTTGATCC
DgAPMAP-seq-F2	GGGGCTTCACCAAATCCTGT
DgAPMAP-seq-F3	CCATTCGTCACACTACACGC
DgAPMAP-seq-R1	ATCAGGATCTTTCCGTGCTC
DgAPMAP-seq-R2	CAACGGCAACTTCCTTGCGA
DgAPMAP-seq-R3	GGTCACGTACTTTGCGCTAA

Table III-2. Primers used in *in vitro* characterization.

Primer	Primer sequences (5' - 3')
Dg-Cys-F	GTCTTTGCCTTCCAGTCGAG
Dg-Cys-R	GGTCTAGCTTGCTCCAAACG
Dg-Ctr1-RT-F	TGGACCACAGTAACCACGAA
Dg-Ctr1-RT-R	GCTAGGCACGAACCAAACAT
Dg-APMAP-RT-F	AGCTCCAGCTGGTTTTCGTA
Dg-APMAP-RT-R	ACTGGGTTCCGGTGTAGATG
Elf1a1-F	GTCGGTGTCATCAAGTCCGT
Elf1a1-R	AGGGTCGAGAGTGTAGGGTC
FLAG-Dg-Ctr1-F	CCGGATATCGACTATGTGCCAGACTCGCA
FLAG-Dg-Ctr1-R	CGGGGTACCTCATCCGCAGTGATCCGAGG

*Restriction enzyme recognition sites are underlined.

Table III-3. Primers used in preparation of the recombinant proteins.

Primer	Primer sequences (5' - 3')
pBIC-Dg-Cys-F	GATGACGATGACAAAGGCCTTTCGGACGTGGCCG
pBIC-Dg-Cys-R	CATCCTGTTAAGCTTTTAATTCTCGCACCGCTTC
pBIC-Dg-Ctr1-F	GATGACGATGACAAAGACTATGTGCCAGACTCGCA
pBIC-Dg-Ctr1-R	CATCCTGTTAAGCTTTTAATTTTGTGTCTTCCACCCG
pBIC-APMAP-F1	GATGACGATGACAAACTCGACTTTGATCCGGC
pBIC-APMAP-F2	GATGACGATGACAAAATCGATATCAAGACAGGC
pBIC-APMAP-F3	GATGACGATGACAAAACTAAGGGTAAGTTGACG
pBIC-APMAP-R1	CATCCTGTTAAGCTTTTACTTATGTTTCAAACG
pBIC-APMAP-R2	CATCCTGTTAAGCTTTTAGCGAGGCGATCGGCGCAG
pBIC-APMAP-R3	CATCCTGTTAAGCTTTTAGGCAAATAGCAGTTTCGAC

*Recombination sites are underlined.

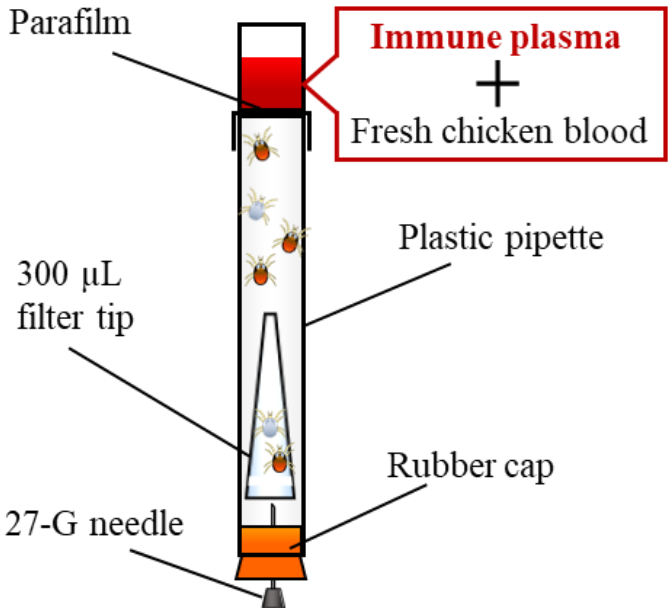

Figure III-1. The device for *in vitro* feeding assay adopted from Ariizumi *et al* (2021). Disposable plastic pipettes (10 mL) were cut and assembled across stretched parafilm. Approximately 100 starved PRMs were collected using 300 µL filter tips, and they were enclosed in the devices. The cut ends of the devices were closed with rubber caps, and the rubber caps were penetrated with 27-G needles for ventilation. Fresh chicken blood containing plasma derived from immunized chickens was added in the devices. Blood-feeding was performed at 40°C for 4 h.

RESULTS

Cloning and sequence analysis of *Dg-Cys*, *Dg-Ctr1*, and *Dg-APMAP* from PRMs

From the dataset of RNA-Seq analysis in Chapter I, the transcripts of the cystatin-like molecule (Dg-Cys), copper transporter 1-like molecule (Dg-Ctr1), and adipocyte plasma membrane-associated protein-like molecule (Dg-APMAP) were identified. The expression intensity of *Dg-Ctr1* was significantly higher in starved PRMs, whereas *Dg-APMAP* expression was higher in blood-fed PRMs. In contrast, no significant difference was observed in the expression of *Dg-Cys* between blood-fed and starved PRMs (Table III-4). The 5′ and 3′ RACE analyses revealed that the full-length cDNA of *Dg-Cys* was 669 bp, and the ORF was 423 bp, encoding a 140 amino-acid sequence. The deduced amino acid sequence of *Dg-Cys* contained a putative signal peptide in positions 1–29, and a cystatin-conserved domain at positions 85–98 (Figure III-2A). Phylogenetic analysis using cystatins from mites, ticks, chickens, and mammals indicated that *Dg-Cys* formed a distinct cluster but was closer to secreted cystatins (cystatin 2 and cystatin C) rather than intracellular ones (stefin, cystatin A and B; Figure III-2B). The deduced amino acid sequence of *Dg-Ctr1* contained three putative transmembrane domains at positions 54–76, 110–127, and 133–152, and a large extracellular domain at the N-terminal position 1–53 (Figure III-3A). Phylogenetic analysis showed that *Dg-Ctr1* was closer to copper transporters of mites and ticks than those of chickens and mammals (Figure III-3B). The deduced amino acid sequence of *Dg-APMAP* contained a putative transmembrane domain at positions 7–29 and a strictosidine synthase domain at positions 167–252 (Figure III-4A). Phylogenetic analysis revealed that *Dg-APMAP* was close to that of the mite *Galendromus occidentalis* (Figure III-4B).

Gene expression profiles of *Dg-Cys*, *Dg-Ctr1*, and *Dg-APMAP*

To examine the gene expression profiles of *Dg-Cys*, *Dg-Ctr1*, and *Dg-APMAP*, RT-PCR and qRT-PCR analyses were performed using cDNA from different life-stages and blood-feeding states of PRMs. Except for *Dg-Cys* in eggs, mRNA of target molecules was expressed in all life stages regardless of the feeding state (Figures III-5A and 6). Next, to analyze the gene expression of these molecules in different tissues of PRMs, LCM and RT-PCR/nested PCR were conducted using tissue samples from salivary glands, midguts, and ovaries. The gene expression of all molecules was clearly detected in the midguts and ovaries, whereas none of them was expressed in the salivary glands (Figure III-5B).

Expression of Dg-Ctr1 on the plasma membrane

To confirm the expression of Dg-Ctr1 on the plasma membrane, the N-terminal FLAG epitope-tagged recombinant Dg-Ctr1 (FLAG-Dg-Ctr1) was prepared in the Sf9 insect cells. The subcellular localization of Dg-Ctr1 was examined by flow cytometric analysis using the anti-DYKDDDDK (FLAG) antibody. FLAG-Dg-Ctr1-expressing cells were more frequently recognized by the anti-FLAG antibody compared to mock-transfected cells (Figure III-7), demonstrating that Dg-Ctr1 is a plasma membrane protein, as predicted by the IPR program.

Preparation of recombinant proteins

The recombinant proteins of Dg-Cys, the N-terminal sides of the extracellular domain of Dg-Ctr1, and the extracellular domain of Dg-APMAP were expressed as fusion proteins with a His-tag (Dg-Cys-his, Dg-Ctr1-N-his, and Dg-APMAP-his) using BIC system. With respect to Dg-APMAP-his, the secretion level of the recombinant protein into the supernatants was low, although the protein was expressed in the cultured bacteria (Figure III-8A). To facilitate the secretion of the recombinant protein into the cultural supernatants, truncated versions of the extracellular domain of Dg-APMAP was designed and analyzed for their secretory efficiencies into the supernatants. Among the 5 fragments examined (Dg-APMAP-N-his, Dg-APMAP-C-his, Dg-APMAP-N2-his, Dg-APMAP-D-his, and Dg-APMAP-C2-his; Figure III-8B), Dg-APMAP-N-his was efficiently secreted into the supernatants (Figure III-8C). Each recombinant protein was then purified from the culture supernatants of the transformed bacteria, and the purities of the proteins were confirmed by SDS polyacrylamide gel electrophoresis (SDS-PAGE) and by staining with Coomassie brilliant blue. Each recombinant protein was detected at the predicted molecular weight (Dg-Cys-his, approximately 13.4 kDa; Dg-Ctr1-N-his, approximately 10.6 kDa; Dg-APMAP-N-his, approximately 28.9 kDa; Figure III-9).

Enzymatic activity of Dg-Cys-his

The inhibitory properties of Dg-Cys-his against cysteine proteases were examined. The enzymatic activities of cysteine proteases, cathepsins L and S, were suppressed in the presence of Dg-Cys-his in a dose-dependent manner (50% inhibitory concentration for cathepsins L and S: 666.8 nM and 36.1 nM, respectively), while that of cathepsin B was not interrupted (Figure III-10). These results indicated that Dg-Cys-his acts as an inhibitor of cysteine proteases.

Immunization with recombinant proteins and acaricidal potential of the plasmas from the immunized chickens

Chickens were subcutaneously immunized with purified recombinant proteins in an emulsion with light liquid paraffin, and the plasmas were collected according to the schedule described in Figure III-11. The antibody titers in the immune plasmas were determined by ELISA, and 2 of 4 chickens immunized with Dg-Cys-his (Cys2 and 4), 3 of 6 chickens immunized with Dg-Ctr1-N-his (Ctr3, 5, and 6), and all the chickens immunized with Dg-APMAP-N-his exhibited higher antibody titers against immunized antigens (Table III-5). Additionally, the production of the specific antibodies against immunized antigens in in those chickens was further confirmed by western blot analyses (Figure III-12).

Next, plasmas showing higher antibody titers from the immunized chickens and those from control chickens were pooled separately and subjected to *in vitro* feeding assay to evaluate anti-PRM effects. After *in vitro* feeding, the blood-fed PRMs were collected, and the vaccine efficacies were assessed based on two criteria: the survival rate (SR) and the reproductive capacity (RC). The acaricidal effects by the immune plasmas against Dg-Cys-his, Dg-Ctr-N-his, Dg-APMAP-N-his, and by their combination are shown in the following 4 sections.

1. Acaricidal effects of Dg-Cys-his-immunized plasma

In the first experiment, protonymphs and adults were subjected to evaluate the acaricidal effects of immune plasmas based on the SR and RC. The RC of PRMs that fed on the immune plasmas from Cys2 and Cys4 was significantly reduced (Table III-6 and Figure III-13A), whereas no difference was observed in the SR of PRMs between the groups (Table III-6 and Figure III-13B). In the second experiments, protonymphs and deutonymphs were subjected to the same analysis. In contrast to the result of the first experiment, the SR of PRMs fed on the immune plasmas were significantly lower than that of PRMs fed on control plasmas, as indicated by Kaplan-Meier curve analysis and the log-rank test (Figure III-13C). Additionally, Fisher's exact test and odds ratio analysis showed that the SR of PRMs fed on immune plasmas is decreased from 5 days post-feeding (Table III-7). These results suggest that the plasma from chickens immunized with Dg-Cys increases the mortality of PRMs, especially nymphs, and interrupt their reproductive activity.

2. Acaricidal effects of Dg-Ctr1-N-his-immunized plasma

In the first experiment, nymphs were subjected to the analysis. The Kaplan-Meier

curve analysis and the log-rank test showed that PRMs fed on the immune plasmas from Ctr3, Ctr5, and Ctr6, exhibited a significant reduction in survival rate (Figure III-14A). In addition, Fisher's exact test and odds ratio analysis indicated that the SR of PRMs fed on immune plasmas was decreased from 7 days post-feeding (Table III-8). In the second experiment, to assess the acaricidal effects of immune plasmas on PRMs of different life stages, nymphs and adults were analyzed independently. Fisher's exact test and odds ratio analysis showed that the SR of PRMs fed on immune plasmas was significantly lower than that of control groups at 10 days post-feeding when analyzed in total PRMs (Table III-9), whereas no significant difference was shown by the log-rank test (Figure III-14B). For adults, neither the log-rank test nor Fisher's exact test showed significant differences in the SR between the control and immunized groups (Figure III-14C and Table III-10). Meanwhile, consistent with the results of the first experiment, the SR of nymphs fed on immune plasmas was significantly lower than that of the control groups (Figure III-14D), and this decrease in the SR was observed 8–10 days post-feeding (Table III-11). In this experiment, the RC was not analyzed, as oviposition was not observed in both groups. These data show that the plasmas from chickens immunized with Dg-Ctr1-N-his have the acaricidal potential on PRMs, and as observed in the result of Dg-Cys-his-immunization, nymphs tended to be more susceptible to the acaricidal effects of immune plasmas.

3. Acaricidal effects of Dg-APMAP-N-his-immunized plasma

To evaluate the effects of Dg-APMAP-N-his-immunization on different life stages of PRMs, adults and nymphs were collected separately and analyzed independently by the *in vitro* feeding assay. A comparison of the Kaplan-Meier curves revealed that the SR of mixed stages of PRMs fed on plasmas from APM1–4 was significantly lower than that of PRMs fed on plasmas from unimmunized chickens (Figure III-15A). Additionally, Fisher's exact test and odds ratio analysis indicated that the SR of PRMs fed on immunized plasmas is decreased from 4 days post-feeding (Table III-12). Importantly, the Kaplan-Meier curve analysis and the log-rank test revealed that the SR was lower in both adults and nymphs fed on immune plasmas, compared to those fed on unimmunized plasmas (Figures III-15B and C). This reduction in the SR was observed at 7 and 4 days post-feeding for adults and nymphs, respectively (Tables III-13 and 14). Regarding the RC, however, no significant difference was observed between each group (Figure III-15D). Collectively, plasmas from chickens immunized with Dg-APMAP-N-his increased the mortality in both adults and nymphs, and thus, Dg-APMAP could be one of the candidates for vaccine antigens.

4. Enhanced acaricidal effects by the combination of immune plasmas

Although plasmas from chickens immunized with each of three antigens identified in this study exhibited anti-PRM properties, their acaricidal effects on adults were limited. In ticks, several studies have demonstrated that the "cocktail vaccine", which combines different vaccine antigens, potentially have enhanced acaricidal efficacy than single antigen-based vaccines [Almazán *et al*., 2012; Pérez-Sánchez *et al*., 2019]. Therefore, the acaricidal effects of the combined use of immune plasmas were examined. The plasmas from Dg-Cys-his-immunized chickens were mixed with those from chickens immunized with Dg-Ctr1-N-his or Dg-APMAP-N-his, and their acaricidal effects on adult PRMs were evaluated. In the assessment using the immune plasmas against Dg-Cys and Dg-Ctr1, the immune plasmas against Dg-Cys-his showed significant reduction in the SR at days 5 and 7 post-feeding compared to the control plasmas, whereas no acaricidal effect was observed in PRMs fed on the immune plasmas against Dg-Ctr1 (Table III-15 and Figure III-16A). Remarkably, PRMs fed on the mixed plasmas containing antibodies against both Dg-Cys and Dg-Ctr1 exhibited significant reduction in the SR at 7 and 9 days post-feeding compared to those fed on the control plasmas. In addition, at 10 days post-feeding, the SR of PRMs fed on the mixed plasmas was lower than those of PRMs fed on single immune plasmas against each antigen (Dg-Cys, 10% lower; Dg-Ctr1, 18 % lower), although the differences were not statistically significant (Table III-15 and Figure III-16A). In the evaluation of the immune plasmas of Dg-Cys and Dg-APMAP, the single treatment of immune plasmas against each antigen did not elicit acaricidal effects (Table III-16 and Figure III-16B). Conversely, the combination of the plasmas exhibited a prominent reduction in the SR from 8 days post-feeding compared to those of PRMs fed on Dg-Cys-his-immunized plasmas. Furthermore, the SR of PRMs fed on the plasmas cocktail was significantly lower than those of all of the other groups at day 10-post feeding (Table III-16 and Figure III-16B). Taken together, these data show that the cocktail vaccine have a great potential as an effective control strategy of PRMs.

Table III-4. Gene expression profiles of vaccine antigen candidates tested in this study.

	FPKM value[a]		Predicted motifs/domains[b]	*p* value	FDR[c]
	Blood-fed	Starved			
Dg-Cys	168.82	116.68	Proteinase inhibitor I25, cystatin, conserved site	0.177	0.244
Dg-Ctr1	102.55	377.99	Ctr copper transporter	0.023	0.050
Dg-APMAP	38.22	0.66	Strictosidine synthase	8.65E-14	5.25E-12

(a) FPKM: Fragment per kilobase of exon per million mapped reads.
(b) The motifs/domains were predicted using the InterProScan program v5.32-71.0.
(c) FDR: False discovery rate.

(A)

```
   1 CAGCGTTTCTCTACACATTTTCGATATGCAAAGCAACCGCGTCAATAGCAGCAGCAACAT  60

  61 CAGCAGCAGAAACAGTCATAACAACAACACCTGCGGCAGCCAGCAGTGCAACTGACAGTG 120

 121 GAATCAACACGATCGCAACATCGACAACTTTGACTTCTACAACAAAGTACCGCCGAAACC 180

 181 TTCAGCGCGAGCAACATGGCGCGCGTGTTTATTCGTACTGCTGCTGCTGTTGCAGCCGCC 240
   1                M  A  R  V  F  I  R  T  A  A  A  V  A  A  A  15

 241 TTGCAGTTTGTAGTGATCGGTCTTTGCCTTCCAGTCGAGGCTGGCCTTTCGGACGTGGCC 300
  16  L  Q  F  V  V  I  G  L  C  L  P  V  E  A  G  L  S  D  V  A  35

 301 GTGTCACAGTGCGAGCCATCGTTTGGGATTTCCGGTACCGAAACTCATCTCCTGGGCGGT 360
  36  V  S  Q  C  E  P  S  F  G  I  S  G  T  E  T  H  L  L  G  G  55

 361 TTCACCAACGTCGACTGTGGCAGCGAGATTGTTCAAAAACTCGCGGCGGCTGCCGATCTC 420
  56  F  T  N  V  D  C  G  S  E  I  V  Q  K  L  A  A  A  A  D  L  75

 421 GAACCCGCAGAGGTGTACGCGGTCACCAGCCAGCTGGTAGCCGGAAGGAAGTACGTGTTG 480
  76  E  P  A  E  V  Y  A  V  T  S  Q  L  V  A  G  R  K  Y  V  L  95

 481 TTCGTTGAGGTGTCGGGCAGTTGTTACCGAGTGCCCGTTTGGAGCAAGCTAGACCAAACG 540
  96  F  V  E  V  S  G  S  C  Y  R  V  P  V  W  S  K  L  D  Q  T 115

 541 GTCTCCGTACTGTCGGACGAAATCTGCCGCGACCAAGACCATTGCTCGGCTGTTCCGGTG 600
 116  V  S  V  L  S  D  E  I  C  R  D  Q  D  H  C  S  A  V  P  V 135

 601 AAGCGGTGCGAGAATTAAATTCTATTCTAGTCGTACGAAAAAAAAAAAAAAAAAAAAAAA 660
 136  K  R  C  E  N  *                                           141

 661 AAAAAAAAA 669
```

(B)

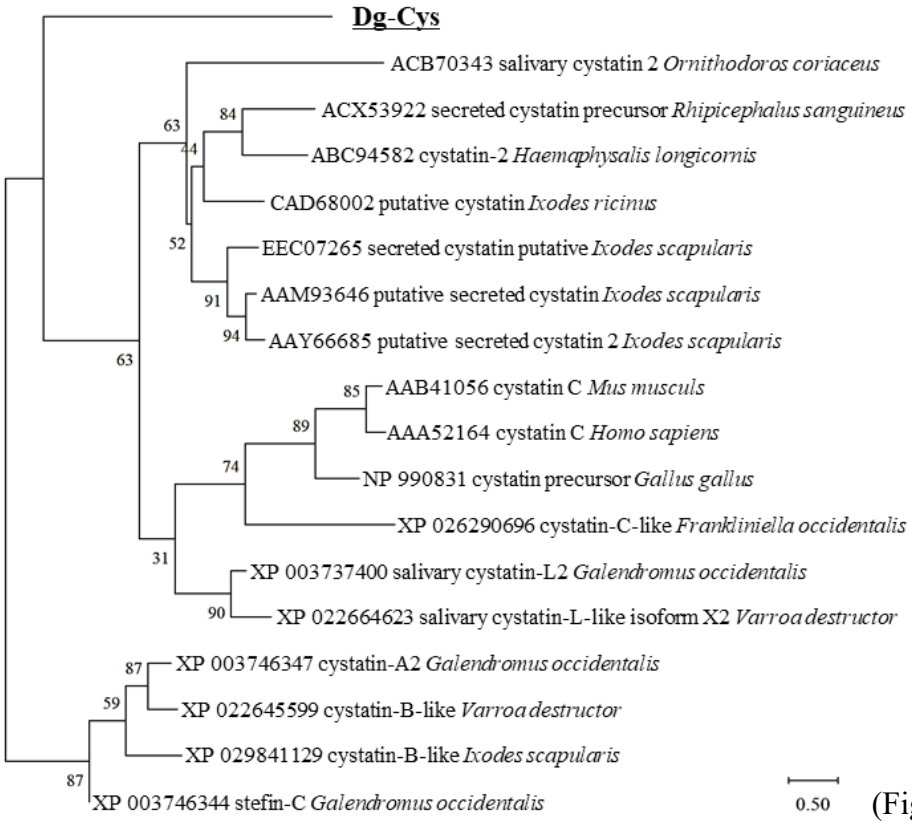

(Figure III-2 continued)

Figure III-2. Cloning of a cystatin-like molecule from *Dermanyssus gallinae*.
(A) Nucleotide and deduced amino acid sequences of cDNA encoding a *D. gallinae* cystatin-like molecule (*Dg-Cys*). Putative signal peptide sites were underlined, and the cystatin-conserved site was boxed. (B) A phylogenic tree based on the deduced amino acid sequence of *Dg-Cys*. The tree was built with the maximum likelihood method using the MEGA X software [Kumar *et al*., 2018]. Numbers indicate bootstrap percentage (1,000 replicates). The scale indicates the divergence time.

(A)

```
  1 ATGGACTATGTGCCAGACTCGCACCCGGCCGGCGATATGGACCACAGTAACCACGAAGGA 60
  1  M  D  Y  V  P  D  S  H  P  A  G  D  M  D  H  S  N  H  E  G  20

 61 CACGACCATAACGAAGGAGATCACTCGATGATGATGCAAATGACTTTCTATGCCTCGTCA 120
 21  H  D  H  N  E  G  D  H  S  M  M  M  Q  M  T  F  Y  A  S  S  40

121 GTAGTCACCATCCTGTTTGACGGGTGGAAGACACAAAATGCTGCACAAATGTTTGGTTCG 180
 41  V  V  T  I  L  F  D  G  W  K  T  Q  N  A  A  Q  M  F  G  S  60

181 TGCCTAGCCGTGTTTGCCCTGGCTGTCCTGTTTGAGGGCCTGCGGGCGTATCGGGAGCAC 240
 61  C  L  A  V  F  A  L  A  V  L  F  E  G  L  R  A  Y  R  E  H  80

241 CTCTACGTAAAGACGCGCAGCGAAAGCAGCACGTCTCTTGTCGACAGCCAAAACCAGTGG 300
 81  L  Y  V  K  T  R  S  E  S  S  T  S  L  V  D  S  Q  N  Q  W  100

301 CTCATGGCCATGTTAGCCACGCGGCATCTTGCCCAAACGGCTCTCTACGGACTTCAGATC 360
101  L  M  A  M  L  A  T  R  H  L  A  Q  T  A  L  Y  G  L  Q  I  120

361 ACACTTGGCTACATGTTGATGCTCATCTTCATGACTTACAATGTCTACGTGTGCATTGCC 420
121  T  L  G  Y  M  L  M  L  I  F  M  T  Y  N  V  Y  V  C  I  A  140

421 GTTGTGCTCGGGGCTACCTTCGGCTTTTTGCTGTTCGGCTGCAGAAAGTGGACCATCCTT 480
141  V  V  L  G  A  T  F  G  F  L  L  F  G  C  R  K  W  T  I  L  160

481 GAGATGACCTCGGATCACTGCGGATGA 507
161  E  M  T  S  D  H  C  G  *  169
```

(B)

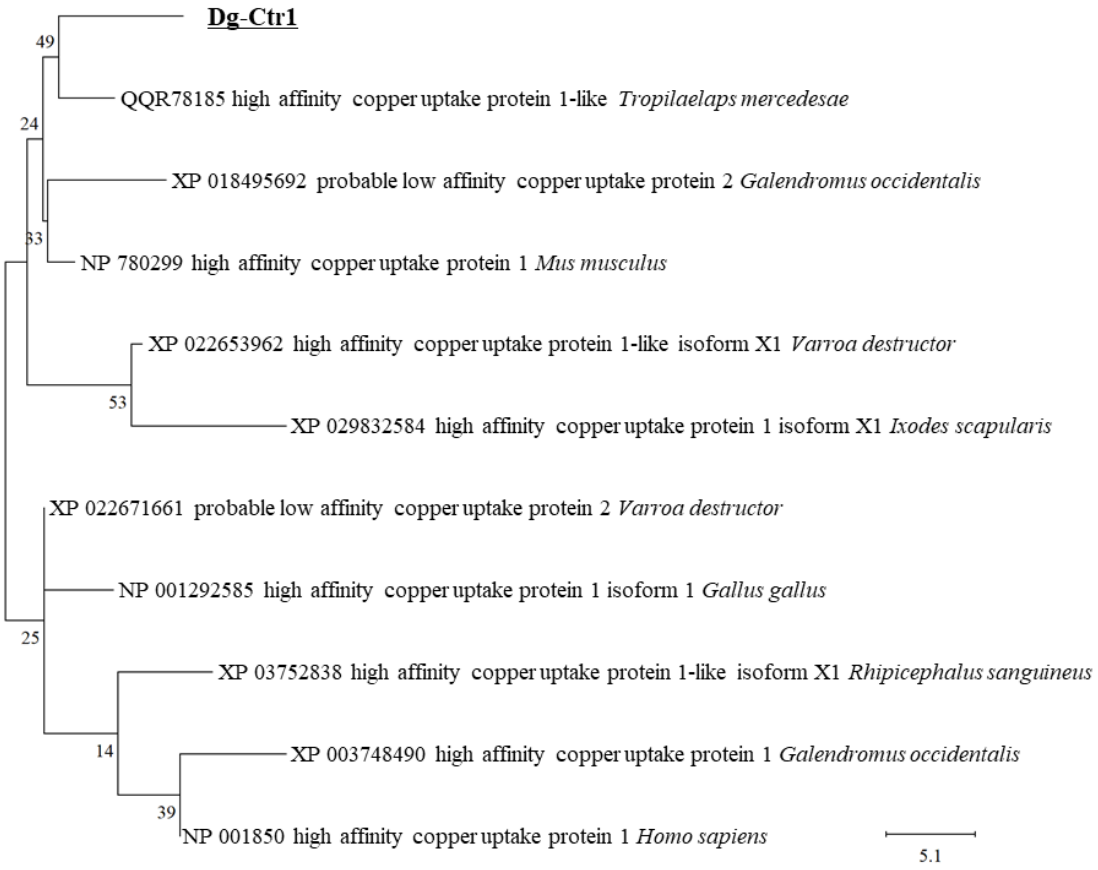

(Figure III-3 continued)

Figure III-3. Cloning of a copper transporter 1-like molecule from *Dermanyssus gallinae*.

(A) Nucleotide sequences and deduced amino acid sequences of cDNA encoding *D. gallinae* copper transporter 1-like molecule (*Dg-Ctr1*). Putative transmembrane sites were underlined. (B) A phylogenic tree based on the deduced amino acid sequence of *Dg-Ctr1*. The tree was built with the maximum likelihood method using the MEGA X software [Kumar *et al*., 2018]. Numbers indicate bootstrap percentage (1,000 replicates). The scale indicates the divergence time.

(A)

```
1   ATGTATAAACTGGTGAAACTTCAGCTCCAGCTGGTTTTCGTATCGCTGCTGGCTTTACTGAGCCTCCCGTTTATGCCCATTCCGCTCGAC  90
1   M  Y  K  L  V  K  L  Q  L  Q  L  V  F  V  S  L  L  A  L  L  S  L  P  F  M  P  I  P  L  D  30

91  TTTGATCCGGCCGCCTACAATGTGACGTTGCCCGCCTTCGAGGGCGTCCTAGCACCGAACGATGCGCTCGACCGGGCCAAGATGCTCTTC  180
31  F  D  P  A  A  Y  N  V  T  L  P  A  F  E  G  V  L  A  P  N  D  A  L  D  R  A  K  M  L  F  60

181 CAGCAGCGGCTGCGCGGTCCTGAGTCGCTAGCCGTCAAAGACGGGCTCATCTACACCGGAACCCAGTTCGGGGACGTGTTTGCTATCGAT  270
61  Q  Q  R  L  R  G  P  E  S  L  A  V  K  D  G  L  I  Y  T  G  T  Q  F  G  D  V  F  A  I  D  90

271 CCCGTTAAGGAGACTCTAACAAAGGTAGCGAATACGGGAAGTAGTTGCAACGGTTTGCACGACGAGGAAAAATGCGGACGGGTACTTGGA  360
91  P  V  K  E  T  L  T  K  V  A  N  T  G  S  S  C  N  G  L  H  D  E  E  K  C  G  R  V  L  G  120

361 CTTCGCTTTGCGCCTAATGGTGATCTTTATGCTGCCGACGCCTACAAGGGACTGCTGAAAATCGATATCAAGACAGGCAAGGTCGAGACG  450
121 L  R  F  A  P  N  G  D  L  Y  A  A  D  A  Y  K  G  L  L  K  I  D  I  K  T  G  K  V  E  T  150

451 CTGGTGGCCAGTGGATCGTACGTGGGAACGTCGAAACTGCTATTTGCCGACGATCTCGATATCGACAACAATGGCGTTATCTACTATTCG  540
151 L  V  A  S  G  S  Y  V  G  T  S  K  L  L  F  A  D  D  L  D  I  D  N  N  G  V  I  Y  Y  S  180

541 CAAGGAAGTTGCCGTTGGGGGCTTCACCAAATCCTGTACATCATCATGGAATTCGATACCACTGGAAGGATCCTGACCTACGACACGAAG  630
181 Q  G  S  C  R  W  G  L  H  Q  I  L  Y  I  I  M  E  F  D  T  T  G  R  I  L  T  Y  D  T  K  210

631 ACAAAGAAGAGCGGAGTTCTCCTCGAAGGACTGGCCTTTCCGAACGGCGTTCAGCTGACAGAAGACCGAAGCGCACTGCTCTTCTCCGAG  720
211 T  K  K  S  G  V  L  L  E  G  L  A  F  P  N  G  V  Q  L  T  E  D  R  S  A  L  L  F  S  E  240

721 CTCGGAAAGAAGCGCATCATGAAGTACCAGCTGACAGGCGCCACTAAGGGTAAGTTGACGGTATTTGCCGAAAACCTGCCCGGTGGTCCG  810
241 L  G  K  K  R  I  M  K  Y  Q  L  T  G  A  T  K  G  K  L  T  V  F  A  E  N  L  P  G  G  P  270

811 GATAATCTGCGCCGATCGCCTCGCGGAACATACTGGGTGGGCATCGATATTGCCCGCTCGAACACAACGCAGCCCCTCGGCGATCTGATC  900
271 D  N  L  R  R  S  P  R  G  T  Y  W  V  G  I  D  I  A  R  S  N  T  T  Q  P  L  G  D  L  I  300

901 GCCCCGTATCCGCTCGTGGCCAAGGCGACTATGCGATTTTGCTGGTTGACGGGTCAGGCTCTCAAACAGATTGACAGCTTCGTAGATCAT  990
301 A  P  Y  P  L  V  A  K  A  T  M  R  F  C  W  L  T  G  Q  A  L  K  Q  I  D  S  F  V  D  H  330

991 CCAACGCTCCAGGATCTCAGCGCCGATTTTGAGCACGGAAAGATCCTGATCAATACGGTACCAAATCGGGGTATCATTCTCGAGCTGGGT  1080
331 P  T  L  Q  D  L  S  A  D  F  E  H  G  K  I  L  I  N  T  V  P  N  R  G  I  I  L  E  L  G  360

081 CCTGACGGAAAAATACTTCGAAGCCTCCATTCGTCACACTACACGCTCTTTTCGGAGGTTTTAGAATACGGTGGACACCTCTACATTGGC  1170
361 P  D  G  K  I  L  R  S  L  H  S  S  H  Y  T  L  F  S  E  V  L  E  Y  G  G  H  L  Y  I  G  390

171 TCGTTCATTAAGCCCTATCTCTTACGTTTGAAACATAAGTAA  1212
391 S  F  I  K  P  Y  L  L  R  L  K  H  K  *  404
```

(B)

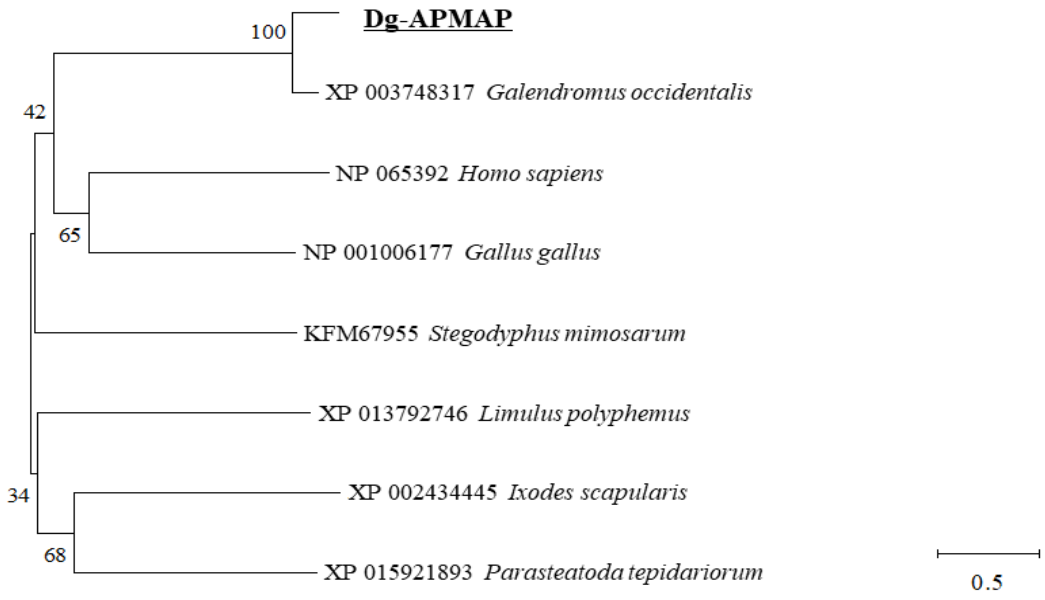

(Figure III-4 continued)

Figure III-4. Cloning of an adipocyte plasma membrane-associated protein-like molecule from *Dermanyssus gallinae*.

(A) Nucleotide sequences and deduced amino acid sequences of cDNA encoding *D. gallinae* adipocyte plasma membrane-associated protein-like molecule (*Dg-APMAP*). Putative transmembrane sites were underlined. (B) A phylogenic tree based on the deduced amino acid sequence of *Dg-APMAP*. The tree was built with the maximum likelihood method using the MEGA X software [Kumar *et al*., 2018]. Numbers indicate bootstrap percentage (1,000 replicates). The scale indicates the divergence time.

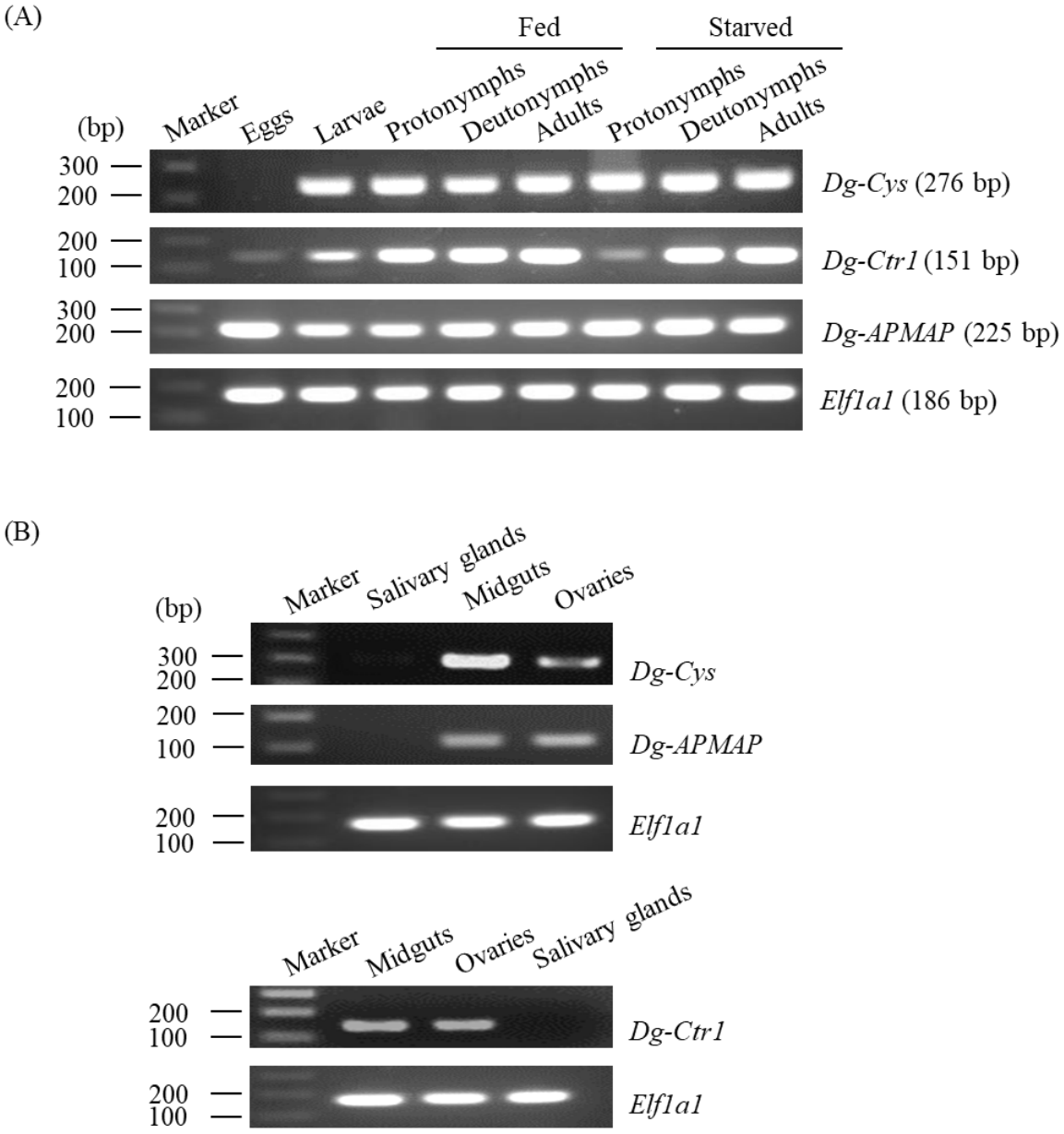

Figure III-5. Gene expression analyses of each antigen candidate.

mRNA expressions of *Dg-Cys*, *Dg-Ctr1*, and *Dg-APMAP* were analyzed by RT-PCR/nested PCR for (A) each life stage and blood-feeding state and (B) tissue type (salivary glands, ovaries, and midguts). *Elf1a1* was amplified as an internal control.

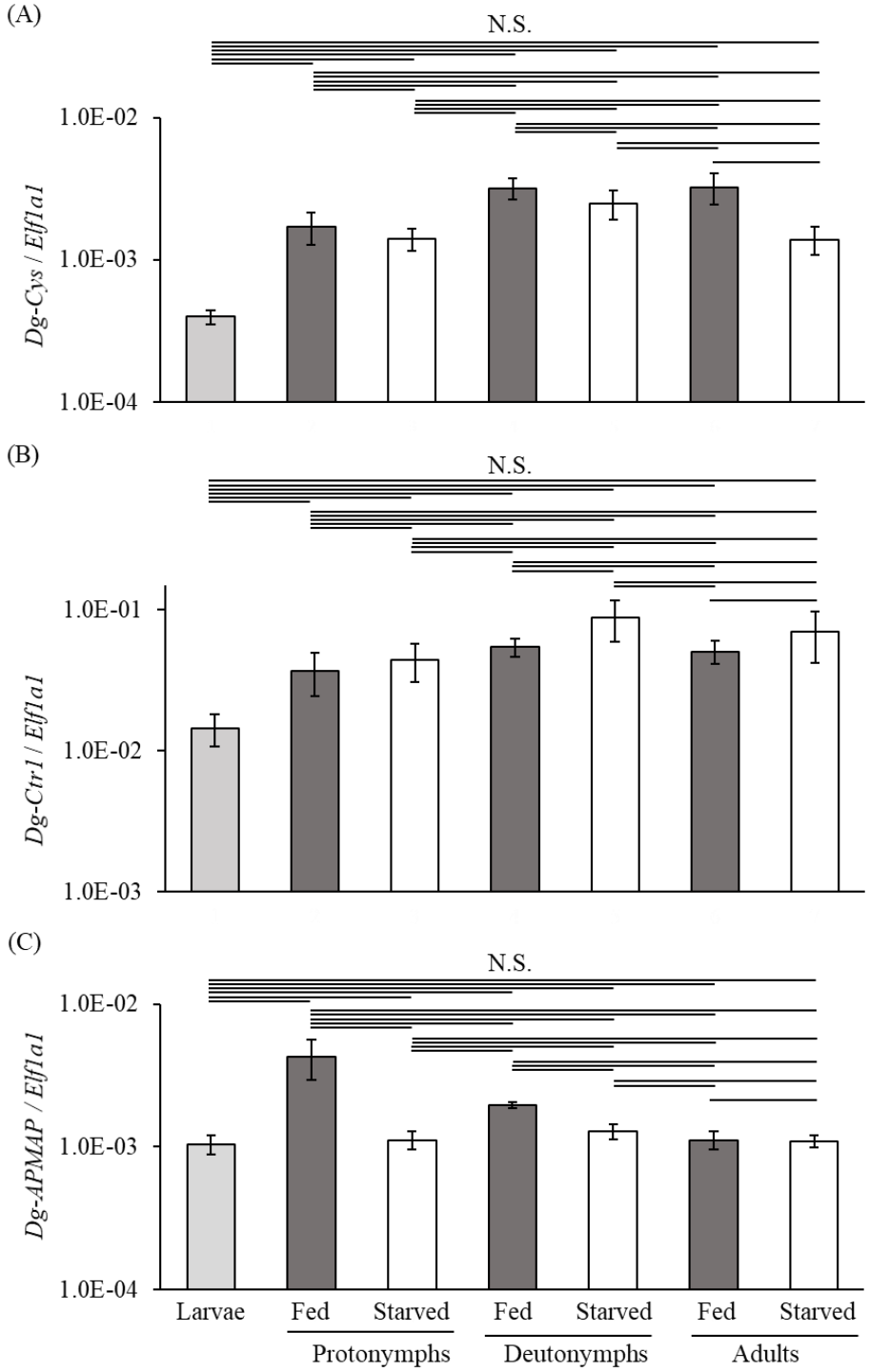

Figure III-6. Gene expression profiles of antigen candidates.

qRT-PCR was performed to quantify the mRNA expression of (A) *Dg-Cys*, (B) *Dg-Ctr1*, and (C) *Dg-APMAP* at each life stage and feeding state. *Elf1a1* was amplified as an internal control. The extent of the expression of each target gene was calculated by dividing the copy numbers of each target by those of *Elf1a1*. Error bars indicate standard error of the mean.

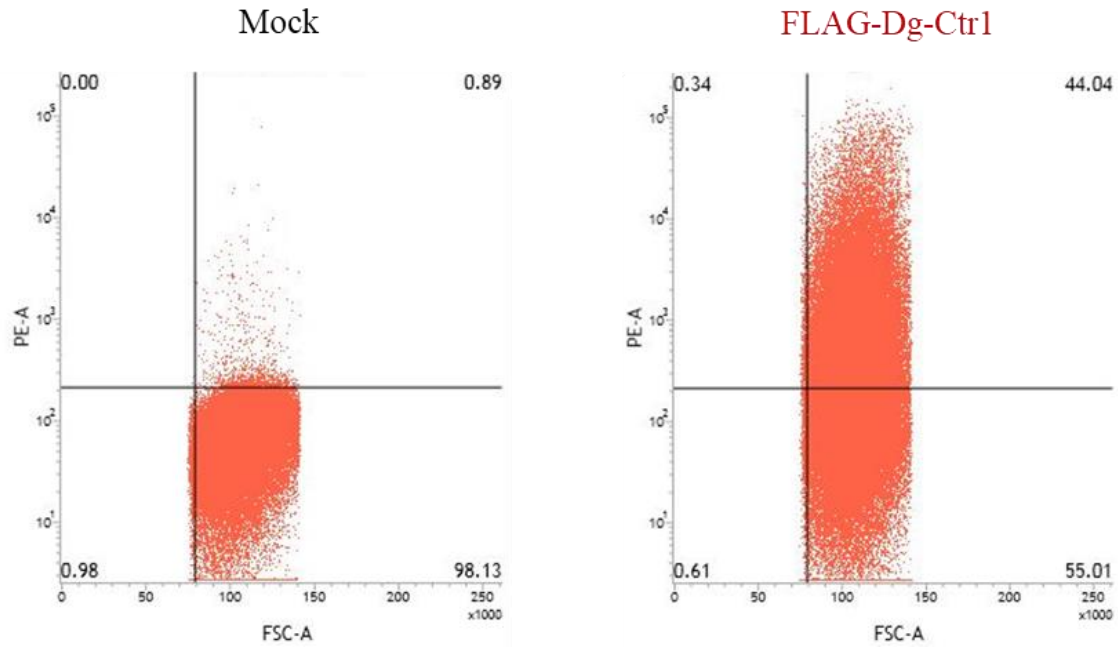

Figure III-7. Expression of Dg-Ctr1 on the plasma membrane.

FLAG epitope-tagged recombinant protein of Dg-Ctr1 (FLAG-Dg-Ctr1) was expressed in Sf9 insect cells. The expression of Dg-Ctr1 on the plasma membrane was confirmed by flow cytometric analysis.

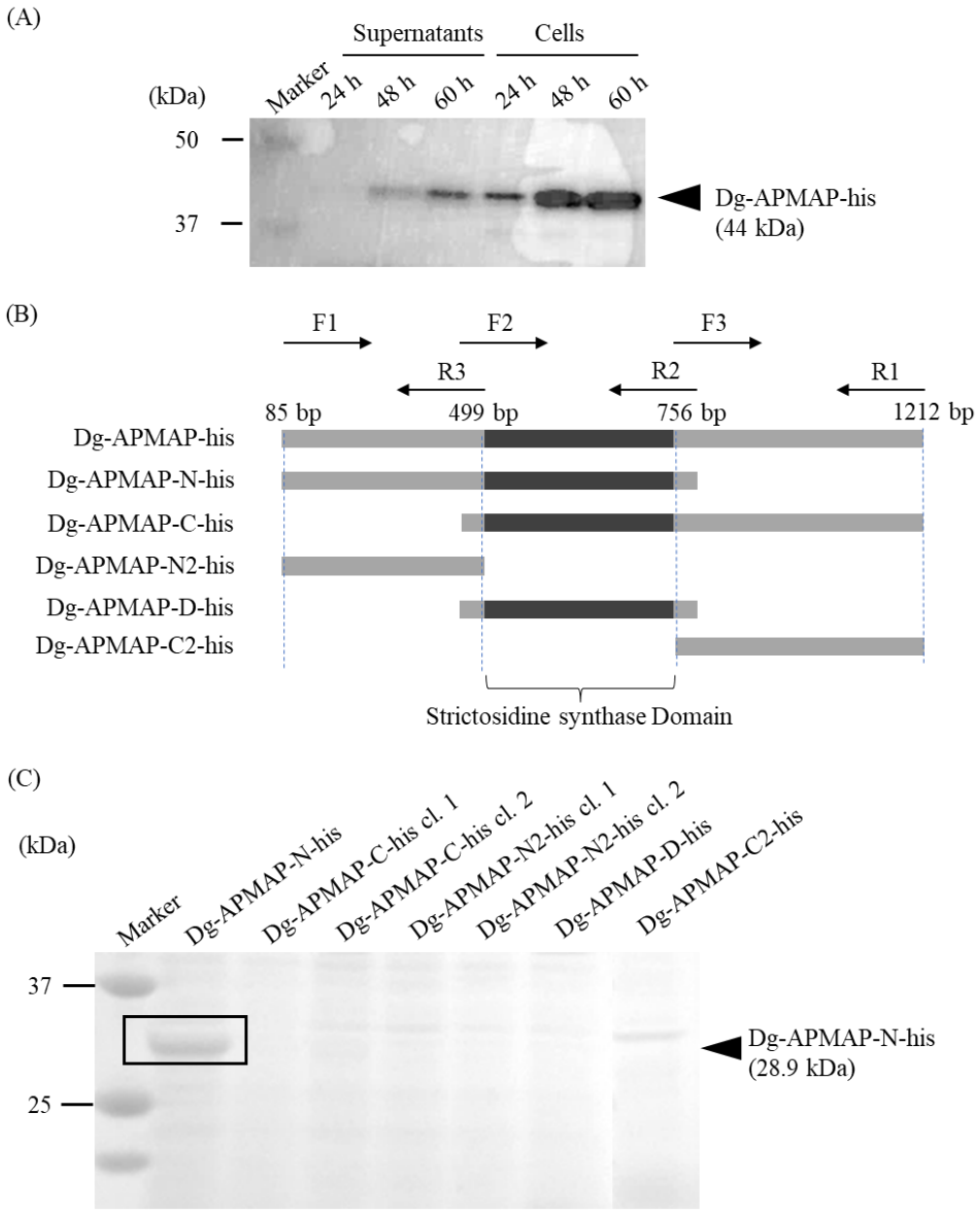

Figure III-8. Expression of recombinant protein of Dg-APMAP.

(A) The recombinant protein of the extracellular domain of Dg-APMAP (Dg-APMAP-his) was expressed using the BIC system. Culture supernatants and bacterial fractions at 24, 48, and 60 h after cultivation were applied to western blotting to confirm the expression of Dg-APMAP-his. (B) The truncated extracellular domain of Dg-APMAP and the expression plasmids encoding each fragment. Arrows indicate primers used to amplify the target fragments (see also Table III-3). (C) The recombinant proteins prepared using the BIC system. Secretion of the proteins into the cultural supernatants was confirmed by SDS-PAGE.

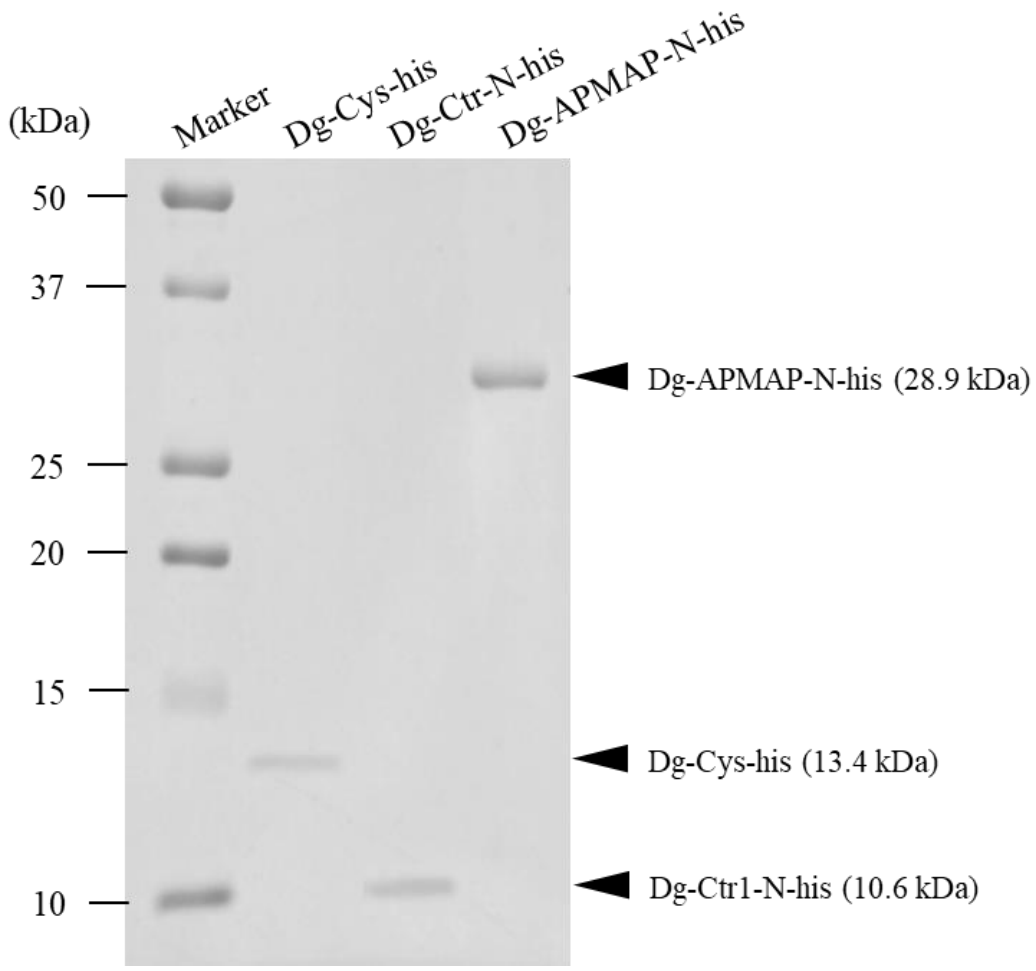

Figure III-9. Preparation of the recombinant proteins.

The recombinant proteins of Dg-Cys (Dg-Cys-his), N-terminal extracellular domain of Dg-Ctr1 (Dg-Ctr1-N-his), and N-terminal side of the extracellular domain of Dg-APMAP (Dg-APMAP-N-his) were prepared using BIC system. Purified proteins were separated by SDS-PAGE and visualized by staining with Coomassie brilliant blue.

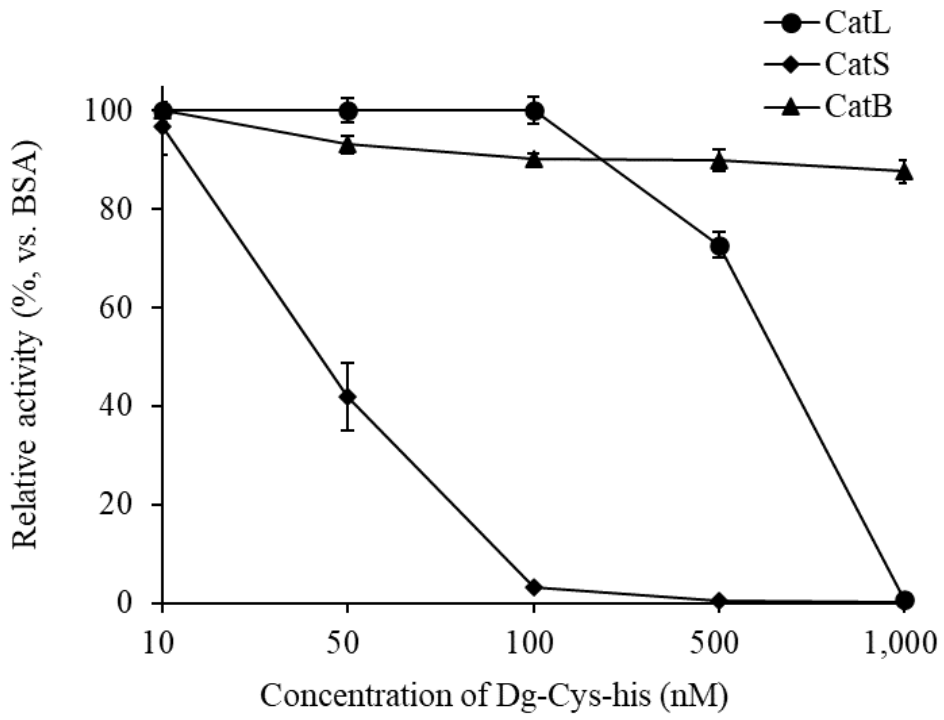

Figure III-10. Functional analysis of recombinant Dg-Cys.

Inhibitory properties of Dg-Cys-his against cysteine proteases were assessed. Cathepsins L, S, and B were incubated with their fluorometric substrates in the presence of Dg-Cys-his or bovine serum albumin (BSA). The X-axis indicates the concentrations of Dg-Cys-his, and the Y-axis indicates relative enzymatic activities of each cysteine protease in the presence of Dg-Cys-his compared to those incubated with BSA. The experiments were performed in triplicate, and error bars indicate ±standard error of the mean.

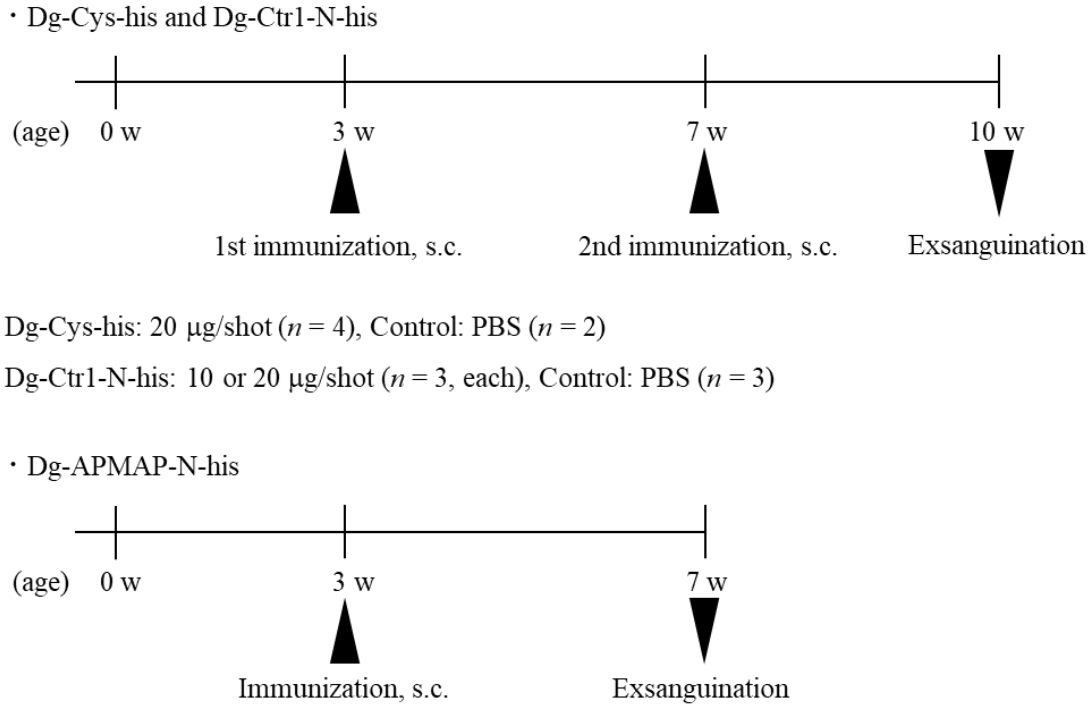

Figure III-11. The schedule of immunization and sample collection.

Chickens were immunized with the recombinant proteins to provide immune plasmas. Each recombinant protein was mixed with light liquid paraffin adjuvant and immunized subcutaneously. An emulsion of PBS with light liquid paraffin was prepared as a control. Four weeks later, heparinized blood was collected from unimmunized and Dg-APMAP-N-his-immunized chickens, and chickens immunized with Dg-Cys-his, Dg-Ctr1-N-his, or PBS were immunized with the same doses of Dg-Cys-his, Dg-Ctr-N-his, or PBS. The heparinized blood was collected 3 weeks after second immunization.

Table III-5. Antibody titers in the plasmas from chickens immunized with the recombinant proteins.

Group	Chicken	Antibody titer
Dg-Cys-his		
Control	PBS-Cys1	< 1,000
	PBS-Cys2	< 1,000
Immunized	Cys1	2,000
	Cys2	8,000
	Cys3	1,000
	Cys4	16,000
Dg-Ctr1-N-his		
Control	PBS-Ctr1	< 1,000
	PBS-Ctr2	< 1,000
	PBS-Ctr3	< 1,000
Immunized	Ctr1	< 1,000
	Ctr2	4,000
	Ctr3	32,000
	Ctr4	4,000
	Ctr5	> 64,000
	Ctr6	> 64,000
Dg-APMAP-N-his		
Control	UN1	< 1,000
	UN2	< 1,000
	UN3	< 1,000
	UN4	< 1,000
Immunized	APM1	64,000
	APM2	64,000
	APM3	64,000
	APM4	64,000

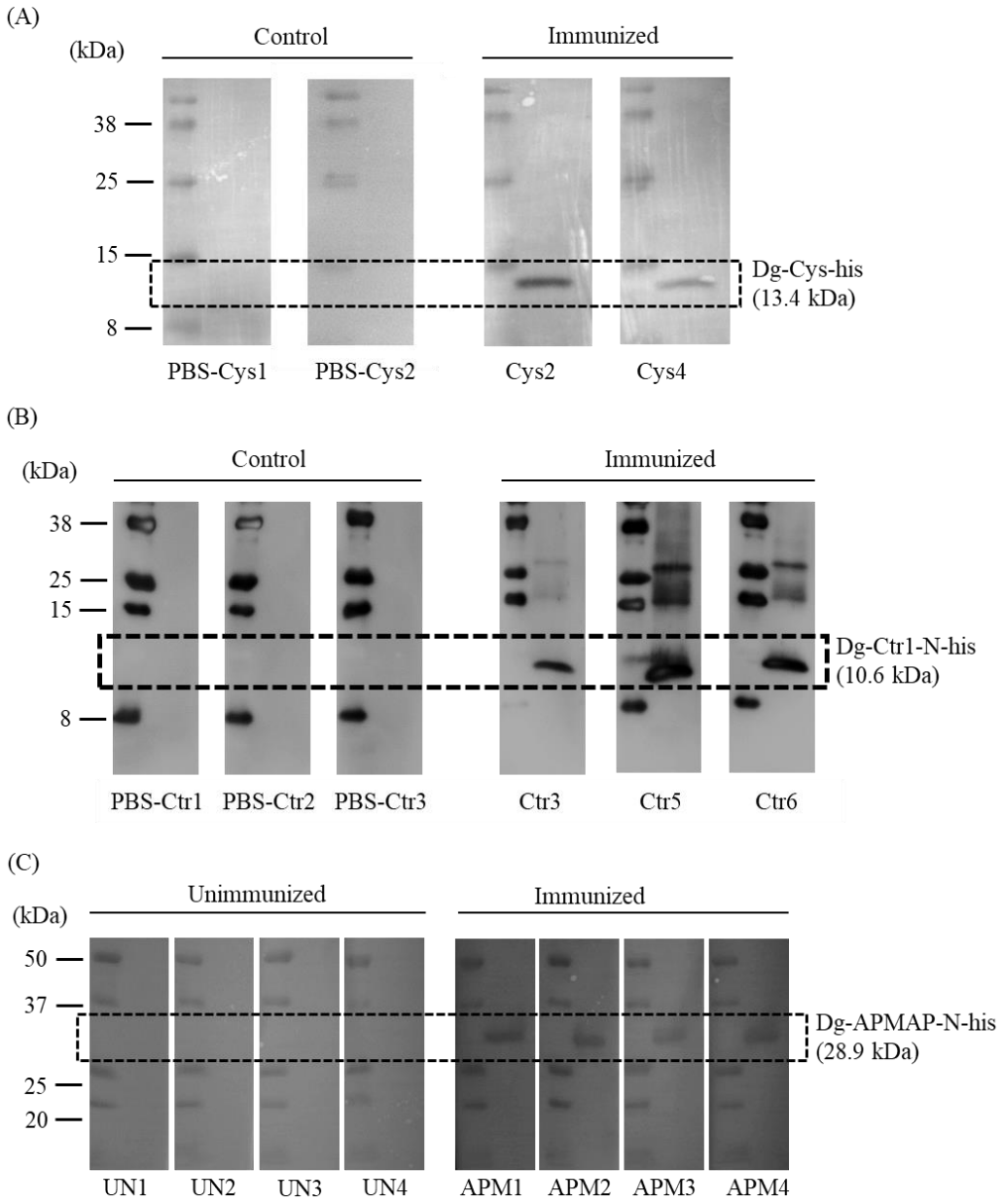

Figure III-12. Production of the specific antibodies against each antigen in immunized chickens.

Production of the specific antibodies against (A) Dg-Cys-his, (B) Dg-Ctr1-N-his, and (C) Dg-APMAP-N-his in immunized chickens was examined. The recombinant proteins were reacted with the plasmas from immunized chickens (A: Cys2 and Cys4; B: Ctr3, Ctr5, and Ctr6; C: APM1–4) and control chickens (A: PBS-Cys1 and PBS-Cys2; B: PBS-Ctr1–3; C: UN1–4) by western blotting. The predicted molecular sizes of Dg-Cys-his, Dg-Ctr1-N-his, and Dg-APMAP-N-his are approximately 13.4, 10.6, and 28.9 kDa, respectively, and the specific signals were detected in the plasmas from the immunized chickens.

Table III-6. Summary of anti-PRM property of Dg-Cys-his immunization (First experiment).

	Days post-feeding							RC
	1	2	3	4	5	6	7	
Immunized (n = 255, nymphs: n = 38, adults: n = 219)								
No. of dead PRMs	5	12	16	21	35	38	45	1.29
SR (%)	98.04	95.29	93.73	91.76	86.27	85.10	82.35	
Control (n = 211, nymphs: n = 51, adults: n = 160)								
No. of dead PRMs	1	4	13	15	23	26	37	2.24
SR (%)	99.53	98.10	93.84	92.89	89.10	87.68	82.46	
p value	0.228	0.126	1	0.729	0.399	0.499	1	2.38E-05*
Odds ratio	4.19	2.55	1.01	1.17	1.30	1.25	1.01	0.57
95% CI (lower limit)	0.46	0.76	0.45	0.56	0.72	0.71	0.61	0.44
95% CI (upper limit)	199.39	11.02	2.36	2.52	2.39	2.22	1.68	0.75

The data are compared by Fisher's exact test between immunized and control groups.
SR, survival rate; RC, reproductive capacity.
*$p < 0.05$ was considered statistically significant.

Table III-7. Summary of anti-PRM property of Dg-Cys-his immunization (Second experiment).

	Days post-feeding						
	1	2	3	4	5	6	7
Immunized (n = 189, all nymphs)							
No. of dead PRMs	5	6	10	13	34	57	74
SR (%)	97.35	96.83	94.71	93.12	82.01	69.84	60.85
Control (n = 150, all nymphs)							
No. of dead PRMs	1	3	4	4	14	28	38
SR (%)	99.33	98.00	97.33	97.33	90.67	81.33	74.67
p value	0.233	0.736	0.280	0.085	0.028*	0.017*	0.008*
Odds ratio	4.04	1.60	2.04	2.69	2.13	1.88	1.89
95% CI (lower limit)	0.44	0.34	0.57	0.81	1.06	1.09	1.16
95% CI (upper limit)	192.59	10.08	9.07	11.57	4.48	3.28	3.13

The data are compared by Fisher's exact test between immunized and control groups.
SR, survival rate.
*$p < 0.05$ was considered statistically significant.

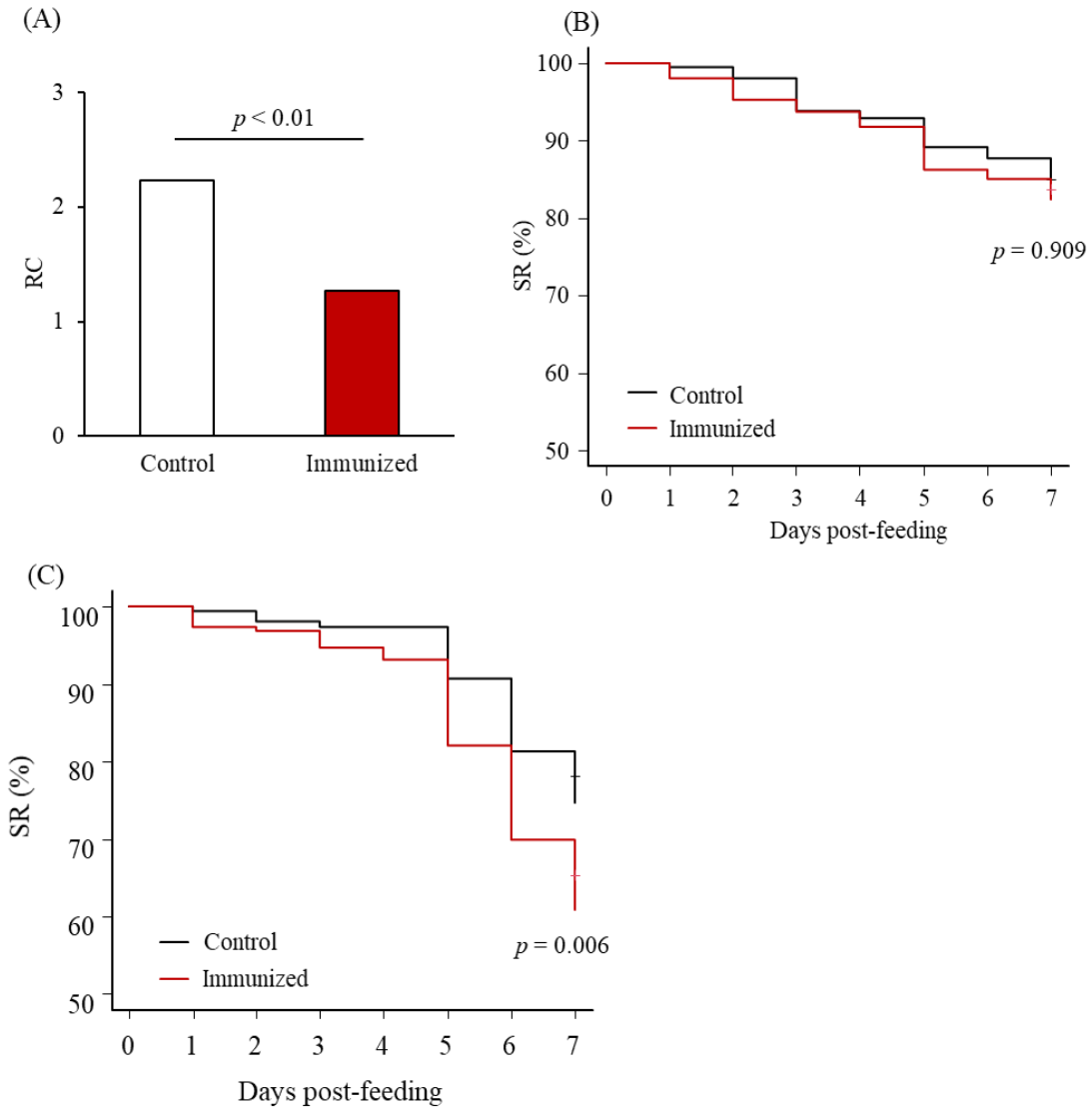

Figure III-13. Anti-PRM effects of plasmas from chickens immunized with Dg-Cys-his.

Anti-PRM properties of Dg-Cys-his immunization were examined by the *in vitro* feeding assay (A and B: first experiment, C: second experiment). (A) The reproductive capacity (RC) at 7 days post-feeding was assessed. Statistical analysis was performed using Fisher's exact test. (B and C) The survival rate (SR) of PRMs fed with the plasmas from immunized chickens was assessed every day for a 1-week period. The Kaplan-Meier Curves were generated to indicate the survival rate of PRMs. Statistical analysis was performed using the log-rank test.

Table III-8. Summary of anti-PRM property of Dg-Ctr1-N-his immunization (First experiment).

	Days post-feeding									
	1	2	3	4	5	6	7	8	9	10
Immunized (n = 167, nymphs)										
No. of dead PRMs	1	3	10	14	30	50	75	102	125	134
SR (%)	99.40	98.20	94.01	91.62	82.04	70.06	55.09	38.92	25.15	19.76
Control (n = 98, nymphs)										
No. of dead PRMs	0	4	5	7	12	19	31	39	49	61
SR (%)	100	95.92	94.90	92.86	87.76	80.61	68.37	60.20	50.00	37.76
p value	1	0.429	1.000	0.817	0.296	0.061	0.037*	0.001*	5.400E-05*	0.002*
Odds ratio	-	0.43	1.18	1.19	1.57	1.77	1.76	2.37	2.96	2.45
95% CI (lower limit)	-	0.06	0.36	0.43	0.73	0.94	1.01	1.38	1.70	1.35
95% CI (upper limit)	-	2.61	4.55	3.62	3.55	3.44	3.09	4.09	5.22	4.47

The data are compared by Fisher's exact test between immunized and control groups.
SR, survival rate.
*$p < 0.05$ was considered statistically significant.

Table III-9. Summary of anti-PRM property of Dg-Ctr1-N-his immunization (Second experiment, total).

	Days post-feeding									
	1	2	3	4	5	6	7	8	9	10
Immunized (n = 252)										
No. of dead PRMs	2	13	20	26	52	87	110	137	173	192
SR (%)	99.21	94.84	92.06	89.68	79.37	65.48	56.35	45.63	31.35	23.81
Control (n = 241)										
No. of dead PRMs	6	16	26	33	47	74	102	122	145	164
SR (%)	97.51	93.36	89.21	86.31	80.50	69.29	57.68	49.38	39.83	31.95
p value	0.168	0.567	0.283	0.269	0.822	0.388	0.785	0.418	0.060	0.045*
Odds ratio	0.31	0.77	0.71	0.73	1.07	1.19	1.06	1.16	1.45	1.50
95% CI (lower limit)	0.03	0.33	0.37	0.40	0.67	0.80	0.73	0.80	0.98	0.99
95% CI (upper limit)	1.78	1.74	1.37	1.30	1.71	1.77	1.53	1.68	2.14	2.28

The data are compared by Fisher's exact test between immunized and control groups.
SR, survival rate.
*$p < 0.05$ was considered statistically significant.

Table III-10. Summary of anti-PRM property of Dg-Ctr1-N-his immunization (Second experiment, adults).

	Days post-feeding									
	1	2	3	4	5	6	7	8	9	10
Immunized (n = 95)										
No. of dead PRMs	1	7	9	10	15	22	26	32	43	55
SR (%)	98.95	92.63	90.53	89.47	84.21	76.84	72.63	66.32	54.74	42.11
Control (n = 80)										
No. of dead PRMs	1	9	13	17	21	22	30	33	36	42
SR (%)	98.75	88.75	83.75	78.75	73.75	72.50	62.50	58.75	55.00	47.50
p value	1	0.436	0.252	0.059	0.095	0.600	0.193	0.347	1	0.542
Odds ratio	0.84	0.63	0.54	0.44	0.53	0.80	0.63	0.72	1.01	1.24
95% CI (lower limit)	0.01	0.19	0.19	0.17	0.23	0.38	0.32	0.37	0.53	0.65
95% CI (upper limit)	66.76	2.01	1.46	1.09	1.18	1.67	1.25	1.40	1.92	2.36

The data are compared by Fisher's exact test between immunized and control groups.
SR, survival rate.

Table III-11. Summary of anti-PRM property of Dg-Ctr1-N-his immunization (Second experiment, nymphs).

	Days post-feeding									
	1	2	3	4	5	6	7	8	9	10
Immunized (n = 157)										
No. of dead PRMs	1	6	11	16	37	65	84	105	130	137
SR (%)	99.36	96.18	92.99	89.81	76.43	58.60	46.50	33.12	17.20	12.74
Control (n = 161)										
No. of dead PRMs	5	7	13	16	26	52	72	89	109	122
SR (%)	96.89	95.65	91.93	90.06	83.85	67.70	55.28	44.72	32.30	24.22
p value	0.215	1.000	0.833	1	0.121	0.104	0.145	0.039*	0.002*	0.009*
Odds ratio	0.20	0.87	0.86	1.03	1.60	1.48	1.42	1.63	2.29	2.18
95% CI (lower limit)	0.00	0.24	0.34	0.46	0.88	0.91	0.89	1.01	1.31	1.17
95% CI (upper limit)	1.82	3.12	2.15	2.29	2.92	2.40	2.27	2.64	4.07	4.18

The data are compared by Fisher's exact test between immunized and control groups.
SR, survival rate.
*$p < 0.05$ was considered statistically significant.

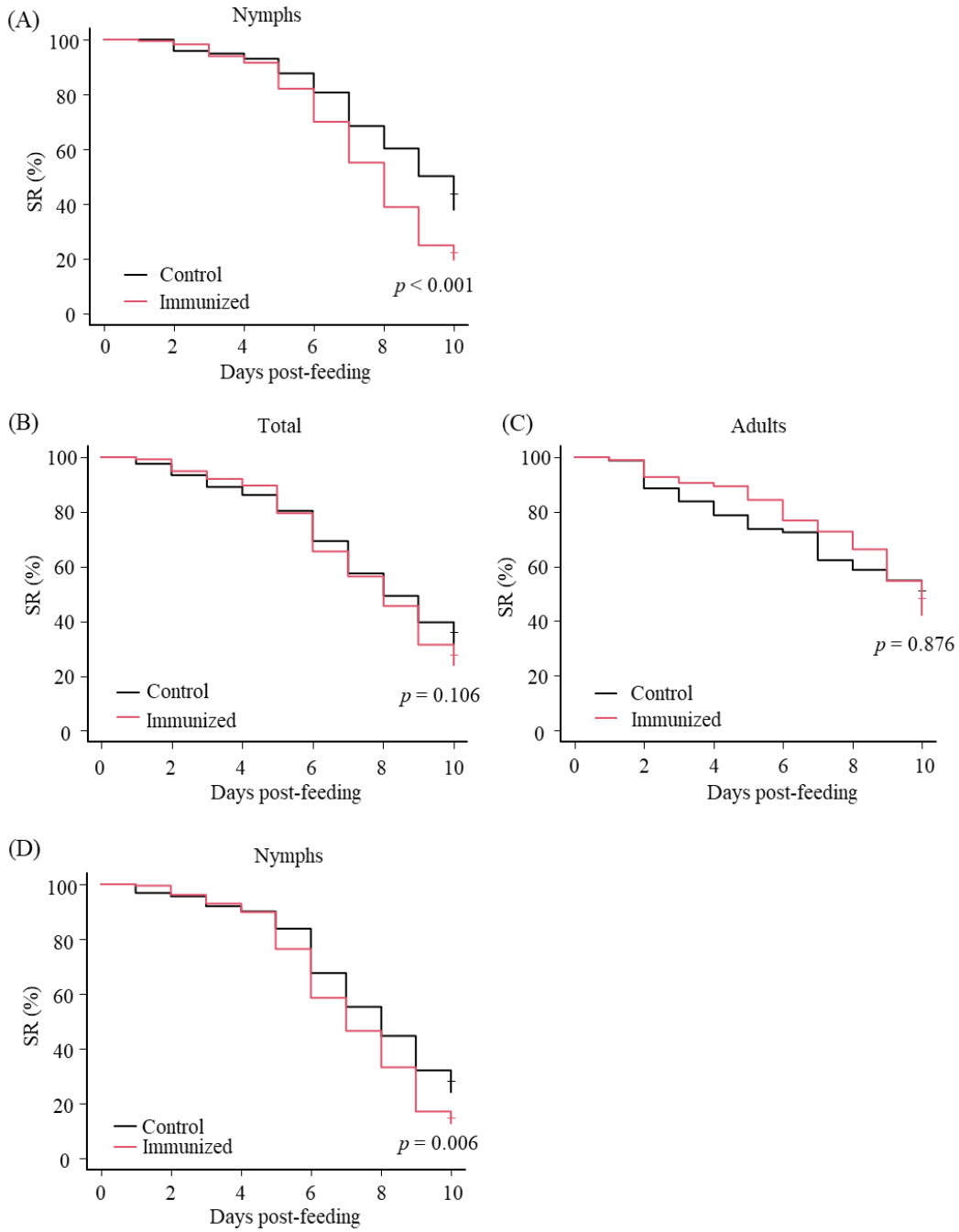

Figure III-14. Anti-PRM effects of plasmas from chickens immunized with Dg-Ctr1-N-his.

Anti-PRM properties of Dg-Ctr1-N-his immunization were examined by the *in vitro* feeding assay (A: first experiment; B–D: second experiment). The survival rate (SR) of PRMs fed with the plasma from immunized chickens was assessed every day for a 10-day period. The Kaplan-Meier Curves were generated to indicate the survival rate in total PRMs (B), adults (C), and nymphs (A and D). Statistical analysis was performed using the log-rank test.

Table III-12. Summary of anti-PRM property of Dg-APMAP-N-his immunization (total).

	Days post-feeding						
	1	2	3	4	5	6	7
Immunized (n = 181)							
No. of dead PRMs	3	7	13	38	65	85	112
SR (%)	98.34	96.13	92.82	79.01	64.09	53.04	38.12
Control (n = 210)							
No. of dead PRMs	4	12	19	27	42	59	85
SR (%)	98.10	94.29	90.95	87.14	80.00	71.90	59.52
p value	1	0.483	0.581	0.041*	9.56E-04*	1.47E-04*	3.04E-05*
Odds ratio	0.112	0.664	0.778	1.798	2.172	2.261	2.382
95% CI (lower limit)	6.563	0.217	0.342	1.016	1.352	1.459	1.557
95% CI (upper limit)	0.859	1.879	1.719	3.22	3.516	3.524	3.663

The data are compared by Fisher's exact test between immunized and control groups.
SR, survival rate.
*$p < 0.05$ was considered statistically significant.

Table III-13. Summary of anti-PRM property of Dg-APMAP-N-his immunization (adults).

	Days post-feeding							RC
	1	2	3	4	5	6	7	
Immunized (n = 65)								
No. of dead PRMs	0	2	5	11	18	29	40	0.246
SR (%)	100	96.92	92.31	83.08	72.31	55.38	38.46	
Control (n = 110)								
No. of dead PRMs	1	3	7	13	21	33	48	0.218
SR (%)	99.09	97.27	93.64	88.18	80.91	70.00	56.36	
p value	1	1	0.763	0.369	0.194	0.072	0.028*	0.722
Odds ratio	0	1.131	1.225	1.516	1.619	1.873	2.058	1.128
95% CI (lower limit)	0	0.092	0.293	0.572	0.735	0.945	1.057	0.519
95% CI (upper limit)	65.933	10.158	4.712	3.956	3.546	3.726	4.065	2.400

The data are compared by Fisher's exact test between immunized and control groups.
SR, survival rate; RC, reproductive capacity.
*$p < 0.05$ was considered statistically significant.

Table III-14. Summary of anti-PRM property of Dg-APMAP-N-his immunization (nymphs).

	Days post-feeding						
	1	2	3	4	5	6	7
Immunized (n = 116)							
No. of dead PRMs	3	5	8	27	47	56	72
SR (%)	97.41	95.69	93.10	76.72	59.48	51.72	37.93
Control (n = 100)							
No. of dead PRMs	3	9	12	14	21	26	37
SR (%)	97.00	91.00	88.00	86.00	79.00	74.00	63.00
p value	1	0.178	0.242	0.117	0.005*	1.16E-03*	3.64E-04*
Odds ratio	0.859	0.457	0.545	1.858	2.405	2.644	2.772
95% CI (lower limit)	0.112	0.116	0.184	0.872	1.275	1.439	1.546
95% CI (upper limit)	6.563	1.582	1.523	4.109	4.639	4.946	5.031

The data are compared by Fisher's exact test between immunized and control groups.
SR, survival rate.
*$p < 0.05$ was considered statistically significant.

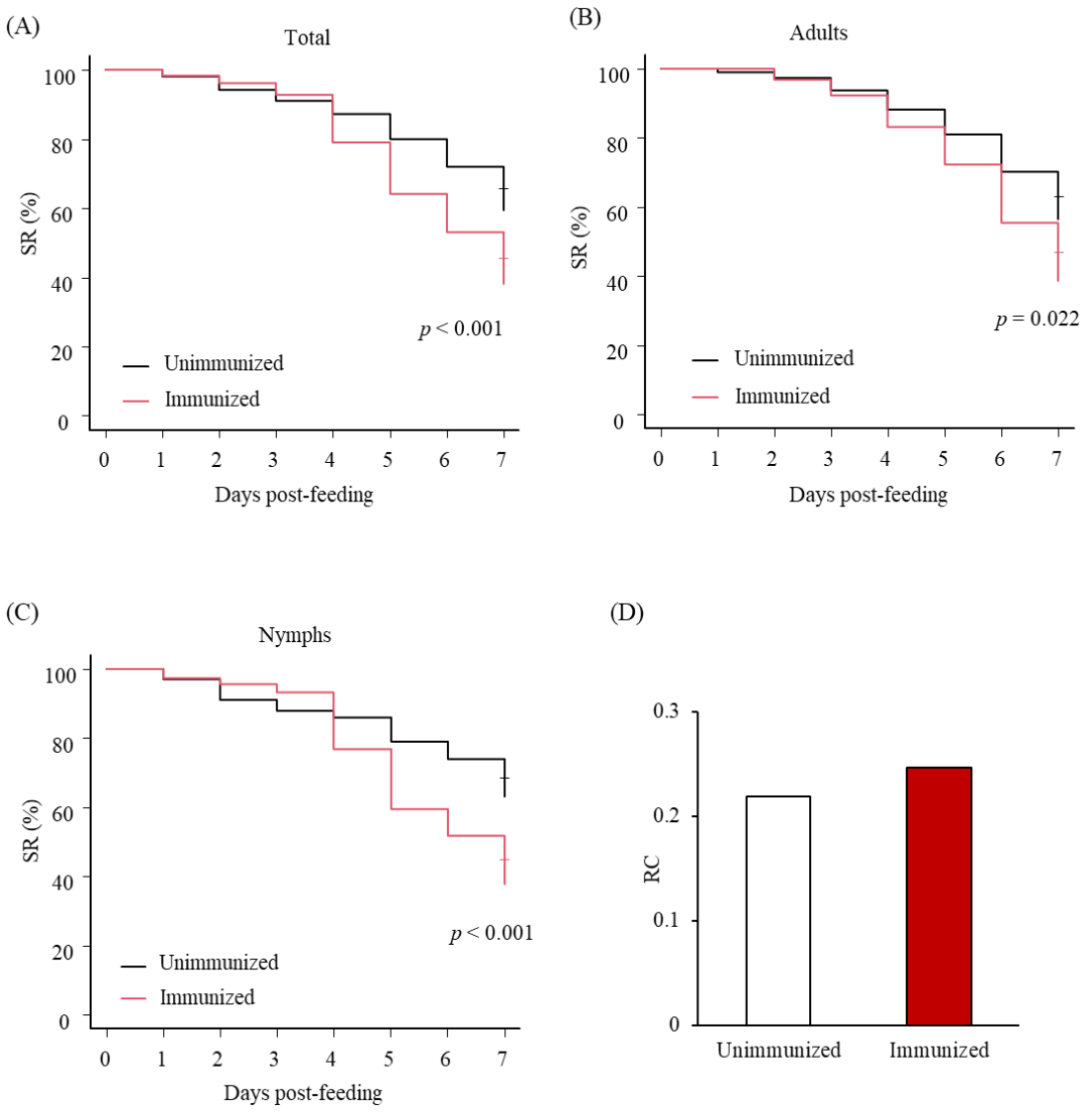

Figure III-15. Anti-PRM effects of plasmas from chickens immunized with Dg-APMAP-N-his.

Anti-PRM properties of Dg-APMAP-N-his immunization were examined by the *in vitro* feeding assay. (A–C) The survival rate (SR) of PRMs fed with the plasma from immunized chickens was assessed every day for a 1-week period. The Kaplan-Meier Curves were generated to indicate the survival rate in total PRMs (A), adults (B), and nymphs (C). Statistical analysis was performed using the log-rank test. (D) The reproductive capacity (RC) at 7 days post-feeding was assessed. Statistical analysis was performed using Fisher's exact test.

Table III-15. Summary of the acaricidal effects of combined immune plasmas on adult PRMs (Dg-Cys and Dg-Ctr1).

	Days post-feeding									
	1	2	3	4	5	6	7	8	9	10
Control (n = 70)										
No. of dead PRMs	0	1	2	2	3	5	8	19	25	34
SR (%)	100	98.57	97.14	97.14	95.71	92.86	88.57	72.86	64.29	51.43
Dg-Cys (n = 78)										
No. of dead PRMs	0	5	7	11	16	18	24	32	38	46
SR (%)	100	93.59	91.03	85.90	79.49	76.92	69.23	58.97	51.28	41.03
Dg-Ctr1 (n = 57)										
No. of dead PRMs	1	2	4	4	6	7	11	13	21	29
SR (%)	98.25	96.49	92.98	92.98	89.47	87.72	80.70	77.19	63.16	49.12
Combination (n = 80)										
No. of dead PRMs	0	1	5	8	11	16	25	33	47	54
SR (%)	100	98.72	93.59	89.74	85.90	79.49	67.95	57.69	39.74	30.77
p value										
Control vs Dg-Cys	1	1	1	0.116	0.019*	0.068	0.025*	0.256	0.539	0.970
Control vs Dg-Ctr1	1	1	1	1	0.891	0.754	0.634	1	1	0.970
Control vs Combination	1	1	1	0.513	0.254	0.16	0.018*	0.239	0.019*	0.074
Dg-Cys vs Dg-Ctr1	1	1	1	1	0.633	0.491	0.496	0.161	0.595	0.970
Dg-Cys vs Combination	1	1	1	1	0.891	0.847	1	1	0.595	0.970
Dg-Ctr1 vs Combination	1	1	1	1	0.891	0.754	0.468	0.161	0.045*	0.168

The data are compared by Fisher's exact test.
SR, survival rate.
*Holm-adjusted $p < 0.05$ was considered statistically significant.

Table III-16. Summary of the acaricidal effects of combined immune plasmas on adult PRMs (Dg-Cys and Dg-APMAP).

	Days post-feeding									
	1	2	3	4	5	6	7	8	9	10
Control (n = 71)										
No. of dead PRMs	2	4	6	10	11	14	21	27	33	40
SR (%)	97.18	94.37	91.55	85.92	84.51	80.28	70.42	61.97	53.52	43.66
Dg-Cys (n = 52)										
No. of dead PRMs	0	1	2	4	6	8	10	16	20	28
SR (%)	100	98.08	96.15	92.31	88.46	84.62	80.77	69.23	61.54	46.15
Dg-APMAP (n = 74)										
No. of dead PRMs	0	3	4	9	9	18	23	30	38	47
SR (%)	100	95.95	94.59	87.84	87.84	75.68	68.92	59.46	48.65	36.49
Combination (n = 48)										
No. of dead PRMs	0	2	2	5	8	16	20	31	34	41
SR (%)	100	95.83	95.83	89.58	83.33	66.67	58.33	35.42	29.17	14.58
p value										
Control vs Dg-Cys	1	1	1	1	1	1	0.855	1	0.923	1
Control vs Dg-APMAP	1	1	1	1	1	1	0.859	1	0.923	1
Control vs Combination	1	1	1	1	1	0.657	0.855	0.026*	0.070	0.006**
Dg-Cys vs Dg-APMAP	1	1	1	1	1	1	0.772	1	0.611	1
Dg-Cys vs Combination	1	1	1	1	1	0.357	0.104	0.007**	0.008**	0.006**
Dg-APMAP vs Combination	1	1	1	1	1	1	0.855	0.062	0.165	0.050*

The data are compared by Fisher's exact test.
SR, survival rate.
*Holm-adjusted $p < 0.05$ was considered statistically significant.

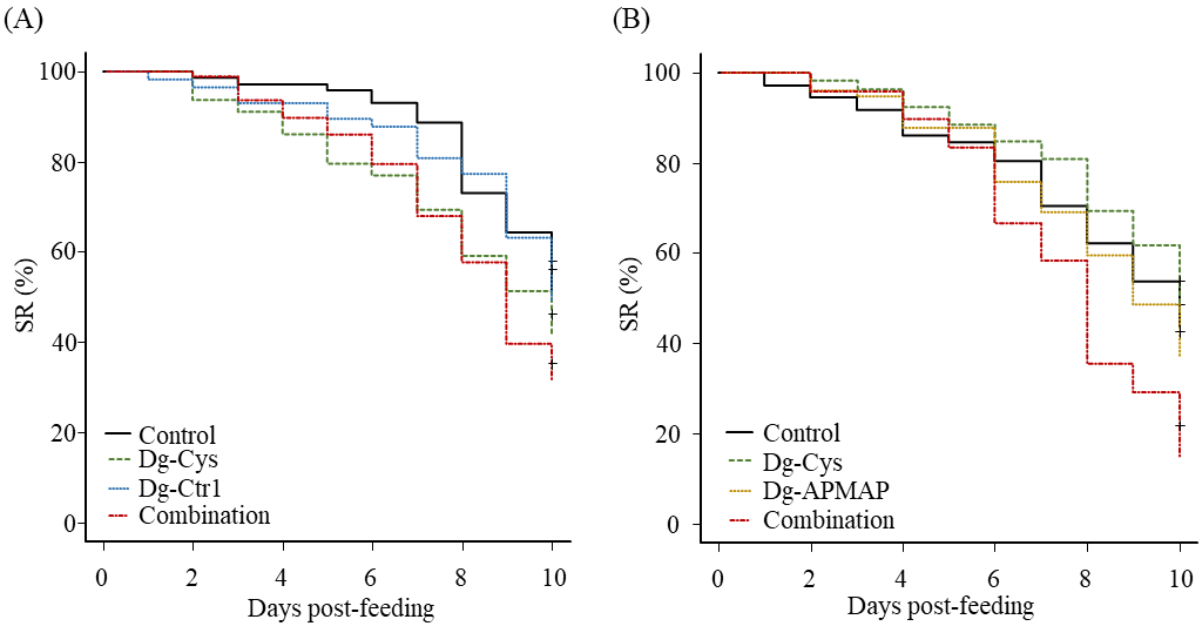

Figure III-16. Acaricidal effects of the combination of the immune plasmas on adult PRMs.

The efficacies of "cocktail vaccine" on adult PRMs were evaluated *in vitro*. The survival rate (SR) of adult PRMs that were fed with the combination of the plasmas from (A) Dg-Cys- and Dg-Ctr1-immunized chickens and (B) Dg-Cys- and Dg-APMAP-immunized chickens was assessed every day for a 10-day period.

DISCUSSION

In the present study, three novel vaccine antigen candidates, *Dg-Cys*, *Dg-Ctr1*, and *Dg-APMAP* were identified by RNA-Seq analysis performed in Chapter I. Whereas the expression intensities of *Dg-Ctr1* and *Dg-APMAP* identified in RNA-Seq data were significantly different between blood-fed and starved PRMs, qPCR analyses showed no difference in their expression levels. As an explanation for these differences, starved PRMs used in RNA-Seq analysis were maintained for a 2-week period without blood meals, while qPCR was performed using PRMs that were kept for a 1-week period. Besides, whilst the expression levels in each life stage of PRMs were quantified in the qPCR analysis, RNA-Seq was conducted using mixed life stages of PRMs, potentially biasing the data. Thus, the expression levels of these antigens may differ dependent upon the period after blood feeding. To clarify the expression profiles of target molecules precisely, their mRNA and protein expressions should be analyzed at several time points after blood feeding.

Previous studies have demonstrated that cystatins play the pivotal roles in biological activities in ticks, such as modulation of host immunity, reproduction, and blood digestion [Karim *et al*., 2005; Schwarz *et al*., 2012]. According to the deduced amino acid sequence and the result of the phylogenetic analysis, Dg-Cys was predicted as a secreted cystatin. Several reports have proposed that cystatins expressed in the midguts are closely associated with blood digestion and/or fecundity in ticks [Lima *et al*., 2006; Alim *et al*., 2008, 2009; Yamaji *et al*., 2009], while those secreted in tick saliva contribute to blood feeding and pathogen transmission by attenuating host immune responses [Lieskovská *et al*., 2015; Chmelař *et al*., 2017; Sajiki *et al*., 2020]. Here, *Dg-Cys* was expressed in the midguts and ovaries, but not in the salivary glands, suggesting its functions in blood digestion and embryogenesis. In contrast, the recombinant protein Dg-Cys-his exhibited inhibitory properties against cathepsins L and S, which play crucial roles in antigen processing and innate immunity [Dai *et al*., 2017; Yan *et al*., 2020]. These results suggest that Dg-Cys is related to the modulations of host immune responses. Meanwhile, Dg-Cys did not inhibit the enzymatic activity of cathepsin B, as previously reported in several cystatins [Lima *et al*., 2006; Turk *et al*., 2008; Zhou *et al*., 2009]. These results indicate the specificity and/or selectivity of Dg-Cys against its targets, and suggest the presence of other cystatin-like molecules in PRMs. Additional experiments, including gene silencing approaches [Chen et al., 2021], are required to elucidate the physiological role of Dg-Cys in PRMs.

In vitro feeding experiments demonstrated that plasmas containing antibodies against

Dg-Cys, Dg-Ctr1, or Dg-APMAP exerted acaricidal effects against PRMs, suggesting that these newly identified molecules have potentials as antigens for anti-PRM vaccines. Meanwhile, the reduction in the RC was observed only in PRMs fed on plasmas from Dg-Cys-immunized chickens. Previous studies have demonstrated the association of cystatins in ticks with the development and hatching of eggs [Wang *et al*., 2015; Rahman *et al*., 2018], suggesting that Dg-Cys is also involved in the embryonic development. Another possible reason is the differences in the expression patterns of each antigen among each life stage; although statistically not significant, qPCR analyses showed that the expression of *Dg-APMAP* in blood-fed states of adult PRMs tended to be lower than that in blood-fed nymphs. Thus, Low expression level of the target molecule in adult PRMs may limit the efficacy of vaccines using Dg-APMAP on the reproductive capacity. These variations in the expression patterns may also cause the differences in acaricidal effects between nymphs and adults; the reduction in the SR of nymphs fed on immune plasmas against Dg-APMAP were markedly high, compared to those of Dg-Cys and Dg-Ctr1. Therefore, the expression profiles of target molecules should be assessed by the LCM and RT-PCR analyses at each life stage in more detail.

In tick studies, vaccines targeting the glycoprotein Bm86, which is expressed on the plasma membrane in the midguts, exhibited conspicuous efficacies, although its physiological function is still unclear [Rand *et al*.,1989; Azhahianambi *et al*., 2009]. Consistently, plasmas containing antibodies against Dg-Ctr1 and Dg-APMAP, both of which are predicted as plasma membrane proteins, exhibited the acaricidal effects on PRMs. In particular, PRMs fed on plasmas from chickens immunized with Dg-APMAP seemed to show higher mortalities than those fed on Dg-Ctr1-immunized plasmas. The strictosidine synthase, which is predicted as a functional domain conserved in APMAP, is associated with the biosynthesis of the monoterpenoid indole alkaloid in plants [Stöckigt *et al*., 2008; Fischereder *et al*., 2014]. Although little is known about the physiological role of APMAP in arthropods, Dg-APMAP possibly plays important roles in PRMs' lives. In contrast, the acaricidal effects of plasmas from Dg-Ctr1-immunzied chickens were observed from 7 or 8 days post-feeding, which were relatively later than the effects of Dg-Cys, Dg-APMAP, and other vaccine candidates previously reported [Bartley *et al*., 2012; Xu *et al*., 2020]. One possible cause is the transient downregulation of Dg-Ctr1 expression driven by the stimulation with copper ion present in the blood meal. Previous reports have demonstrated that the expression of Ctr1 in humans, yeast, and *Arabidopsis thaliana* on the plasma membrane were decreased in response to copper stimulation to strictly regulate copper homeostasis [Petris *et al*., 2003; Liu *et al*., 2007; Li *et al*., 2020]. Further studies on the regulation mechanisms of cell surface Ctr1 expression

in PRMs may help maximize the vaccine efficacy of Dg-Ctr1.

In ticks, mounting studies have suggested that combined treatment of antigens augments the efficacies of vaccines [Almazán *et al*., 2012; Pérez-Sánchez *et al*., 2019; Ndawula Jr and Tabor, 2020]. In the present study, the *in vitro* feeding assays using the immune plasmas containing antibodies against Dg-Cys and Dg-Ctr1/Dg-APMAP revealed that the combined treatment of immune plasmas could elicit acaricidal effects even on adult PRMs, that did not respond to the single treatment of the immune plasmas containing antibodies against each antigen. These data suggest that the combined treatment of antigens can enhance vaccine efficacies. Importantly, the mixed immune plasmas subjected to *in vitro* feeding assays contained half as much antibodies as those present in the single immune plasmas against each antigen. Nevertheless, the acaricidal properties of mixed plasmas predominated those of the single immune plasmas against each antigen. These findings further support the outstanding potential of the cocktail vaccine. Additional experiments, including evaluation of the minimal antibody titers of each antigen required to exert acaricidal effects, are warranted to assess the potential of the cocktail vaccine in more detail. Notably, previous reports have demonstrated that an inappropriate combination of antigens potentially attenuate the efficacies of vaccine, perhaps due to antigenic competitions [McKenna *et al*., 1998; Hope *et al*., 2010; Ndawula Jr and Tabor, 2020]. Collectively, the combination of antigens must be carefully considered, and antigen candidates should be continuously investigated.

Taken together, the results of the present study propose that vaccination with novel antigen candidates, Dg-Cys, Dg-Ctr1, and Dg-APMAP could be an effective strategy to control the number of PRMs in poultry farms, and moreover, the use of cocktail vaccine including Dg-Cys has a great potential to enhance acaricidal efficacies of the vaccines. In this study, however, variations in the antibody responses were observed among the antigens as well as the individuals in the same group. Considering the practical application, therefore, further experiments on the adequate dose, route, and adjuvant are required to improve the immunogenicity and antibody response of each vaccine. In addition, there were differences in SR and RC in control groups among the experiments, making it difficult to compare the acaricidal efficacies of each antigen candidate. These differences were probably due to the physical conditions of PRMs, including mechanical damages during the transport to the laboratory and *in vitro* feeding procedures. Moreover, while PRMs had an opportunity to feed blood during the *in vitro* feeding assay, PRMs usually feed blood repetitively and has several opportunities to be exposed to antibodies in the field. Thus, PRM-infestation trial using immunized chickens should be examined to further evaluate the vaccine efficacies.

SUMMARY

Since current preventive methods of PRMs are insufficient, the development of alternative control strategies is urgently needed. In recent years, vaccination has been in the limelight as a novel method to control PRMs, and a growing number of studies have reported antigen candidates for vaccines and their effectiveness. However, sufficient efficacies of vaccination have not been observed in the field, and hence, antigens for more effective vaccines should be explored.

In Chapter III, three novel antigen candidates of PRMs, Dg-Cys, Dg-Ctr1, and Dg-APMAP, which were identified in the data obtained by the RNA-Seq analysis performed in Chapter I, were characterized *in vitro*. Gene expression analyses revealed that mRNA of each antigen was expressed in the midguts and ovaries, and in all life stages regardless of feeding states. Importantly, PRMs fed on chicken-derived plasmas containing antibodies against Dg-Cys or Dg-Ctr1 showed the significant reduction in the survival rate of nymphs, and immune plasmas of Dg-APMAP exerted an acaricidal effects on both nymphs and adults. In addition, PRMs fed on plasmas from chickens immunized with Dg-Cys exhibited a significant decrease in the reproductive capacity compared to those fed on control plasmas. Furthermore, the combined treatment of Dg-Cys-immunized plasmas with either Dg-Ctr1 or Dg-APMAP-immunized plasmas augmented acaricidal efficacies of vaccines, as represented by the increased mortality observed in adult PRMs. These results suggest that Dg-Cys, Dg-Ctr1, and Dg-APMAP have potentials as antigens for anti-PRM vaccine, and that the use of cocktail vaccines including Dg-Cys could be an effective strategy to protect poultry sectors from PRMs. Further studies including PRM-infestation trials using vaccinated chickens should be performed to evaluate vaccine effectiveness in more detail.

CONCLUSION

The invasion of the poultry red mite (*Dermanyssus gallinae*, PRM), a blood-feeding ectoparasite of avian species, is a global threat to the poultry industry. Mass infestation with PRMs causes various health problems in chickens such as anemia, resulting in serious economic losses. Previous studies have shown that hematophagous arthropods, such as ticks and mosquitoes, mitigate the host immune reactions, especially inflammatory responses, by infestation. In addition, this immunosuppression can be associated with pathogen transmission. Hence, it is important to elucidate the host immunological states in infestation for the establishment of the control strategies not only for parasitical burdens but also for transmission of infectious agents. However, immune responses in chickens infested with PRMs have yet to be documented in detail.

Chemical acaricides, which are commonly used to protect the poultry sector from PRMs, are usually ineffective, because PRMs rapidly develop resistance to acaricides. Thus, the development of alternative control strategies for PRMs is urgently required. In recent years, vaccination has come to draw a lot of attention as a novel method to control PRMs. However, sufficient efficacies of anti-PRM vaccine in the field trials have not been observed as yet, and hence, novel antigens for more effective vaccines must be investigated to improve vaccination strategies.

The present study aimed to examine host immune responses against PRM-infestation and to develop the vaccine as a novel control method for PRMs. To achieve them, transcriptomes of PRMs in blood-fed and starved states were analyzed to scrutinize the biological characteristics of PRMs. Next, chicken-derived transcripts detected in blood-fed PRMs and the expression of representative genes associated with immune responses in PRM-infested chickens were examined. Finally, novel candidate antigens for vaccines were identified from the data of transcriptome analysis, and their potentials as antigens for vaccines were evaluated.

Chapter I: The dynamics of gene expression profiles in PRMs in response to blood feeding were examined. RNA sequencing (RNA-Seq) analysis using blood-fed and starved PRMs revealed that the gene expression patterns of PRMs were dramatically different between the feeding states. A gene ontology enrichment analysis showed that the expression of genes associated with metal ion binding was higher in blood-fed PRMs, suggesting that the uptake, storage, or detoxification of metal ion are promoted in response to the ingestion of host blood-derived ions. Additionally, genes involved in energy synthetic and metabolic processes were more frequently expressed in blood-fed PRMs, whereas starved PRMs predominantly expressed the genes related to metabolism

in the absence of sufficient nutrients, including autophagy and gluconeogenesis. These data are informative to search for the targets of novel control methods for PRMs as well as to investigate the physiology of PRMs in detail.

Chapter II: Immunological states of chickens infested with PRMs were explored. RNA-Seq analysis performed in Chapter I and the analyses using peripheral mononuclear cells (PBMCs) and plasmas collected from PRM-infested and non-infested chickens revealed that a pro-inflammatory C-C chemokine ligand 4 (CCL4) was highly expressed in peripheral blood of PRM-infested chickens. In contrast, no difference was observed in the expression of Th1 and inflammatory cytokines between infested and non-infested chickens. Meanwhile, the expression of anti-inflammatory cytokines and other molecules related to immunosuppression, such as immune checkpoint molecules, were higher in PRM-infested chickens. Additionally, the expression of C-C chemokine receptor 5, a receptor of CCL4, was decreased in infested chickens. These results suggest that the chronic infestation by PRMs suppressively modulate host immunity during infestation. Besides, PRM-derived molecules (soluble mite extract: SME) attenuated inflammatory responses in chicken immune cells, especially macrophage-like cells, *in vitro*, as manifested by the decreased expression of inflammatory cytokines and by the polarization into M2-like phenotype. Importantly, the expression of interferon-α, which plays a central role in the innate immune response, was also decreased in chicken immune cells exposed to SME, suggesting the contribution of PRM-infestation to pathogen transmission.

Chapter III: Three antigen candidates for vaccines, a cystatin-like molecule (*D. gallinae*-cystatin: Dg-Cys), a copper transporter 1-like molecule (*D. gallinae*-copper transporter 1: Dg-Ctr1), and an adipocyte plasma membrane-associated protein-like molecule (*D. gallinae*-adipocyte plasma membrane-associated protein: Dg-APMAP), were identified from the data obtained by RNA-Seq performed in Chapter I, and their potentials as antigens for vaccines was evaluated. Gene expression analyses revealed that mRNA of each candidate gene is expressed in all life stages of PRMs regardless of the feeding states, and expressed in the midguts. Next, the potential of each candidate molecule as antigens for vaccines was assessed *in vitro* by monitoring the acaricidal effects on PRMs fed on plasmas from chickens immunized with recombinant proteins of each molecule. All the plasmas tested exerted acaricidal effects on PRMs, and in addition, PRMs fed on plasmas from chickens immunized with Dg-Cys exhibited a significant reduction in the reproductive capacity of PRMs. These results suggest that vaccines targeting Dg-Cys, Dg-Ctr1, and Dg-APMAP could be effective to control PRMs. Furthermore, the combined treatment of the plasmas containing antibodies against Dg-

Cys and either Dg-Ctr1 or Dg-APMAP elicited higher acaricidal effects than those of single plasmas against each antigen. These results propose the great potential of the cocktail vaccine including Dg-Cys as a novel control method for PRMs.

In conclusion, this study characterizes the transcriptomic profiles of PRMs in each feeding state, and demonstrates that the host inflammatory responses are attenuated by PRM-infestation. Moreover, anti-PRM vaccine targeting Dg-Cys and Dg-Ctr1 or Dg-APMAP exerts significant acaricidal effects on PRMs. These findings could provide informative evidence for establishing novel control strategies for PRMs as well as understanding the impacts of PRM erosion on affected chickens. Further studies are required to clarify the association of PRM-infestation with pathogen transmission and to corroborate the efficacies of the vaccines to apply anti-PRM vaccines in the field.

ACKNOWLEDGEMENT

I would like to express my deepest appreciation to Dr. Kazuhiko Ohashi, Dr. Satoru Konnai, and Dr. Shiro Murata, Laboratory of Infectious Diseases, Department of Disease Control, Faculty of Veterinary Medicine, Hokkaido University, Sapporo, Japan, Dr. Tomohiro Okagawa and Dr. Naoya Maekawa, Department of Advanced Pharmaceutics, Faculty of Veterinary Medicine, Hokkaido University, for their continuous mentoring, guidance, assistance, and encouragement while this work.

I would like to express my deepest my gratitude to Dr. Nariaki Nonaka and Dr. Ryo Nakao, Laboratory of Parasitology, Department of Disease Control, Faculty of Veterinary Medicine, Hokkaido University, for their invaluable supervision and critical review on the manuscript.

I would like to express my sincere appreciation to Dr. Akira Taneno, Dr. Eiji Oishi, and Mr. Takumi Sato, Vaxxinova Japan K.K., Tokyo, Japan, for the provision of the materials and their cooperation in the animal experiments, and their support throughout the study.

I am deeply grateful to Dr. Osamu Ichii, Laboratory of Anatomy, Department of Basic Veterinary Sciences, Faculty of Veterinary Medicine, Hokkaido University, for his kind assistance and comprehensive supervision on laser-capture microdissection and helpful support.

I owe a deep dept of gratitude to Dr. Tsukasa Okada, Hokkaido System Science Co., Ltd., Hokkaido, Japan, and Dr. Junya Yamagishi, Division of Collaboration and Education, International Institute for Zoonosis Control, Hokkaido University, for their technical assistance and valuable advice on bioinformatic analyses.

I greatly appreciate all farmers, Dr. Wataru Hashimoto, Japan Layer K.K., Gifu, Japan, and Dr. Akio Enya for their kind assistance in the collection of the blood and PRM samples throughout the study.

Sincere special thanks are extended to all of colleagues in Laboratory of Infectious Diseases, Department of Disease Control, Faculty of Veterinary Medicine, Hokkaido University for their kind help and warm friendship.

I thank the Japan Society for the Promotion of Science (JSPS) for the fellowship that supported the current studies. I would like to express my sincere condolences on the death of experimental animals used for this thesis.

I would like to express my deepest appreciation to my family and friends for their encouragement and dedicated support of my education and research. Finally, I would like to sincerely thank all of the people who helped me and this research.

REFERENCES

Abbas RZ, Zaman MA, Colwell DD, Gilleard J, Iqbal Z. 2014. Acaricide resistance in cattle ticks and approaches to its management: the state of play. *Vet Parasitol* **203**: 6–20.

Abdel-Ghaffar F, Semmler M, Al-Rasheid K, Mehlhorn H. 2009. *In vitro* efficacy of ByeMite and Mite-Stop on developmental stages of the red chicken mite *Dermanyssus gallinae*. *Parasitol Res* **105**: 1469–1471.

Abdigoudarzi M, Mirafzali MS, Belgheiszadeh H. 2014. Human infestation with *Dermanyssus gallinae* (Acari: Dermanyssidae) in a family referred with pruritus and skin lesions. *J Arthropod Borne Dis* **8**: 119–123.

Ali W, George DR, Shiel RS, Sparagano OA, Guy JH. 2012. Laboratory screening of potential predators of the poultry red mite (*Dermanyssus gallinae*) and assessment of *Hypoaspis miles* performance under varying biotic and abiotic conditions. *Vet Parasitol* **187**: 341–344.

Alim MA, Tsuji N, Miyoshi T, Islam MK, Huang X, Hatta T, Fujisaki K. 2008. HlLgm2, a member of asparaginyl endopeptidases/legumains in the midgut of the ixodid tick *Haemaphysalis longicornis*, is involved in blood-meal digestion. *J Insect Physiol* **54**: 573–585.

Alim MA, Tsuji N, Miyoshi T, Islam MK, Huang X, Hatta T, Fujisaki K. 2009. Legumains from the hard tick *Haemaphysalis longicornis* play modulatory roles in blood feeding and gut cellular remodelling and impact on embryogenesis. *Int J Parasitol* **39**: 97–107.

Almazán C, Moreno-Cantú O, Moreno-Cid JA, Galindo RC, Canales M, Villar M, de la Fuente J. 2012. Control of tick infestations in cattle vaccinated with bacterial membranes containing surface-exposed tick protective antigens. *Vaccine* **30**: 265–272.

Amiard JC, Amiard-Triquet C, Barka S, Pellerin J, Rainbow PS. 2006. Metallothioneins in aquatic invertebrates: their role in metal detoxification and their use as biomarkers. *Aquat Toxicol* **76**: 160–202.

Ariizumi, T, Murata, S, Fujisawa, S, Isezaki, M, Maekawa, N, Okagawa, T, Sato, T, Oishi, E, Taneno, A, Konnai, S, Ohashi, K. 2021. Selection of reference genes for quantitative PCR analysis in poultry red mite (*Dermanyssus gallinae*). *J Vet Med Sci* **83**: 558–565.

Arkle S, Harrington D, Kaiser P, Rothwell L, De Luna C, George D, Guy J, Sparagano OAE. 2008. Immunological control of the poultry red mite. *Ann N Y Acad Sci* **1149**: 36–40.

Axtell RC. 1999. Poultry integrated pest Management: status and future. *Integr pest manag rev* **4**: 53–73.

Azhahianambi P, Ray DD, Chaudhuri P, Gupta R, Ghosh S. 2009. Vaccine efficacy of Bm86 ortholog of *H. a. anatolicum*, rHaa86 expressed in prokaryotic expression system. *J Parasitol Res* **2009**: 165812.

Bartley K, Huntley JF, Wright HW, Nath M, Nisbet AJ. 2012. Assessment of cathepsin D and L-like proteinases of poultry red mite, *Dermanyssus gallinae* (De Geer), as potential vaccine antigens. *Parasitology* **139**: 755–765.

Bartley K, Turnbull F, Wright HW, Huntley JF Palarea-Albaladejo J, Nath M, Nisbet AJ. 2017. Field evaluation of poultry red mite (*Dermanyssus gallinae*) native and recombinant prototype vaccines. *Vet Parasitol* **244**: 25–34.

Beug H, von Kirchbach A, Döderlein G, Conscience JF, Graf T. 1979. Chicken hematopoietic cells transformed by seven strains of defective avian leukemia viruses display three distinct phenotypes of differentiation. *Cell* **18**: 375–390.

Bowman AS, Nuttall PA. 2008. Ticks: biology, disease and control. *Cambridge University Press*, New York.

Brake DK, Pérez de León AA. 2012. Immunoregulation of bovine macrophages by factors in the salivary glands of *Rhipicephalus microplus*. *Parasit Vectors* **5**: 38.

Brossard M, Wikel SK. 2004. Tick immunobiology. *Parasitology* **129** (Suppl.): S161–176.

Cahill Jr GF. 2006. Fuel metabolism in starvation. *Annu Rev Nutr* **26**: 1–22.

Champagne DE. 2005. Antihemostatic molecules from saliva of blood-feeding arthropods. *Pathophysiol Haemost Thromb* **34**: 221–227.

Chauve C. 1998. The poultry red mite *Dermanyssus gallinae* (De Geer, 1778): current situation and future prospects for control. *Vet Parasitol* **79:** 239–245.

Chen G, Severo MS, Sohail M, Sakhon OS, Wikel SK, Kotsyfakis M, Pedra JHF. 2012. *Ixodes scapularis* saliva mitigates inflammatory cytokine secretion during *Anaplasma phagocytophilum* stimulation of immune cells. *Parasit Vectors* **5**: 229.

Chen W, Bartley K, Nunn F, Bowman AS, Sternberg JM, Burgess STG, Nisbet AJ, Price DRG. 2021. RNAi gene knockdown in the poultry red mite, *Dermanyssus gallinae* (De Geer 1778), a tool for functional genomics. *Parasit Vectors* **14**: 57.

Chmelař J, Kotál J, Langhansová H, Kotsyfakis, M. 2017. Protease inhibitors in tick saliva: the role of serpins and cystatins in tick-host–pathogen interaction. *Front Cell Infect Microbiol* **7**: 216.

Christensen BM, Li J, Chen CC, Nappi AJ. 2005. Melanization immune responses in mosquito vectors. *Trends Parasitol* **21**: 192–199.

Cosoroaba I. 2001. Massive *Dermanyssus gallinae* invasion in battery-husbandry raised fowls. *Rev Med Vet-Toulouse* **152**: 89–96.

Cross ML, Cupp EW, Enriquez FJ. 1994. Differential modulation of murine cellular immune responses by salivary gland extract of *Aedes aegypti*. *Am J Trop Med Hyg* **51**: 690–696.

Dai LS, Chu SH, Yu XM, Li YY. 2017. A role of cathepsin L gene in innate immune response of crayfish (*Procambarus clarkii*). *Fish Shellfish Immunol* **71**, 246–254.

Dairaghi DJ, Franz-Bacon K, Callas E, Cupp J, Schall TJ, Tamraz SA, Boehme SA, Taylor N, Bacon KB. 1998. Macrophage inflammatory protein-1β induces migration and activation of human thymocytes. *Blood* **91:** 2905–2913.

de la Fuente J, Kocan KM. 2006. Strategies for development of vaccines for control of ixodid tick species. *Parasite Immunol* **28**: 275–283.

de la Fuente J, Contreras M. 2015. Tick vaccines: current status and future directions. *Expert Rev Vaccines* **14**: 1367–1376.

Di Palma A, Leone F, Albanese F, Beccati M. 2018. A case report of *Dermanyssus gallinae* infestation in three cats. *Vet Dermatol* **29**: 348-e124.

Eriksson H, Jansson DS, Johansson KE, Båverud V, Chirico J, Aspán A. 2009. Characterization of *Erysipelothrix rhusiopathiae* isolates from poultry, pigs, emus, the poultry red mite and other animals. *Vet Microbiol* **137**: 98–104.

Fischereder E, Pressnitz D, Kroutil W, Lutz S. 2014. Engineering strictosidine synthase: rational design of a small, focused circular permutation library of the b-propeller fold enzyme. *Bioorg Med Chem* **22**: 5633–5637.

Flochlay AS, Thomas E, Sparagano O. 2017. Poultry red mite (*Dermanyssus gallinae*) infestation: a broad impact parasitological disease that still remains a significant challenge for the egg-laying industry in Europe. *Parasit Vectors* **10**: 357.

George DR, Shiel RS, Appleby WG, Knox A, Guy JH. 2010. *In vitro* and *in vivo* acaricidal activity and residual toxicity of spinosad to the poultry red mite, *Dermanyssus gallinae*. *Vet Parasitol*. **173**: 307–316.

Gillespie RD, Dolan MC, Piesman J, Titus RG. 2001. Identification of an IL-2 binding protein in the saliva of the Lyme disease vector tick, *Ixodes scapularis*. *J Immunol* **166**: 4319–4326.

Grunclová L, Horn M, Vancová M, Sojka D, Franta Z, Mares M, Kopácek P. 2006. Two secreted cystatins of the soft tick *Ornithodoros moubata*: differential expression pattern and inhibitory specificity. *Biol Chem* **387**: 1635–1644.

Guerrero D, Cantaert T, Missé D. 2020. *Aedes* mosquito salivary components and their effect on the immune response to arboviruses. *Front Cell Infect Microbiol* **10**: 407.

Haas BJ, Papanicolaou A, Yassour M, Grabherr M, Blood PD, Bowden J, Couger MB, Eccles D, Li B, Lieber M, MacManes MD, Ott M, Orvis J, Pochet N, Strozzi F, Weeks N, Westerman R, William T, Dewey CN, Henschel R, LeDuc RD, Friedman N, Regev A. 2013. *De novo* transcript sequence reconstruction from RNA-seq using the Trinity platform for reference generation and analysis. *Nat Protoc* **8**: 1494–1512.

Hajdusek O, Almazán C, Loosova G, Villar M, Canales M, Grubhoffer L, Kopacek P, de la Fuente J. 2010. Characterization of ferritin 2 for the control of tick infestations *Vaccine* **28**: 2993–2998.

Hajnická V, Kocáková P, Sláviková M, Slovák M, Gasperík J, Fuchsberger N, Nuttall PA. 2001. Anti-interleukin-8 activity of tick salivary gland extracts. *Parasite Immunol* **23**: 483–489.

Hannier S, Liversidge J, Sternberg JM, Bowman AS. 2003. *Ixodes ricinus* tick salivary gland extract inhibits IL-10 secretion and CD69 expression by mitogen-stimulated murine splenocytes and induces hyporesponsiveness in B lymphocytes. *Parasite Immunol* **25**: 27–37.

Hardbower DM, Asim M, Murray-Stewart T, Casero Jr RA, Verriere T, Lewis ND, Chaturvedi R, Piazuelo MB, Wilson KT. 2016. Arginase 2 deletion leads to enhanced M1 macrophage activation and upregulated polyamine metabolism in response to *Helicobacter pylori* infection. *Amino Acids* **48**: 2375–2388.

Hope M, Jiang X, Gough J, Cadogan L, Josh P, Jonsson N, Willadsen P. 2010. Experimental vaccination of sheep and cattle against tick infestation using recombinant 5'-nucleotidase. *Parasite Immunol* **32**: 135–142.

Hughes AL. 2013. Evolution of the salivary apyrases of blood-feeding arthropods. *Gene* **527**: 123–130.

Hunter MS, Perlman SJ, Kelly SE. 2003. A bacterial symbiont in the Bacteroidetes induces cytoplasmic incompatibility in the parasitoid wasp *Encarsia pergandiella*. *Proc Biol Sci* **270**: 2185–2190.

Huong CT, Murano T, Uno Y, Usui T, Yamaguchi T. 2014. Molecular detection of

avian pathogens in poultry red mite (Dermanyssus gallinae) collected in chicken farms. *J Vet Med Sci* **76**: 1583–1587.

Ibelli AMG, Kim TK, Hill CC, Lewis LA, Bakshi M, Miller S, Porter L, Mulenga A. 2014. A blood meal-induced *Ixodes scapularis* tick saliva serpin inhibits trypsin and thrombin, and interferes with platelet aggregation and blood clotting. *Int J Parasitol* **44**: 369–379.

Ichii O, Ohta H, Horino T, Nakamura T, Hosotani M, Mizoguchi T, Morishita K, Nakamura K, Hoshino Y, Takagi S, Sasaki N, Takiguchi M, Sato R, Oyamada K, Kon Y. 2017. Urinary exosome-derived microRNAs reflecting the changes of renal function and histopathology in dogs. *Sci Rep* **7**: 40340.

Jones DT, Taylor WR, Thornton JM. 1992. The rapid generation of mutation data matrices from protein sequences. *Comput Appl Biosci* **8**: 275–282.

Kanehisa M, Goto S. 2000. KEGG: kyoto encyclopedia of genes and genomes. *Nucleic Acids Res* **28**: 27–30.

Kaoud HA, El-Dahshan AR. 2010. Effect of red mite (*Dermanyssus gallinae*) infestation on the performance and immune profile in vaccinated broiler breeder flocks. *J Am Sci* **6**: 72–78.

Karim S, Miller NJ, Valenzuela J, Sauer JR, Mather TN. 2005. RNAi-mediated gene silencing to assess the role of synaptobrevin and cystatin in tick blood feeding. *Biochem Biophys Res Commun* **334**: 1336–1342.

Kazimirova M, Stibraniova I. 2013. Tick salivary compounds: their role in modulation of host defences and pathogen transmission. *Front Cell Infect Microbiol* **3**: 43.

Kotsyfakis M, Sá-Nunes A, Francischetti IM, Mather TN, Andersen JF, Ribeiro JMC. 2006. Antiinflammatory and immunosuppressive activity of sialostatin L, a salivary cystatin from the tick *Ixodes scapularis*. *J Biol Chem* **281**: 26298–26307.

Kotsyfakis M, Schwarz A, Erhart J, Ribeiro JMC. 2015. Tissue- and time-dependent transcription in *Ixodes ricinus* salivary glands and midguts when blood feeding on the

vertebrate host. *Sci Rep* **5**: 9103.

Kotál J, Langhansová H, Lieskovská J, Andersen JF, Francischetti IMB, Chavakis T, Kopecký J, Pedra JHF, Kotsyfakis M, Chmelař J. 2015. Modulation of host immunity by tick saliva. *J Proteomics* **128**: 58–68.

Kowalski A, Sokół R. 2009. Influence of *Dermanyssus gallinae* (poultry red mite) invasion on the plasma levels of corticosterone, catecholamines and proteins in layer hens. *Pol J Vet Sci* **12**: 231–235.

Koziatek-Sadłowska SK, Sokół R. 2020. Changes in the percentages of B- and T-lymphocytes and antibody titres in laying hens infested with *Dermanyssus gallinae*-A preliminary study. *Animals* (Basel) **10**: 987.

Krausgruber T, Blazek K, Smallie T, Alzabin S, Lockstone H, Sahgal N, Hussell T, Feldmann M, Udalova IA. 2011. IRF5 promotes inflammatory macrophage polarization and TH1-TH17 responses. *Nat Immunol* **12**: 231–238.

Kumar S, Stecher G, Li M, Knyaz C, Tamura K. 2018. MEGA X: molecular evolutionary genetics analysis across computing platforms. *Mol Biol Evol* **35**: 1547–1549.

Kuthejlová M, Kopecký J, Stepánová G, Macela A. 2001. Tick salivary gland extract inhibits killing of *Borrelia afzelii* spirochetes by mouse macrophages. *Infect Immun* **69**: 575–578.

Kýcková K, Kopecký J. 2006. Effect of tick saliva on mechanisms of innate immune response against *Borrelia afzelii*. *J Med Entomol* **43**: 1208–1214.

Lesna I, Sabelis MW, van Niekerk TG, Komdeur J. 2012. Laboratory tests for controlling poultry red mites (*Dermanyssus gallinae*) with predatory mites in small 'laying hen' cages. *Exp Appl Acarol* **58**: 371–383.

Li J, Yuan J, Wang H, Zhang H, Zhang H. 2020. *Arabidopsis* copper transporter 1 undergoes degradation in a proteasome-dependent manner. *J Exp Bot* **71**: 6174–6186.

Li P, Allen H, Banerjee S, Franklin S, Herzog L, Johnston C, McDowell J, Paskind

M, Rodman L, Salfeld J, Towne E, Tracey D, Wardwell S, Wei F-Y, Wong W, Kamen R, Seshadri T. 1995. Mice deficient in IL-1 beta-converting enzyme are defective in production of mature IL-1 beta and resistant to endotoxic shock. *Cell* **80**: 401–411.

Liebisch G, Hack R, Smid G. 2011. Efficacy of spinosad against the poultry red mite, *Dermanyssus gallinae* (Mesostigmata: Dermanyssidae), in laboratory and field trials. *Zoosymposia* **6**: 282–287.

Lieskovská J, Páleníková J, Širmarová J, Elsterová J, Kotsyfakis M, Chagas AC, Calvo E, Růžek D, Kopecký J. 2015. Tick salivary cystatin sialostatin L2 suppresses IFN responses in mouse dendritic cells. *Parasite Immunol* **37**: 70–78.

Lima CA, Sasaki SD, Tanaka AS. 2006. Bmcystatin, a cysteine proteinase inhibitor characterized from the tick *Boophilus microplus*. *Biochem Biophys Res Commun* **347**: 44–50.

Lima-Barbero JF, Contreras M, Mateos-Hernández L, Mata-Lorenzo FM, Triguero-Ocaña R, Sparagano O, Finn RD, Strube C, Price DRG, Nunn F, Bartley K, Höfle U, Boadella M, Nisbet AJ, de la Fuente J, Villar M. 2019. A vaccinology approach to the identification and characterization of *Dermanyssus Gallinae* candidate protective antigens for the control of poultry red mite infestations. *Vaccines* **7**: 190.

Liu J, Sitaram A, Burd CG. 2007. Regulation of copper-dependent endocytosis and vacuolar degradation of the yeast copper transporter, Ctr1p, by the Rsp5 ubiquitin ligase. *Traffic* (Copenhagen, Denmark) **8**: 1375–1384.

Liu XY, Bonnet SI. 2014. Hard tick factors implicated in pathogen transmission. *PLoS Negl Trop Dis* **8**: e2566.

Lu AR, Zhang QL, Zhang J, Yang B, Wu K, Xie W, Luan YX, Ling E. 2014. Insect prophenoloxidase: the view beyond immunity. *Front Physiol* **5**: 252.

Marangi M, Cafiero MA, Capelli G, Camarda A, Sparagano OAE, Giangaspero A. 2009. Evaluation of the poultry red mite, *Dermanyssus gallinae* (Acari: Dermanyssidae) susceptibility to some acaricides in field populations from Italy. *Exp Appl Acarol* **48**: 11–18.

McKenna RV, Riding GA, Jarmey JM, Pearson RD, Willadsen, P. 1998. Vaccination of cattle against the *Boophilus microplus* using a mucin-like membrane glycoprotein. *Parasite Immunol* **20**: 325–336.

Mejri N, Rutti B, Brossard M. 2002. Immunosuppressive effects of *Ixodes ricinus* tick saliva or salivary gland extracts on innate and acquired immune response of BALB/c mice. *Parasitol Res* **88**: 192–197.

Meyer-Kühling B, Pfister K, Müller-Lindloff J, Heine J. 2007. Field efficacy of phoxim 50% (ByeMite) against the poultry red mite Dermanyssus gallinae in battery cages stocked with laying hens. *Vet Parasitol* **147**: 289–296.

Mirzaei M, Ghashghaei O, Yakhchali M. 2016. Prevalence of ectoparasites of indigenous chickens from Dalahu region, Kermanshah province, Iran. *Turkiye Parazitol Derg* **40**: 13–16.

Mohr SE, Killilea DW. 2018. Editorial: metal biology takes flight: the study of metal homeostasis and detoxification in insects. *Front Genet* **9**: 221.

Mori A, Konnai S, Yamada S, Hidano A, Murase Y, Ito T, Takano A, Kawabata H, Onuma M, Ohashi K. 2010. Two novel Salp 15-like immunosuppressant genes from salivary glands of *Ixodes persulcatus* Schulze tick. *Insect Mol Biol* **19**: 369–365.

Moro CV, De Luna CJ, Tod A, Guy JH, Sparagano OAE, Zenner L. 2009. The poultry red mite (*Dermanyssus gallinae*): a potential vector of pathogenic agents. *Exp Appl Acarol* **48**: 93–104.

Mul M, Van Niekerk T, Chirico J, Maurer V, Kilpinen O, Sparagano O, Thind B, Zoons J, Moore D, Bell B, Gjevre A.-G, Chauve C. 2009. Control methods for *Dermanyssus gallinae* in systems for laying hens: results of an international seminar. *Worlds Poult Sci J* **65**: 589–600.

Müller M, Schmidt O, Angelova M, Faserl K, Weys S, Kremser L, Pfaffenwimmer T, Dalik T, Kraft C, Trajanoski Z, Lindner H, Teis D. 2015. The coordinated action of the MVB pathway and autophagy ensures cell survival during starvation. *eLife* **4**: e07736.

Murano T, Namiki K, Shiina K, Yasukawa H. 2008. The development of resistance by *Dermanyssus gallinae* to commercial acaricides in Japan. *Journal of Japan Veterinary Medical Association* **61**: 287–293.

Murano T, Namiki K, Shiina K, Yasukawa H. 2015. Resistance development of *Dermanyssus gallinae* against commercial acaricides in poultry farms in Japan. *Journal of Japan Veterinary Medical Association* **68**: 509–514.

Muttkowski RA. 1921. Copper in animals and plants. *Science* **53**: 453–454.

Narasimhan S, Montgomery RR, DePonte K, Tschudi C, Marcantonio N, Anderson JF, Sauer JR, Cappello M, Kantor FS, Fikrig E. 2004. Disruption of *Ixodes scapularis* anticoagulation by using RNA interference. *Proc Natl Acad Sci USA* **101**: 1141–1146.

Ndawula Jr C, Tabor AE. 2020. Cocktail anti-tick vaccines: The unforeseen constraints and approaches toward enhanced efficacies. *Vaccines (Basel)* **8**: 457.

Niwa H, Yamamura K, Miyazaki J. 1991. Efficient selection for high-expression transfectants with a novel eukaryotic vector. *Gene* **108**: 193–199.

Nordenfors H, Höglund J, Uggla A. 1999. Effects of temperature and humidity on oviposition, molting, and longevity of *Dermanyssus gallinae* (Acari: Dermanyssidae). *J Med Entomol* **36**: 68–72.

Nuttall PA, Trimnell AR, Kazimirova M, Labuda M. 2006. Exposed and concealed antigens as vaccine targets for controlling ticks and tick-borne diseases. *Parasite Immunol* **28**: 155–163.

Nuttall PA. 2019. Tick saliva and its role in pathogen transmission. *Wien Klin Wochenschr* Online ahead of print.

Oleaga A, Obolo-Mvoulouga P, Manzano-Román R, Pérez-Sánchez R. 2018. *De novo* assembly and analysis of midgut transcriptome of the argasid tick *Ornithodoros erraticus* and identification of genes differentially expressed after blood feeding. *Ticks Tick Borne Dis* **9**: 1537–1554.

Oliveira CJF, Cavassani KA, Moré DD, Garlet GP, Aliberti JC, Silva JS, Ferreira BR. 2008. Tick saliva inhibits the chemotactic function of MIP-1alpha and selectively impairs chemotaxis of immature dendritic cells by down-regulating cell-surface CCR5. *Int J Parasitol* **38**: 705–716.

Perez MH, Noriega FG. 2014. Sublethal metal stress response of larvae of *Aedes aegypti*. *Physiol Entomol* **39**: 111–119.

Pérez-Sánchez R, Manzano-Román R, Obolo-Mvoulouga P, Oleaga A. 2019. *In silico* selection of functionally important proteins from the mialome of *Ornithodoros erraticus* ticks and assessment of their protective efficacy as vaccine targets. *Parasit Vectors* **12**: 508.

Petris MJ, Smith K, Lee J and Thiele DJ. 2003. Copper-stimulated endocytosis and degradation of the human copper transporter, hCtr1. *J Biol Chem* **278**: 9639–9649.

Poole NM, Mamidanna G, Smith RA, Coons LB, Cole JA. 2013. Prostaglandin E(2) in tick saliva regulates macrophage cell migration and cytokine profile. *Parasit Vectors* **6**: 261.

Pritchard J, Kuster T, Sparagano OAE, Tomley F. 2015. Understanding the biology and control of the poultry red mite *Dermanyssus gallinae*: a review. *Avian Pathol* **44**: 143–153.

Pugliese N. Circella E, Marino M, De Virgilio C, Cocciolo G, Lozito P, Cafiero MA, Camarda A. 2019. Circulation dynamics of *Salmonella enterica* subsp. *enterica* ser. Gallinarum biovar Gallinarum in a poultry farm infested by *Dermanyssus gallinae*. *Med Vet Entomol* **33**: 162–170.

Qu Y, Franchi L, Nunez G, Dubyak GR. 2007. Nonclassical IL-1 beta secretion stimulated by P2X7 receptors is dependent on inflammasome activation and correlated with exosome release in murine macrophages. *J Immunol* **179**: 1913–1925.

Rahman MK, Islam MS, You M. 2018. Impact of subolesin and cystatin knockdown by RNA interference in adult female *Haemaphysalis longicornis* (Acari: Ixodidae) on blood engorgement and reproduction. *Insects* **9**: 39.

Ramachandra RN, Wikel SK. 1992. Modulation of host-immune responses by ticks (*Acari*: *Ixodidae*): effect of salivary gland extracts on host macrophages and lymphocyte cytokine production. *J Med Entomol* **29**: 818–826.

Rand KN, Moore T, Sriskantha A, Spring K, Tellam R, Willadsen P, Cobon GS.1989. Cloning and expression of a protective antigen from the cattle tick *Boophilus microplus*. *Proc Natl Acad Sci USA* **86**: 9657–9661.

Ribeiro JMC, Mather TN. 1998. *Ixodes scapularis*: salivary kininase activity is a metallo dipeptidyl carboxypeptidase. *Exp Parasitol* **89**: 213–221.

Ribeiro JMC, Francischetti IMB. 2003. Role of arthropod saliva in blood feeding: sialome and post-sialome perspectives. *Annu Rev Entomol* **48**: 73–88.

Rivera-Perez C, Clifton ME, Noriega FG. 2017. How micronutrients influence the physiology of mosquitoes. *Curr Opin Insect Sci* **23**: 112–117.

Rodriguez-Vivas RI, Jonsson NN, Bhushan C. 2018. Strategies for the control of *Rhipicephalus microplus* ticks in a world of conventional acaricide and macrocyclic lactone resistance. *Parasitol Res* **117**: 3–29.

Rolníková T, Kazimírová M, Buc M. 2003. Modulation of human lymphocyte proliferation by salivary gland extracts of ixodid ticks (*Acari*: *Ixodidae*): effect of feeding stage and sex. *Folia Parasitol* (Praha) **50**: 305–312.

Sajiki Y, Konnai S, Ochi A, Okagawa T, Githaka N, Isezaki M, Yamada S, Ito T, Ando S, Kawabata H, Logullo C, da Silva Vaz Jr I, Maekawa N, Murata S, Ohashi K. 2020. Immunosuppressive effects of sialostatin L1 and L2 isolated from the taiga tick *Ixodes persulcatus* Schulze. *Ticks Tick Borne Dis* **11**: 101332.

Sajiki Y, Konnai S, Ikenaka Y, Gulay KCM, Kobayashi A, Parizi LF, João BC, Watari K, Fujisawa S, Okagawa T, Maekawa N, Logullo C, da Silva Vaz I Jr, Murata S, Ohashi K. 2021. Tick saliva-induced programmed death-1 and PD-ligand 1 and its related host immunosuppression. *Sci Rep* **11**: 1063.

Satoh T, Takeuchi O, Vandenbon A, Yasuda K, Tanaka Y, Kumagai Y, Miyake T,

Matsushita K, Okazaki T, Saitoh T, Honma K, Matsuyama T, Yui K, Tsujimura T, Standley DM, Nakanishi K, Nakai K, Akira S. 2010. The Jmjd3-*Irf4* axis regulates M2 macrophage polarization and host responses against helminth infection. *Nat Immunol* **11**: 936–944.

Saxton RA, Tsutsumi N, Su LL, Abhiraman GC, Mohan K, Henneberg LT, Aduri NG, Gati C, Garcia KC. 2021. Structure-based decoupling of the pro- and anti-inflammatory functions of interleukin-10. *Science* **371**: eabc8433.

Schicht S, Qi W, Poveda L, Strube C. 2014. Whole transcriptome analysis of the poultry red mite *Dermanyssus gallinae*. *Parasitology* **141**: 336–346.

Schneider BS, Soong L, Zeidner NS, Higgs S. 2004. *Aedes aegypti* salivary gland extracts modulate anti-viral and TH1/TH2 cytokine responses to Sindbis virus infection. *Viral Immunol* **17**: 565–573.

Schneider BS, Higgs S. 2008. The enhancement of arbovirus transmission and disease by mosquito saliva is associated with modulation of the host immune response. *Trans R Soc Trop Med Hyg* **102**: 400–408.

Schwarz A, Valdés JJ, Kotsyfakis, M. 2012. The role of cystatins in tick physiology and blood feeding. *Ticks Tick Borne Dis* **3**: 117–127.

Shanmugasundaram R, Selvaraj RK. 2011. Regulatory T cell properties of chicken CD4+CD25+ cells. *J Immunol* **186**: 1997–2002.

Šimo L, Kazimirova M, Richardson J, Bonnet SI. 2017. The essential role of tick salivary glands and saliva in tick feeding and pathogen transmission. *Front Cell Infect Microbiol* **7**: 281.

Skallova A, Iezzi G, Ampenberger F, Kopf M, Kopecky J. 2008. Tick saliva inhibits dendritic cell migration, maturation, and function while promoting development of Th2 responses. *J Immunol* **180**: 6186–6192.

Smulders FJM, Rietjens IMCM, Rose M. 2018. Case report: fipronil contamination of chickens in the Netherlands and surrounding countries. *ECVPH Food safety assurance* **7**:

670.

Sommer D, Heffels-Redmann U, Köhler K, Lierz M, Kaleta EF. 2016. Role of the poultry red mite (*Dermanyssus gallinae*) in the transmission of avian influenza A virus. *Tierarztl Prax Ausg G Grosst Nutztiere* **44**: 26–33.

Sparagano OAE, Pavlićević A, Murano T, Camarda A, Sahibi H, Kilpinen O, Mul M, van Emous R, le Bouquin S, Hoel K, Cafiero MA. 2009. Prevalence and key figures for the poultry red mite *Dermanyssus gallinae* infections in poultry farm systems. *Exp Appl Acarol* **48**: 3–10.

Sparagano OAE, George DR, Harrington DW, Giangaspero A. 2014. Significance and control of the poultry red mite, *Dermanyssus gallinae*. *Annu Rev Entomol* **59**: 447–466.

Steenberg T, Kilpinen O. 2003. Fungus infection of the chicken mite *Dermanyssus gallinae*. *IOBC WPRS Bull* **26**: 23–26.

Stöckigt J, Barleben L, Panjikar S, Loris EA. 2008. 3D-Structure and function of strictosidine synthase-the key enzyme of monoterpenoid indole alkaloid biosynthesis. *Plant Physiol Biochem* **46**: 340–355.

Tavassoli M, Allymehr M, Pourseyed SH, Ownag A, Bernousi I, Mardani K, Ghorbanzadegan M, Shokrpoor S. 2011. Field bioassay of *Metarhizium anisopliae* strains to control the poultry red mite *Dermanyssus gallinae*. *Vet Parasitol* **178**: 374–378.

Thind BB, Ford HL. 2007. Assessment of susceptibility of the poultry red mite *Dermanyssus gallinae* (Acari: Dermanyssidae) to some acaricides using an adapted filter paper based bioassay. *Vet Parasitol* **144**: 344–348.

Thomas E, Zoller H, Liebisch G, Alves LFA, Vettorato L, Chiummo RM, Sigognault-Flochlay A. 2018. *In vitro* activity of fluralaner and commonly used acaricides against *Dermanyssus gallinae* isolates from Europe and Brazil. *Parasit Vectors* **11**: 361.

Tsuda A, Mulenga A, Sugimoto C, Nakajima M, Ohashi K, Onuma M. 2001. cDNA cloning, characterization and vaccine effect analysis of *Haemaphysalis longicornis* tick

saliva proteins. *Vaccine* **19**: 4287–4296.

Tu Q, Hickey ME, Yang T, Gao S, Zhang Q, Qu Y, Du X, Wang J, He J. 2019. A simple and rapid method for detecting the pesticide fipronil on egg shells and in liquid eggs by Raman microscopy. *Food Control* **96**: 16–21.

Turk V, Stoka V, Turk D. 2008. Cystatins: biochemical and structural properties, and medical relevance. *Front Biosci* **13**: 5406–5420.

Uguccioni M, D'Apuzzo M, Loetscher M, Dewald B, Baggiolini M. 1995. Actions of the chemotactic cytokines MCP-1, MCP-2, MCP-3, RANTES, MIP-1 alpha and MIP-1 beta on human monocytes. *Eur J Immunol* **25**: 64–68.

Vancová I, Slovák M, Hajnická V, Labuda M, Šimo L, Peterková K, Hails RS, Nuttall PA. 2007. Differential anti-chemokine activity of *Amblyomma variegatum* adult ticks during blood-feeding. *Parasite Immunol* **29**: 169–177.

Vignali DAA, Collison LW, Workman CJ. 2008. How regulatory T cells work. *Nat Rev Immunol* **8**: 523–532.

Wang Y, Zhou Y, Gong H, Cao J, Zhang H, Li X, Zhou J. 2015. Functional characterization of a cystatin from the tick *Rhipicephalus haemaphysaloides*. *Parasit Vectors* **8**: 140.

Wikel SK. 1982. Influence of *Dermacentor andersoni* infestation on lymphocyte responsiveness to mitogens. *Ann Trop Med Parasitol* **76**: 627–632.

Wikel SK. 1996. Host immunity to ticks. *Annu Rev Entomol* **41**: 1–22.

Wikel SK. 2013. Ticks and tick-borne pathogens at the cutaneous interface: host defenses, tick countermeasures, and a suitable environment for pathogen establishment. *Front Microbiol* **4**: 337.

Willadsen P, Riding GA, McKenna RV, Kemp DH, Tellam RL, Nielsen JN, Lahnstein J, Cobon GS, Gough JM. 1989. Immunologic control of a parasitic arthropod. Identification of a protective antigen from *Boophilus microplus*. *J Immunol* **143**: 1346–

1351.

Willadsen P, Bird P, Cobon GS, Hungerford J. 1995. Commercialisation of a recombinant vaccine against *Boophilus microplus*. *Parasitology* **110** Suppl: S43–50.

Willadsen P. 2004. Anti-tick vaccines. *Parasitology* **129** Suppl: S367–387.

Wright HW, Bartley K, Huntley JF, Nisbet AJ. 2016. Characterisation of tropomyosin and paramyosin as vaccine candidate molecules for the poultry red mite, *Dermanyssus gallinae*. *Parasit Vectors* **9**: 544.

Xu X, Wang C, Huang Y, Zhang S, Yu H, Meng J, Pan B. 2020. Evaluation of the vaccine efficacy of three digestive protease antigens from *Dermanyssus gallinae* using an in vivo rearing system. *Vaccine* **38**: 7842–7849.

Xu XL, Cheng TY, Yang H, Liao ZH. 2016 *De novo* assembly and analysis of midgut transcriptome of *Haemaphysalis flava* and identification of genes involved in blood digestion, feeding and defending from pathogens. *Infect Genet Evol* **38**: 62–72.

Yamaji K, Tsuji N, Miyoshi T, Islam MK, Hatta T, Alim MA, Anisuzzaman, Takenaka A, Fujisaki K. 2009. Hemoglobinase activity of a cysteine protease from the ixodid tick *Haemaphysalis longicornis*. *Parasitol Int* **58**: 232–237.

Yan X, Wu Z, Wang B, Yu T, Hu Y, Wang S, Deng C, Zhao B, Nakanishi H, Zhang X. 2020. Involvement of cathepsins in innate and adaptive immune responses in periodontitis. *Evid Based Complement Alternat Med* **2020**: 4517587.

Zchori-Fein E, Perlman SJ. 2004. Distribution of the bacterial symbiont *Cardinium* in arthropods. *Mol Ecol* **13**: 2009–2016.

Zdybel J, Karamon J, Cencek T. 2011. *In vitro* effectiveness of selected acaricides against red poultry mites (*Dermanyssus gallinae*, De Geer, 1778) isolated from laying hen battery cage farms localised in different regions of Poland. *Bull Vet Inst Pulawy* **55**: 411–416.

Zhou J, Liao M, Ueda M, Gong H, Xuan X, Fujisaki K. 2009. Characterization of an

intracellular cystatin homolog from the tick *Haemaphysalis longicornis*. *Vet Parasitol* **160**: 180–183.

SUMMARY IN JAPANESE

和文要旨

ワクモ (*Dermanyssus gallinae*) はニワトリを含む鳥類に寄生して吸血を行うダニの一種であり、日本を含む世界中に分布している。ワクモに重度に吸血されたニワトリは貧血や産卵率の低下を呈し、生産性の著しい低下を招く。ワクモと同じく吸血性の外部寄生虫であるマダニや蚊においては、吸血時に様々な生理活性物質を唾液中に分泌することで、宿主の生体応答を抑制的に調節していることが知られている。このような免疫抑制は病原体の媒介や宿主の易感染化に関与していることが報告されており、外部寄生虫は貧血等の直接的な被害に加えて感染症リスクの増大等、間接的な被害をも引き起こす可能性がある。したがってワクモによる寄生が宿主免疫応答に与える影響を解明することは、養鶏場における吸血被害ならびに感染症の制御を検討する上で重要である。しかしながら、ワクモの寄生に対するニワトリの免疫応答に関する詳細な知見は乏しい。

現在、養鶏場におけるワクモの防除には主に殺ダニ剤が用いられる。しかし、薬剤による生産物や環境の汚染や薬剤耐性ワクモの出現が社会的な問題となっており、新たな防除法の開発が強く望まれている。同じ吸血性の節足動物であるマダニにおいては、ワクチンを用いた防除法が有効性を示し、家畜生産現場での実用例が知られている。近年、ワクモに対する新規防除法として、抗マダニワクチンを応用した抗ワクモワクチンが注目されており、組換えワクモ由来タンパク質を抗原として用いたワクチン試験において一定の抗ワクモ効果が報告されている。しかしながら野外試験において充分な有効性を示すワクチン抗原は報告されておらず、抗ワクモワクチンは未だ実用化に至っていない。そのため、抗ワクモワクチンによる制御法を樹立するためにはより有効なワクチン抗原の探索が不可欠である。抗ワクモワクチンは、免疫鶏により産生されたワクチン抗原に対する抗体が吸血時にワクモに取り込まれることで抗ワクモ効果を発揮するため、ワクチン抗原としては吸血時に高い発現を示す分子が望ましい。そのような分子を効率的、且つ網羅的に探索するためには、遺伝子発現を含むワクモの生物学的特徴を吸血状態別に精査することが必要である。しかしながら、吸血及び飢餓状態における遺伝子発現の変動については未だ解析されていない。

本稿ではワクモの吸血が宿主に及ぼす影響をより詳細に解明すること、及び効果的な抗ワクモワクチンの候補抗原を探索することを目的として、まず吸血状態別のワクモのトランスクリプトーム解析を行った。次に、ワクモ汚染農場及び非汚染農場由来のニワトリから血液を採材し、ワクモの寄生が宿主の免疫応答に与える影響を解析した。さらに、トランスクリプトーム解析の結果をもとに新規ワクチン抗原候補分子を同定し、*in vitro* における性状解析とワクチン抗原としての有用性の検討を行った。

第 1 章:吸血及び飢餓ワクモを用いた RNA シーケンスにより各吸血状態のワクモのトランスクリプトームを比較解析した結果、吸血によりワクモの遺伝子発現パターンが大きく変動することが明らかとなった。Gene ontology 解析の結果、吸血状態のワクモでは金属イオンの結合に関する遺伝子が高頻度で発現しており、ニワトリ血液中に含まれる金属イオンの運搬、貯蔵、または解毒作用が亢進することが示唆された。また吸血ワクモでは ATP 合成や代謝に関する遺伝子の発現頻度が高い一方、飢餓状態のワクモでは代謝抑制やオートファジー、糖新生に関する遺伝子群の発現が高頻度に認められた。

第 2 章:ワクモの吸血に対する宿主免疫応答の解析を行った。第 1 章で行った吸血ワクモを用いた RNA シーケンスで得られたニワトリ由来遺伝子の解析、さらにワクモ汚染農場及び非汚染農場由来のニワトリから得た血液サンプルを用いた解析結果から、ワクモに吸血されたニワトリの末梢血では炎症性ケモカイン C-C chemokine ligand 4 (CCL4) が非常に高く発現していることが明らかとなった。一方、Th1 サイトカインや炎症性サイトカインの発現には変化は認められなかった。それに対して抗炎症性サイトカインや、免疫チェックポイント分子などの免疫抑制因子については汚染農場由来のニワトリにおいて非常に高い発現が認められた。また、CCL4 の受容体である C-C chemokine receptor 5 は汚染農場由来のニワトリで低い発現を示した。そのため、ワクモに慢性的に曝露されたニワトリは免疫抑制状態にあることが示唆された。次に、ニワトリの免疫細胞をワクモ由来可溶性抽出物 (SME) 存在下で培養したところ、特にマクロファージ様細胞における炎症性サイトカイン遺伝子の発現が低下し、さらに M2 様マクロファージのマーカー遺伝子の発現が上昇することが示された。以上より、ワクモ由来分子が直接的にニワトリの免疫応答を抑制的に調節することが示唆された。さらに、SME で刺激した免疫細胞において、自然免疫応答に中心的な役割を担うインターフェロンαの発現が低下したことから、ワクモの吸血が宿主の易感染化に寄与している可能性が示された。

第 3 章:第 1 章で行った RNA シーケンスの結果を基にシスタチン様分子 (*D. gallinae*-cystatin: Dg-Cys)、銅イオントランスポーター様分子 (*D. gallinae*-copper transporter 1: Dg-Ctr1)、及び adipocyte plasma membrane-associated protein 様分子 (*D. gallinae*-adipocyte plasma membrane-associated protein: Dg-APMAP) の 3 種類を同定した。遺伝子発現解析の結果、いずれの候補分子もワクモの全ての発育ステージで吸血状態を問わず発現しており、また吸血された血液が貯蔵される中腸に発現していることが示された。次に各候補分子の組換えタンパク質を免疫したニワトリから得た免疫血漿をワクモに吸血させることで、抗ワクモ効果の検討を行った。その結果、いずれの免疫血漿を吸血したワクモでも陰性対照群と比べて生存率の低下が認められた。さらに、Dg-Cys の免疫血漿を吸血したワクモでは、繋殖能力が低下した。これらの結果より、本研究で同定した 3 種類の分子のワクチン抗原としての有用性が示唆され

た。さらに、Dg-Cys の免疫血漿と Dg-Ctr1 または Dg-APMAP の免疫血漿と組み合わせた混合血漿による抗ワクモ効果を検証したところ、単独で免疫血漿を用いた場合と比較して殺ダニ効果の増強が認められた。以上より、Dg-Cys を含む複数の抗原を組み合わせたカクテルワクチンが、ワクモ被害に対する新規防除法として有用である可能性が示された。

本研究では吸血状態別のワクモの遺伝子情報を明らかにし、またワクモによる吸血が宿主の免疫応答を抑制することが示唆された。さらに Dg-Cys、Dg-Ctr1、及び Dg-APMAP を標的とした抗ワクモワクチン、さらにそれらを組み合わせたカクテルワクチンが、有効な新規ワクモ制御法となり得ることを示した。今後は実験的寄生モデルを用いることでワクモが病原体の媒介に与える影響やその分子基盤を検討することに加え、免疫鶏を用いたワクチンの臨床試験を行い、本研究を基にした新規制御法の効果をより詳細に評価する必要がある。